

A-315-03710-5



National Library of Canada

Bibliothèque nationale du Canada

Canadian Theses Division / Division des thèses canadiennes

Ottawa, Canada  
K1A 0N4

51605

**PERMISSION TO MICROFILM — AUTORISATION DE MICROFILMER**

• Please print or type — Écrire en lettres moulées ou dactylographier

Full Name of Author — Nom complet de l'auteur

Keith Daryl Whitmore

Date of Birth — Date de naissance

26/08/56

Country of Birth — Lieu de naissance

Canada

Permanent Address — Résidence fixe

9611 - 81 Street  
Edmonton, Alberta  
CANADA

Title of Thesis — Titre de la thèse

Microprocessor Controlled Gamma-Ray  
CT Scanner. For Measurement  
of Bone Density

University — Université

U. of Alberta

Degree for which thesis was presented — Grade pour lequel cette thèse fut présentée

M. Sc Elect Eng.

Year this degree conferred — Année d'obtention de ce grade

Spring 1981

Name of Supervisor — Nom du directeur de thèse

F. J. Koles & T. R. Overton

Permission is hereby granted to the NATIONAL LIBRARY OF CANADA to microfilm this thesis and to lend or sell copies of the film.

L'autorisation est, par la présente, accordée à la BIBLIOTHÈQUE NATIONALE DU CANADA de microfilmer cette thèse et de prêter ou de vendre des exemplaires du film.

The author reserves other publication rights, and neither the thesis nor extensive extracts from it may be printed or otherwise reproduced without the author's written permission.

L'auteur se réserve les autres droits de publication; ni la thèse ni de longs extraits de celle-ci ne doivent être imprimés ou autrement reproduits sans l'autorisation écrite de l'auteur.

Date

December 29

Signature

Keith Daryl Whitmore



National Library of Canada  
Collections Development Branch

Canadian Theses on  
Microfiche Service

Bibliothèque nationale du Canada  
Direction du développement des collections

Service des thèses canadiennes  
sur microfiche

## NOTICE

The quality of this microfiche is heavily dependent upon the quality of the original thesis submitted for microfilming. Every effort has been made to ensure the highest quality of reproduction possible.

If pages are missing, contact the university which granted the degree.

Some pages may have indistinct print especially if the original pages were typed with a poor typewriter ribbon or if the university sent us a poor photocopy.

Previously copyrighted materials (journal articles, published tests, etc.) are not filmed.

Reproduction in full or in part of this film is governed by the Canadian Copyright Act, R.S.C. 1970, c. C-30. Please read the authorization forms which accompany this thesis.

**THIS DISSERTATION  
HAS BEEN MICROFILMED  
EXACTLY AS RECEIVED**

## NOTICE

La qualité de cette microfiche dépend grandement de la qualité de la thèse soumise au microfilmage. Nous avons tout fait pour assurer une qualité supérieure de reproduction.

S'il manque des pages, veuillez communiquer avec l'université qui a conféré le grade.

La qualité d'impression de certaines pages peut laisser à désirer, surtout si les pages originales ont été dactylographiées à l'aide d'un ruban usé ou si l'université nous a fait parvenir une photocopie de mauvaise qualité.

Les documents qui font déjà l'objet d'un droit d'auteur (articles de revue, examens publiés, etc.) ne sont pas microfilmés.

La reproduction, même partielle, de ce microfilm est soumise à la Loi canadienne sur le droit d'auteur, SRC 1970, c. C-30. Veuillez prendre connaissance des formules d'autorisation qui accompagnent cette thèse.

**LA THÈSE A ÉTÉ  
MICROFILMÉE TELLE QUE  
NOUS L'AVONS REÇUE**

THE UNIVERSITY OF ALBERTA

Microprocessor Controlled Gamma-Ray CT Scanner For

Measurement Of Bone Density

by

© Keith Daryl Whitmore

A THESIS

SUBMITTED TO THE FACULTY OF GRADUATE STUDIES AND RESEARCH

IN PARTIAL FULFILMENT OF THE REQUIREMENTS FOR THE DEGREE

OF Master of Science

Electrical Engineering

EDMONTON, ALBERTA

Spring 1981

THE UNIVERSITY OF ALBERTA

RELEASE FORM

NAME OF AUTHOR Keith Daryl Whitmore  
TITLE OF THESIS Microprocessor Controlled Gamma-Ray CT  
Scanner For Measurement Of Bone Density  
DEGREE FOR WHICH THESIS WAS PRESENTED Master of Science  
YEAR THIS DEGREE GRANTED Spring 1981

Permission is hereby granted to THE UNIVERSITY OF ALBERTA LIBRARY to reproduce single copies of this thesis and to lend or sell such copies for private, scholarly or scientific research purposes only.

The author reserves other publication rights, and neither the thesis nor extensive extracts from it may be printed or otherwise reproduced without the author's written permission.

(SIGNED) *Keith Daryl Whitmore...*

PERMANENT ADDRESS:

9611-81 Street  
Edmonton, Alberta  
Canada

DATED December 31, 1980

THE UNIVERSITY OF ALBERTA  
FACULTY OF GRADUATE STUDIES AND RESEARCH

The undersigned certify that they have read, and recommend to the Faculty of Graduate Studies and Research, for acceptance, a thesis entitled Microprocessor Controlled Gamma-Ray CT Scanner For Measurement Of Bone Density submitted by Keith Daryl Whitmore in partial fulfilment of the requirements for the degree of Master of Science.

*Z. D. Koles*  
.....  
*Z. D. Koles*  
.....

Supervisors

*Jay Pattison*  
.....  
*Dr. H. H. H. H.*  
.....  
*W. H. H. H.*  
.....  
*Keith D. Whitmore*  
.....

Date.....

## Abstract

The theory, design and construction of a microprocessor controlled gamma-ray CT bone scanner are described. This scanner, with its ability to determine the radiological density of trabecular bone at appendicular sites in the skeleton, provides an order of magnitude increase in sensitivity to changes in bone mineralization over existing techniques such as absorptiometry and radiographic analysis. This technological development could be invaluable to the clinician for diagnosis and in the evaluation of treatments of osteopenia. The design and implementation of both a single and multi-detector rotation-translation scanning system are detailed along with future plans for a fan-beam rotational system.

## Acknowledgements

I would like to express my appreciation to my supervisor, Dr. T.R. Overton for his efforts (in terms of administrative assistance and moral encouragement) which have increased both the value and personal satisfaction of my education. This project has been a team effort and hence there are many people whose efforts I would like to recognize. These include: Mr. I. Yamamoto (for his aid in design and construction of the mechanical components), Mr. R. Heath (for the design, testing, and implementation of the HP programs), Mr. J.D. Ridley (for his aid in evaluation of the scanner), Dr. D. Menon (for his assistance in helping me to understand some of the theoretical aspects of CT and his review of this manuscript) and Dr. T.N. Hangartner (for his efforts in upgrading the CT system and his willingness to share his expertise). Lastly, I would like to express my thanks to my many friends in the Division of Biomedical Engineering who have made my educational experience truly enjoyable.

## Table of Contents

Chapter	Page
I. Historical Aspects .....	1
A. Measurement of Bone at the University of Alberta .....	4
II. Bone Physiology and Pathology .....	7
A. Osteoporosis and Osteomalacia .....	9
B. Physical Evaluation of Bone .....	12
Bone Biopsy .....	12
Radiology (X-rays) .....	12
Absorptiometry .....	13
In Vivo Neutron Activation Analysis (IVNAA) ..	16
Compton Scattering .....	17
Radioisotope CT .....	17
III. Principles of CT Scanners .....	20
A. Back-Projections .....	25
B. Reconstruction Algorithms .....	31
Iterative Technique .....	31
Analytical Technique .....	32
Comparison of Analytical and Iterative Algorithms .....	41
C. Photon Attenuation .....	41
Statistical Considerations .....	42
Dead Time .....	43
Beam Hardening .....	45
D. Detector Types .....	46



Scintillation Detector .....	48
E. Performance Characteristics Of CT Scanners .....	52
Spatial Resolution .....	52
Contrast Resolution .....	56
F. Commercial CT Scanners .....	57
IV. System Design and Construction .....	60
A. Mechanical Operations .....	60
Stand .....	60
Source-Detector Alignment and Motion .....	62
Mechanical Drives .....	62
B. Radioactive Sources and Detectors .....	66
Signal Processing .....	67
C. Scanner Control .....	69
Timing Considerations .....	70
MPU Control .....	73
Reproducibility of Measurements .....	81
Single Stepping .....	83
HP/Microprocessor Interfacing .....	83
D. Multidetector System .....	86
Physical Limitations .....	87
Intervals and Subintervals .....	89
Centering .....	90
E. Data Processing .....	92
Open Count .....	95
Pixel Size and Grey Levels .....	95
Analysis Program .....	96
V. System Evaluation .....	100

- A. Spatial Resolution ..... 100
- B. Precision ..... 105
- C. Accuracy ..... 105
- D. Radiation Dose ..... 107
- Thermo-Luminescent Detectors ..... 115
- E. Contrast Resolution ..... 115
- VI. System Limitations and Future Plans ..... 117
  - A. X-Ray Tube ..... 117
  - B. System Three ..... 118
  - C. Control System ..... 118
  - D. Processing Facilities ..... 119
- References ..... 120
- Appendix A. Iodine 125 Decay Mechanism ..... 127
- Appendix B. MPU Program Flow Chart ..... 128
- Appendix C. MPU Subroutines Used ..... 129
- Appendix D. Read Subroutine ..... 150

List of Tables

Table .....	Page
1. Analysis Program Output .....	97
2. Precision Test - Repeat Measurements .....	106
3. Accuracy Measurements .....	109

## List of Figures

Figure .....	Page
1. Conventional Tomography .....	2
2. Reconstruction Matrix .....	5
3. Absorptiometry .....	15
4. CT Generation 1 .....	21
5. CT Generation 2 .....	21
6. CT Generation 3 .....	23
7. CT Generation 4 .....	23
8. CT Generation 5 .....	24
9. Parallel Beam Format .....	26
10. Rotational Beam Format .....	27
11. Back-Projection .....	29
12. Image Reconstruction Using Back-Projection .....	30
13. Beam Hardening Correction .....	47
14. Photomultiplier Tube and Related Circuitry .....	51
15. Effects of Aperture Size on Spatial Resolution .....	54
16. Effects of Aperture Size on Spatial Resolution .....	55
17. CT System .....	61
18. Plate #1 .....	63
19. Plate #2 .....	64
20. Plate #3 .....	65
21. Preamp Circuit .....	68
22. Stepping Motor and Translator Circuit .....	71
23. Control and Data Processing Block Diagram .....	72
24. Image Obtained From Scout Scan .....	82

25. Single Stepping Circuitry .....	84
26. Current Sink For HP-Micro Signal Conversion .....	85
27. Voltage Divider Circuit .....	85
28. Multi-Detector Holder .....	88
29. The Cause of Centering Artifacts .....	91
30. Centering Artifacts in a Plexiglass Model .....	93
31. Image of a Normal Radius-Ulna .....	98
32. High Speed Spatial Resolution .....	102
33. Medium Speed Spatial Resolution .....	103
34. Low Speed Spatial Resolution .....	104
35. Test Cylinder of $K_2HPO_4$ .....	108
36. Evaluation of System Accuracy .....	110

## I. Historical Aspects

It has long been the goal of medical radiology to obtain clear cross-sectional views of the body. As early as 1921 (1) conventional or focal plane tomography was being used. Conventional tomography involves the movement of both the X-ray tube and film (or even the body itself) in a trajectory (Figure 1) so that only the desired layer remains in focus while all other layers are blurred. This type of tomography which is analogous to a narrow-depth-of-field in photography has the disadvantage of the blurred presence of unwanted fields.

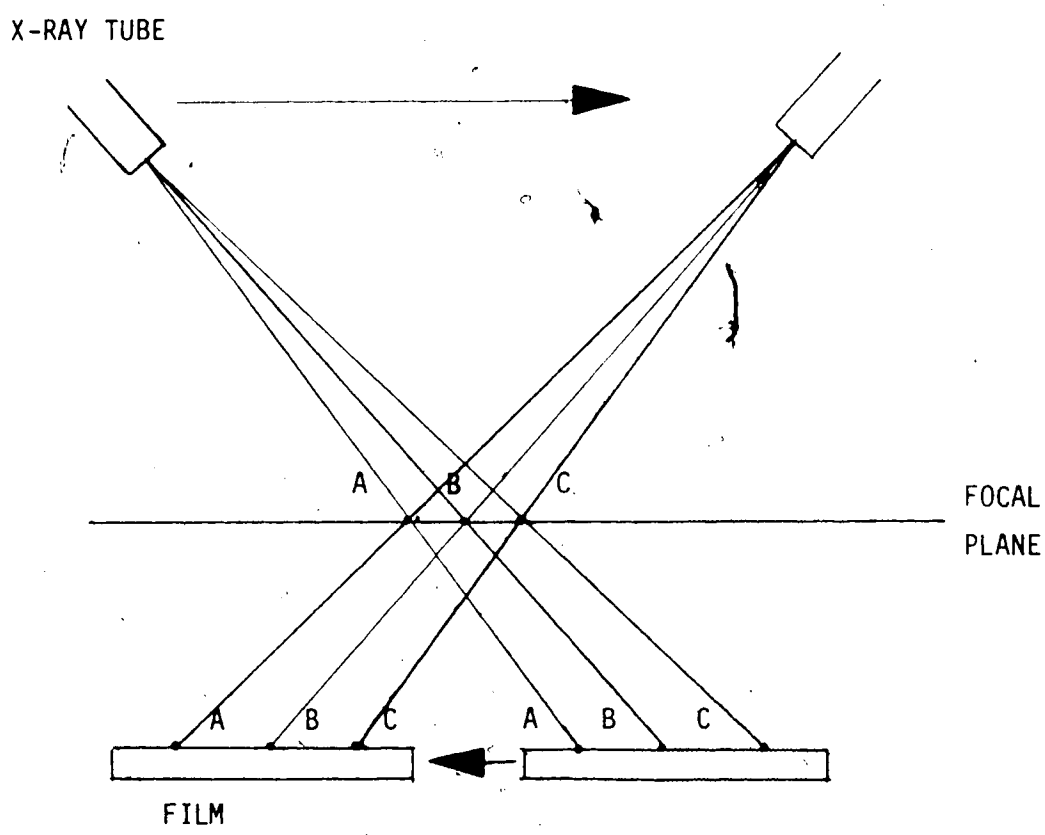
Computed tomography (CT), which is the latest evolution in a series of techniques used in image reconstruction, eliminates these unwanted planes by limiting radiation to the desired plane. CT is based on the principle that if radiological attenuation is measured along a sufficient number of lines passing through a given plane, then the radiological densities throughout that plane can be determined.

The mathematical basis for computed tomography was first described by Radon (2) in 1917. Given that

1.  $f(x,y)$  denotes the attenuation coefficient at a point  $(x,y)$  in the plane, and
2. that  $L$  is any line in the plane:

then, the logarithm of attenuation is equal to the integral of  $f$  along  $L$ ;  $P(L) = \int f(x,y) ds$

where  $s$  indicates a length along  $L$ . The problem then is to



ONLY POINTS ON THE FOCAL PLANE ARE CONTINUALLY REGISTERED ON THE SAME PART OF THE FILM. POINTS IN OTHER PLANES ARE IMAGED ONTO VARYING PARTS OF THE FILM AND HENCE ARE BLURRED.

FIGURE 1. CONVENTIONAL TOMOGRAPHY

invert the equation: that is, given  $P(L)$ , to determine  $f(x,y)$ . Assuming  $P(L)$  is given for all lines  $L$  and that  $f(x,y)$  is continuous with compact support, Radon showed that  $f(x,y)$  could be calculated for all points in the plane. At the time of its development this mathematical basis for image reconstruction was purely theoretical in nature and in actual fact was derived by Radon while he was working with equations dealing with gravitational fields.

It was not until 1956 that this theory was made use of by Bracewell (3) in the field of radioastronomy. Bracewell was able to identify regions on the sun which emitted microwave radiation. However, the antennas being used could only focus on thin strips criss-crossing the solar surface. In order to map out the solar regions of microwave activity it was necessary to convert these strips into a representative plane of solar activity - the exact problem shown by Radon to be mathematically solvable. Bracewell developed both an analytical technique (equivalent to Radon's) and an iterative technique for image reconstruction.

The first medical application appeared 7 years later when Cormack (4) published his first experimental results. Cormack's work involved development of a mathematical technique for the accurate reconstruction of an image from x-ray projections and applications based on measurements of simple phantoms. This technique for reconstruction involved the expansion of  $P$  and  $f$  into Fourier series and the



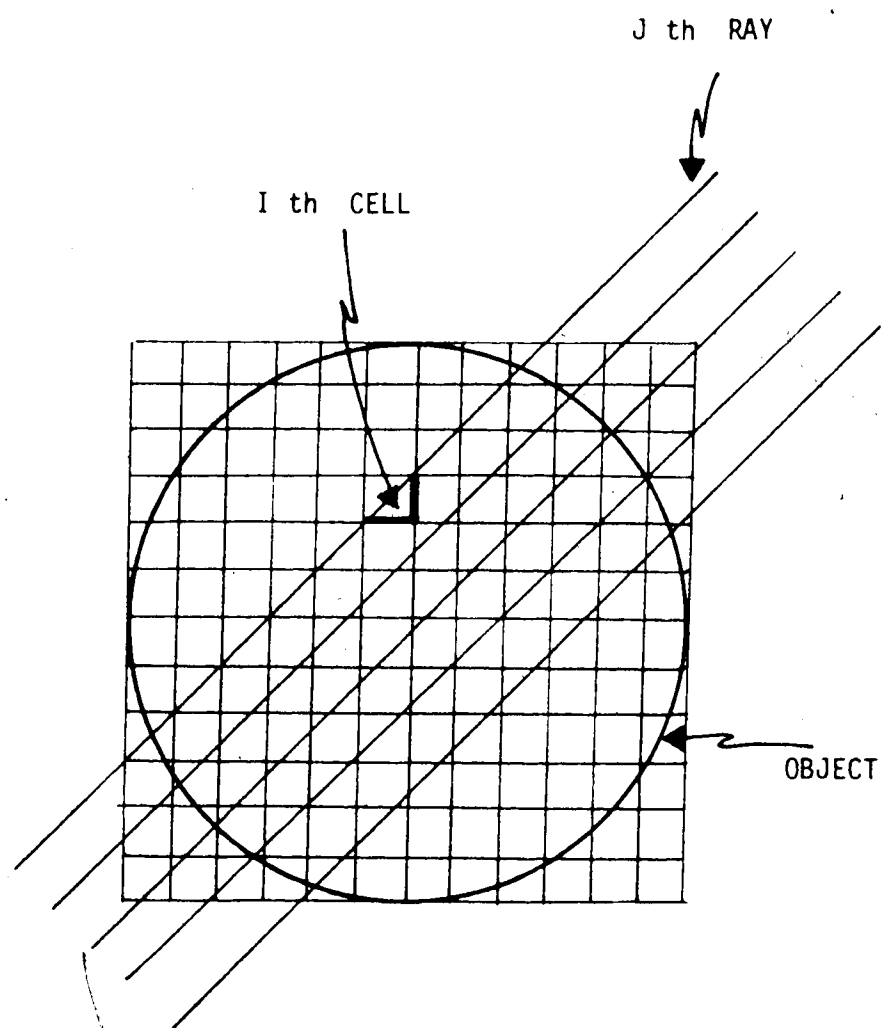
subsequent matching of Fourier coefficients.

The first commercial scanner was the E.M.I. Head Scanner described in 1973 by G. Hounsfield (5). Having realized that the ray-integrals essentially composed a discrete rather than a continuous number of equations, Hounsfield's approach to reconstruction involved an iterative solution to inversion of the equation defined by  $P_j =$  the summation over  $i$  of  $W_{ij} f_i$  (Figure 2) where  $W_{ij}$  is a weighting function of the radiological density,  $f_i$ . This weighting function represents the contribution of the  $i$ th cell to the  $j$ th ray.

From these early days CT has evolved from the point where only scans of the head could be performed to today where scans of the entire body can be made. A 1977 study of the U.S. Department of Commerce (6) predicted that by 1980 there would be some 2500 CT scanners in the U.S. and annual related expenditures of \$1.7 billion. Over a dozen different companies were involved in marketing CT machines in 1976: machines able to delineate differences in soft tissue density as low as 0.5 % (7).

#### A. Measurement of Bone at the University of Alberta

The use of CT for the measurement of bone density, as developed in Zurich by R uegsegger and Elsasser (8), is a relatively new phenomenon. Since changes in bone mineralization occur much more rapidly in trabecular bone than in cortical bone (9), detection of small changes in



THE RECONSTRUCTION MATRIX IS AN  $N$  BY  $N$  ARRAY OF CELLS.  
THE ACTUAL RAYS ARE STRIPS OF FINITE WIDTH. THE CONTRIBUTION  
OF THE  $I$  th CELL TO THE  $J$  th RAY IS DENOTED BY  $w_{ij}$ .

FIGURE 2. RECONSTRUCTION MATRIX

mineral content are only possible if trabecular bone density can be quantified. It is for this reason that CT scans which can be used to produce images of bone cross section are so valuable.

Although the principles involved in reconstruction of an image of bone are the same as in commercial whole body scanners, there are a sufficient number of differences to merit a specially designed CT scanner.

The Division of Biomedical Engineering at the U. of A. has been involved in the clinical determination of bone mineral content using absorptiometric techniques for the past 8 years (10). This clinical experience led to the development of a CT system for the measurement of bone mineral content at the University of Alberta. Based upon an original design by Elsasser (11) an eight detector, translation-rotation gamma-ray CT system has been constructed. With this scanner, measurements can be made of the distal forearm using Iodine 125 as a photon source.

This thesis is concerned primarily with the control system for the scanner. A microprocessor unit or MPU (Motorola 6800 D2 kit) serves as a system master clock, providing control of scanner movement and for data acquisition through the laboratory computer (HP 2100) and CAMAC systems. An MPU based controller was chosen as it was felt that the timing specifications of the scanner would be too tight to be controllable by the HP running under a multi-user operating system.

## II. Bone Physiology and Pathology

In the diagnosis of various diseases of bone it is desirable to measure changes in mineral content of trabecular (spongy) bone. To understand this requirement it is necessary to examine the physiological and pathological characteristics of bone. Once the need for bone mineral density analysis has been described an examination of existing analysis techniques will be presented.

Bone consists of an organic matrix that is greatly strengthened by deposits of calcium salts (12-14). Five percent of this organic matrix is a homogeneous medium called ground substance while the other 95 % is made up of collagen fibers. It is these collagen fibers which give bone its tensile strength while the calcium salts provide its compressional strength. The calcium salts are composed principally of calcium and phosphate and are formed in a crystal called hydroxyapatite. The crystals are between 200 and 400 angstroms in length and between 10 and 30 angstroms in diameter. Under varying nutritional conditions the ratio by weight of calcium to phosphate in these crystals can vary from 1.3 to 2.0.

As we have seen having the obvious structural function the skeleton acts as a reservoir for many of the body's ions, notably calcium and phosphate. Bone contains 99% of the total body calcium and 90% of the total body phosphorus. From 0.4 to 1.0 % of this bone calcium is readily exchangeable and this exchange occurs at points in the bone

undergoing active calcium resorption (remodelling) (15). Thus there is a constant circulation of ions between the skeletal reservoir and body fluids and tissues. Ions not contained in the bone have a wide range of physiological activities. For example; calcium not in the bone affects enzyme activity, cell membrane permeability, cardiac rhythm and neuromuscular excitability. The concentration of calcium in the blood is maintained between 9 and 11 mg per 100 ml and it is the buffering action of bone that provides this control. Exchange of calcium with the bone is controlled mainly by parathyroid hormone from the parathyroids and calcitonin from the thyroid. Another means of control of calcium ion concentration is absorption from the gut. Vitamin D<sub>2</sub>, for example, is required for calcium absorption from the gut.

Bone is made up of 3 types of cells..These cells are scattered throughout an interstitial matrix of fibrous protein and occupy 3% of the total volume of the bone. Osteocytes are the ordinary bone cells and comprise the bulk of the cells. They are incapable of mitosis and hence must be removed before new bone can be formed. Osteoblasts are the cells which secrete the ground substance and collagen onto the bone forming surface. This uncalcified organic matrix is known as osteoid. The osteoblasts produce an enzyme, alkaline phosphatase, which is thought to act by splitting organic phosphate compounds thus upsetting the local calcium-phosphate balance causing precipitation of

calcium salts in the ground substance. Osteoclasts or bone phagocytes are the cells involved in the removal of bone. This occurs by both a phagocytic action and the release of enzymes and acids which cause the simultaneous dissolution of mineral and matrix. Thus bone is continually being deposited by osteoblasts and being resorbed at sites where osteoclasts are active. Osteoblastic deposition is stimulated by physical stress while sex hormones and calcium supplements decrease both bone resorption and formation.

On a macroscopic level there are two main classes of bone: cortical or compact bone, which is the harder outer bone and trabecular or spongy bone which is the less dense inner bone. Average compact bone consists of 25 % by weight matrix and 75 % calcium salts while trabecular bone is made up of a much higher percentage of matrix. Due to a greater surface area it is in this less dense trabecular bone structure where physiological and pathological changes in matrix structure or calcium salt deposition occur more rapidly and hence it is desirable to measure the distribution of density in trabecular bone.

#### A. Osteoporosis and Osteomalacia

Two common diseases of bone are osteomalacia or "adult rickets" and osteoporosis. Osteomalacia is a lack of calcium salts and is due to a lack of calcium and phosphates in the extracellular fluid (16). This is often caused by a lack of calcium absorption from the gut possibly due to a vitamin D

deficiency. Kidney disorders are one common non-nutritional cause of osteomalacia.

Osteomalacia involves an increase in the proportion of uncalcified bone (osteoid) with a corresponding increase in both the number and thickness of osteoid seams. The mineralized bone mass is usually decreased due to a decrease in calcium and phosphate. The bones are soft and skeletal deformities may ensue. Symptoms of osteomalacia include weakness, bone pain and tenderness as well as radiologic evidence of decreased mineralization and pseudofractures of the long bones.

Osteoporosis is abnormal organic matrix formation (17,18) and may be caused by: (1) lack of use of the bones, (2) malnutrition to the extent that sufficient protein matrix cannot be formed, (3) lack of vitamin C, (4) postmenopausal lack of estrogen secretion, and (5) old age (due to dysfunction of various protein anabolic functions). Osteoporosis therefore involves a decrease in bone mass due to the absence of a normal quantity of bone caused by deficient production of bone matrix. The mineral content of the bone however, is grossly normal and there is no excess of osteoid. Thus there is an imbalance between osteoblastic bone deposition and osteoclastic bone resorption. Clinically there is a decrease in the number of and thickness of bony trabeculae. The cortical bone later becomes thinned; however, it is still relatively dense compared to the decreased density of the trabecular bone. There is an

increase in susceptibility to fractures from compression forces (eg. vertebral bone compression fractures).

The density of bone has been shown to decline in all people from the age of 20 onwards, the process accelerating after middle age (16,18). To this extent bone becomes osteoporotic after 50 years of age to a greater extent and somewhat earlier in women than in men.

Decreased bone mineralization, which may accompany osteopenia (general bone disorders), appears radiologically as areas of decreased density. As such, it is possible to use radiographic techniques to diagnose and to evaluate the effectiveness of treatment in diseases related to changes in bone mineralization.

"Since the disorders causing rickets and osteomalacia are generally of long standing and must have profound effects on matrix composition or mineral metabolism before they become apparent clinically, therapy may be necessary for months or years before healing is complete." <sup>1</sup> The same may be said for osteoporosis. Some of the present treatments include mineral supplements, gonadal hormones and physical therapy. Some of these treatments may have other effects. For example, pharmacologic doses of vitamin D may cause hypercalcemia. Treatments then are very dose dependant and/or expensive and hence any technique which will provide an early and accurate means of diagnosis and measurement of changes in bone density has potential for both therapeutic

---

<sup>1</sup> Current Therapy 1977, Edited by Conn: pg 461.



and financial benefit. Since changes in bone density first appear in trabecular bone, a technique is required that is able to measure density of trabecular bone.

## B. Physical Evaluation of Bone

This section will examine some of the techniques presently being used for physical evaluation of bone. These include both invasive and non-invasive techniques.

### Bone Biopsy

Bone biopsies involve the physical removal of a sample of bone usually from the iliac crest (hip bone). This sample is then analyzed, usually by microscopic examination of the number of trabeculae and osteoid in a given area within the sample. Although this technique does provide valuable information the sample removal is an invasive technique and is traumatic for the patient. Results obtained vary greatly from site to site and once bone has been removed the same site cannot be re-examined. This then precludes the use of bone biopsies as an accurate means of monitoring both the course of any diseases such as osteoporosis and osteomalacia as well as the effectiveness of any treatments. Thus the use of bone biopsies is severely limited.

### Radiology (X-rays)

Prior to 1963, diagnosis of osteoporosis and osteomalacia predominantly involved the radiological evaluation of vertebral skeleton. Radiographic techniques or X-rays show total density of a number of planes superimposed

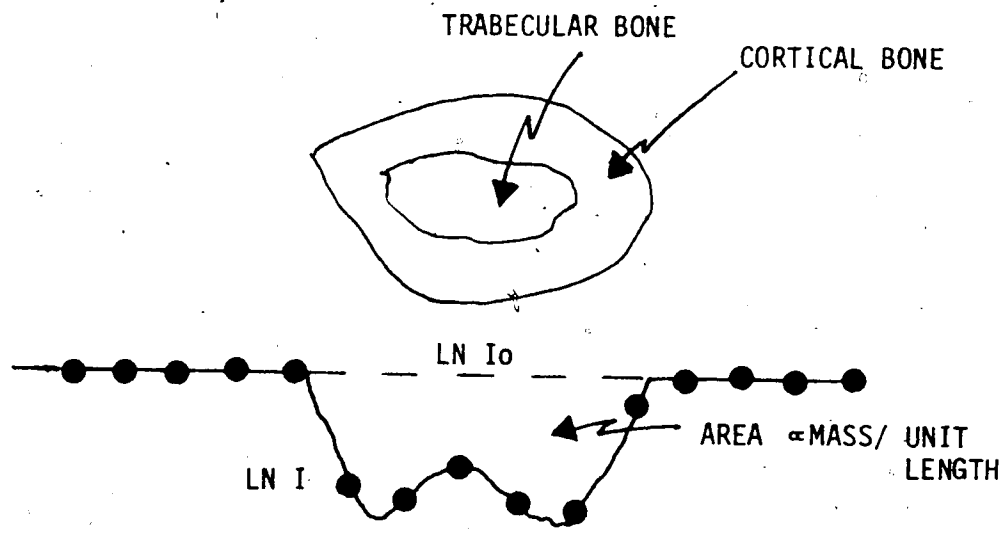
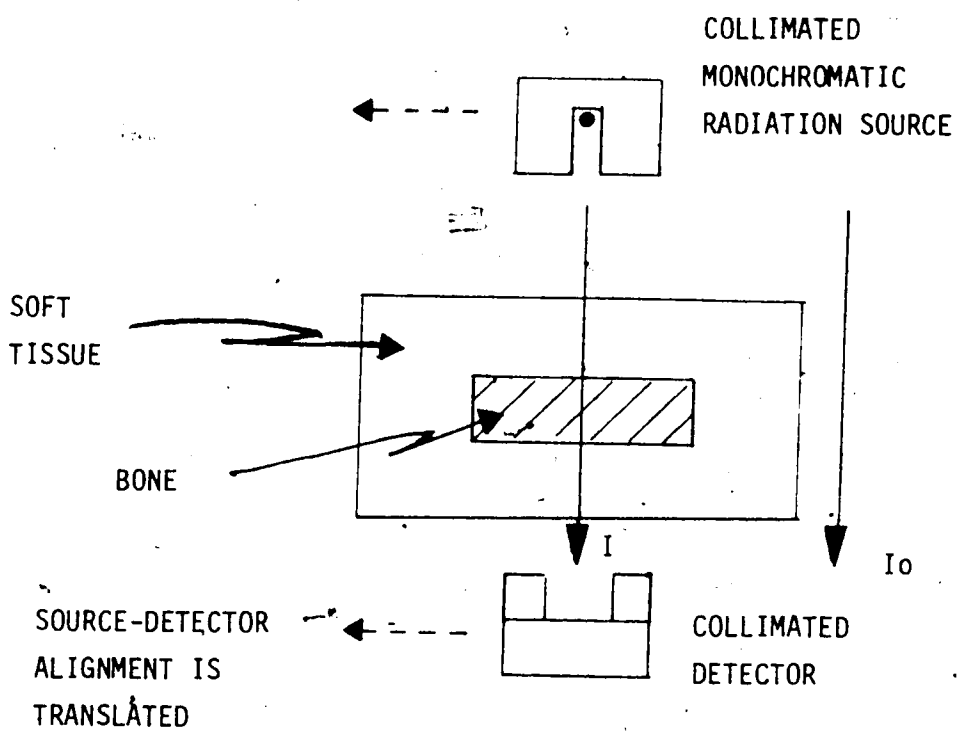
together on one view and hence any one plane of high density will overshadow any of the other planes. Thus it is largely cortical bone that shows on X-rays and hence measurements of density of trabecular bone are not feasible. Accurate diagnosis of either osteoporosis or osteomalacia using X-rays requires the diseases to be significantly advanced involving decreases in bone mass of greater than 25% (16,18) and/or compression fractures. Due to the lack of precision of this technique, longitudinal studies (studies over time) are difficult to perform and it is virtually impossible to evaluate the progress of disease and the effectiveness of treatments. Radiographic distinction between osteoporosis and osteomalacia is also difficult and the two diseases may coexist.

#### Absorptiometry

In 1963, Cameron and Sorenson (19) reported an improved technique, known as absorptiometry, for the in vivo measurement of bone mineral content. Their method involved the use of a nearly monoenergetic collimated source of photons mechanically coupled and collinear with a collimated scintillation detector. The scintillation detector, with appropriate electronics, is able to measure both the energy of, and the number of photons striking it in an interval of time. Therefore, one can measure both the number and energy of photons striking the detector with and without an object placed between them. These measurements allow the amount of energy absorbed by the object to be calculated. In the case

of bone the number of photons removed from the beam by the object is related to the mass of bone present. The measurement technique then involves movement of the source detector system along a linear path across the object with transmission measurements taken at discrete intervals throughout the translation (Figure 3). This results in an absorption profile of the object, the area of which is a function of the number of photons absorbed by the object.

Although this technique is similar to a conventional X-ray in that radiological attenuation is measured, the improved equipment results in marked improvements in both the accuracy and precision of the measurement. Absorptiometry could be considered a digital form of radiology in that quantitative rather than qualitative transmission measurements are made. Measurement of bone mineral content on a cadaver forearm (20) using absorptiometry was found to have an accuracy to within 4-7 % of that obtained from measurements of bone weight. Reproducibility of measurements on a single individual were found to have a coefficient of variation of 2.5 %. These improvements in accuracy and precision of absorptiometry versus conventional X-rays were due to elimination or reduction of such causes of error as film exposure, development and calibration; measurement errors due to scattered radiation and the broad beam polychromatic x-rays as well as errors from soft tissue effects. Variations in quantities of soft tissue are reduced by submersion of the



MEASUREMENTS ARE MADE AT REGULARLY SPACED INTERVALS

FIGURE 3. ABSORPTIOMETRY

limb in water, thus providing a constant pathlength of attenuation. The radiological attenuation of fat, collagen, water and other organic components of soft tissue are all approximately equal.

Loss of vertebral skeletal bone has been shown to be reflected in measurements of radial bone mass, in particular in the distal region. A study was done (21,22) of 169 white women, 113 of whom had no fractures while 56 had radiological evidence of spinal fractures. Those women with no evidence of fractures had higher values of radial bone mass with a significance of 98.8 % for cortical bone and better than 99.9 % for trabecular bone. Although total bone mineral content was found to be a reliable determinant for diagnosis of decreased mineralization it was also found that in cases of very slight or exceptionally heavy built patients, evaluation of mineral content divided by bone width provided a more useful parameter. Absorptiometry studies involve measurement of a single radiation absorption profile. This allows one to evaluate total bone mineral content and thickness of cortical bone but quantitative evaluation of bone mineral density is not possible. Thus, absorptiometry requires a measurable change in the thickness of cortical bone or total bone mineral content to evaluate disease processes and this typically requires a period of several months to years.

#### In Vivo Neutron Activation Analysis (IVNAA)

Neutron activation analysis involves irradiation of a

volume by neutron bombardment and the subsequent detection of emitted radiation to determine the quantity of a particular material present (23). Irradiation of calcium in bone results in the production of a number of different isotopes of calcium. By measuring the radiation given off by one of these isotopes the quantity of that isotope can be calculated. Using the ratio of the quantity of that isotope to total calcium, total bone calcium can be calculated. This technique although providing valuable information is a costly process (requiring 14 MeV neutron sources) with limited accuracy and precision (of the order of 5 %).

#### Compton Scattering

Another technique which has been used for the in vivo measurement of bone mineral density is the Compton scatter technique (24). This technique involves the irradiation of a collimator defined volume and the measurement of Compton scatter from a particular portion of this volume by a collimated detector. From these measurements it is possible to determine the average electron density of the measured volume. The major limitations of the technique relate to the fact that only a relatively small volume of material can be studied and as such repositioning problems (in order to measure the same volume at a future time) are a major concern.

#### Radioisotope CT

Although CT, with its ability to image cross sections, would appear to provide a technique for measurement of bone

density there are a number of problems with standard commercial X-ray scanners that preclude such measurements. These problems are mainly manifest in the areas of beam hardening (due to use of a multi-energy X-ray source), physical resolution (due to the degree of collimation of the source and detectors) and the sample spacing (which is required to cover an abdominal area, leaving too little matrix in an area of bone for sufficient analyses to be carried out). A technique able to measure density of both trabecular and cortical bone with a precision of better than 1 % using a radioisotope CT scanner was first reported by Rügsegger and Elsasser (8) in 1975. The principles behind this special purpose CT scanner are the same as for commercial whole body scanners; however, changes have been made in order to facilitate the measurement of bone rather than soft tissue density. The technique involves performing a scan of the radius and ulna at a distal site, usually 1/10 the distance from the ulna styloid to the proximal point of the ulna. At this site although some 50 % of the bone area is trabecular it contributes only 10 % to the total bone mineral content. Given this relatively large area of trabecular bone it is possible to separately determine the density of both trabecular and cortical bone at this site. The technique is non-invasive, not traumatic to the patient and allows repeat measurements of the same sample to be performed.

It is also hoped that CT may be used to examine the

bone-cement and metal-cement contact on artificial hips (25). Although this problem is somewhat distinct from the measurement of bone density (and will require an X-ray tube photon source) many of the problems encountered are similar (i.e. measurement of radiological attenuation in high density areas such as bone). Upon implantation it is difficult to determine the degree of bonding of artificial hips and subsequent loosening may result.

Use of a photon source with energies higher than the 27.5 KeV of Iodine 125, such as Gadolinium 153 (40 KeV, 100KeV), may allow the CT scanner to be used for examination of bone gaps and degradation in patients who are having knee joints implanted. A higher energy source is required because of the quantity of bone involved and hence the high radiological attenuation. At present it is often necessary to perform an exploratory operation to determine the sizes of bone gaps and the amount of degradation of the bones. It is possible that the CT Scanner may be used to eliminate this exploratory surgery.

In order to fully appreciate the potential uses of a CT Scanner it is first necessary to have a basic understanding of what computed tomography is and how it works. This area will be explored in the next chapter.



### III. Principles of CT Scanners

"CT" or computed tomography (7,26-30) is now the preferred name for "CAT"(computerized (assisted) axial tomography). A tomogram is literally a picture of a slice or section at a given orientation. Radiation in the form of gamma or X-rays are passed through (transmission tomography) or originate (emission tomography) from the desired plane of view without entering other areas. The amount of radiation absorbed along a given pathlength is measured and is an indication of the sum of linear attenuation coefficients or radiological densities along the pathlength. A linear attenuation coefficient is a measure of the absorption of radiation as it traverses a distance in an object. It should be noted that the attenuation coefficient in any object is dependent on the material composition and the incident photon energy. This sum of attenuation coefficients is measured along a sufficient number of pathways so that an image depicting the radiological densities (or attenuation coefficients) throughout the object can be reconstructed. Since this work deals primarily with transmission tomography any further references to CT will be referring to transmission CT.

To this date there have been 5 generations of CT scanners. These generations are identified by the type of mechanical motion used and the number of detectors employed. The first two generations of scanners (Figures 4 & 5) are known as single detector and multiple detector translation-rotation systems. Scans are performed by

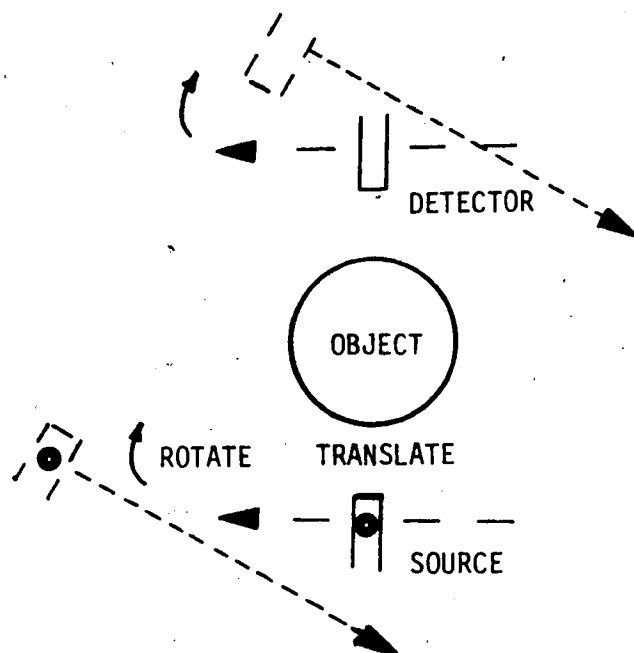


FIGURE 4. CT GENERATION 1

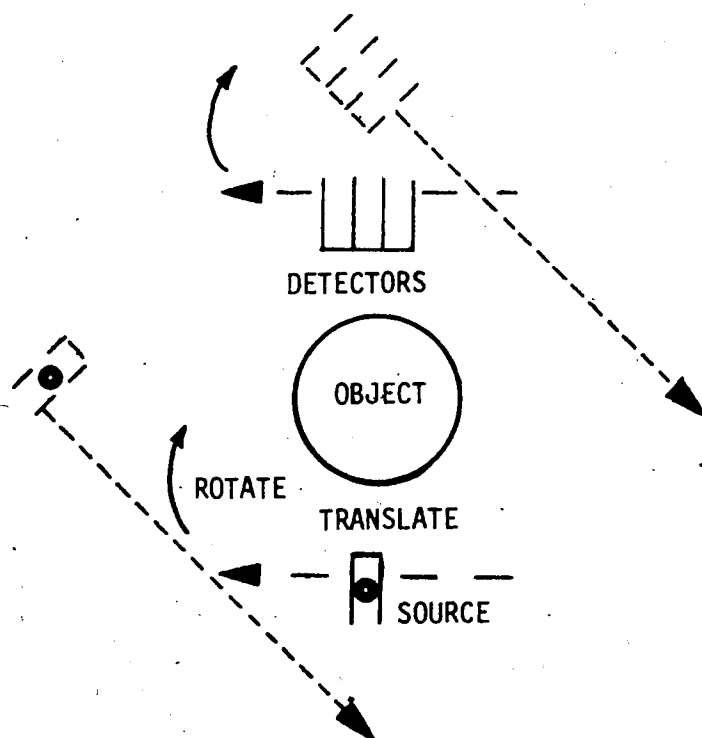


FIGURE 5. CT GENERATION 2

translating the source-detector configuration past the object at which point they are rotated about the object and the translation is repeated in the opposite direction. Measurements of ray-integrals or total radiological attenuation are continually measured during translation. This movement results in a "smoothing" or blurring of the object as the actual measured data is taken over a finite area of the object. Translations and rotations are repeated until the sum of the rotations meets or exceeds the 180 degrees required for complete reconstruction. Multiple detector systems are advantageous in that rotations between translations can be made through a larger angle and hence the number of translations and rotations can be decreased thus reducing scan time.

The third and fourth generation scanners (Figures 6 & 7) are multiple detector rotation-only systems. In the case of the third generation scanner the source and detectors each rotate about the same point through the required circle. In the fourth generation scanner the detectors form a stationary circle of 360 degrees and only the source is rotated. This eliminates the need to rotate the detectors and their associated high voltage and signal cables. The major advantage of the rotation only scanners versus the rotation-translation scanners is the reduction in scanning time. This reduction in scan time is important as it reduces image artifacts that can be caused by patient movement.

The fifth generation scanners (Figure 8) employ both

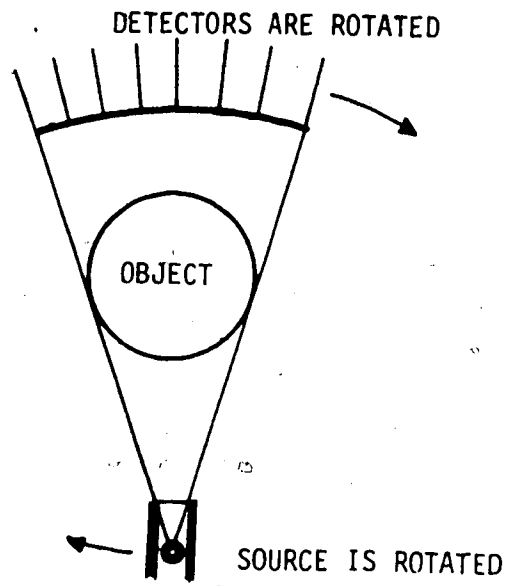


FIGURE 6. CT GENERATION 3

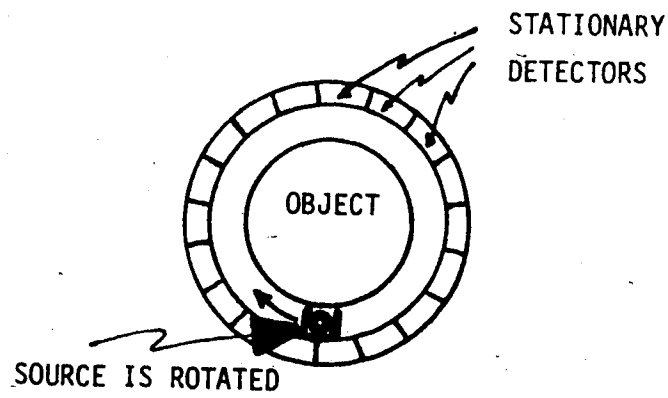


FIGURE 7. CT GENERATION 4

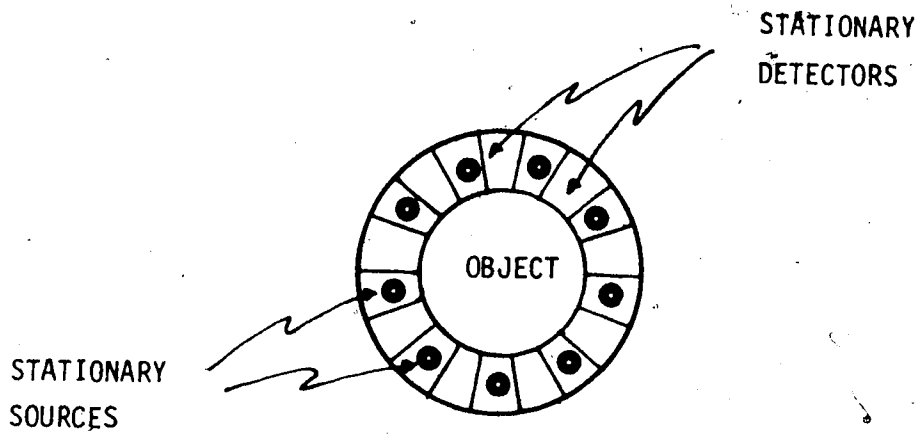


FIGURE 8. CT GENERATION 5

multiple sources and multiple detectors and may allow ultrafast scanning to produce dynamic representations of cardiac motion without special gating or synchronization techniques. Such scanners are a relatively new phenomenon and introduce additional problems in terms of expense and calibration.

Radiological attenuation along lines through the plane is often measured in a parallel beam format associated with the first two generations of scanners. This means that attenuations are measured along a series of regularly spaced parallel lines taken at a number of angular orientations (Figure 9). Each series of measurements taken at a given angular orientation is referred to collectively as a view or profile. In the cases of the third, fourth and fifth generation scanners data is collected in a rotational format (Figure 10). This data can be reordered and interpolated in order to create the parallel beam format thus permitting the same reconstruction algorithms to be used for all generations of scanners. However, special algorithms have been developed for the rotational format (31,32).

#### A. Back-Projections

The first technique (7) used for reconstruction involved a method now referred to as Back-Projection.<sup>2</sup> For

-----  
<sup>2</sup> Capitalization is used to distinguish between Back-Projection as a method of image reconstruction, and back-projection as a process.

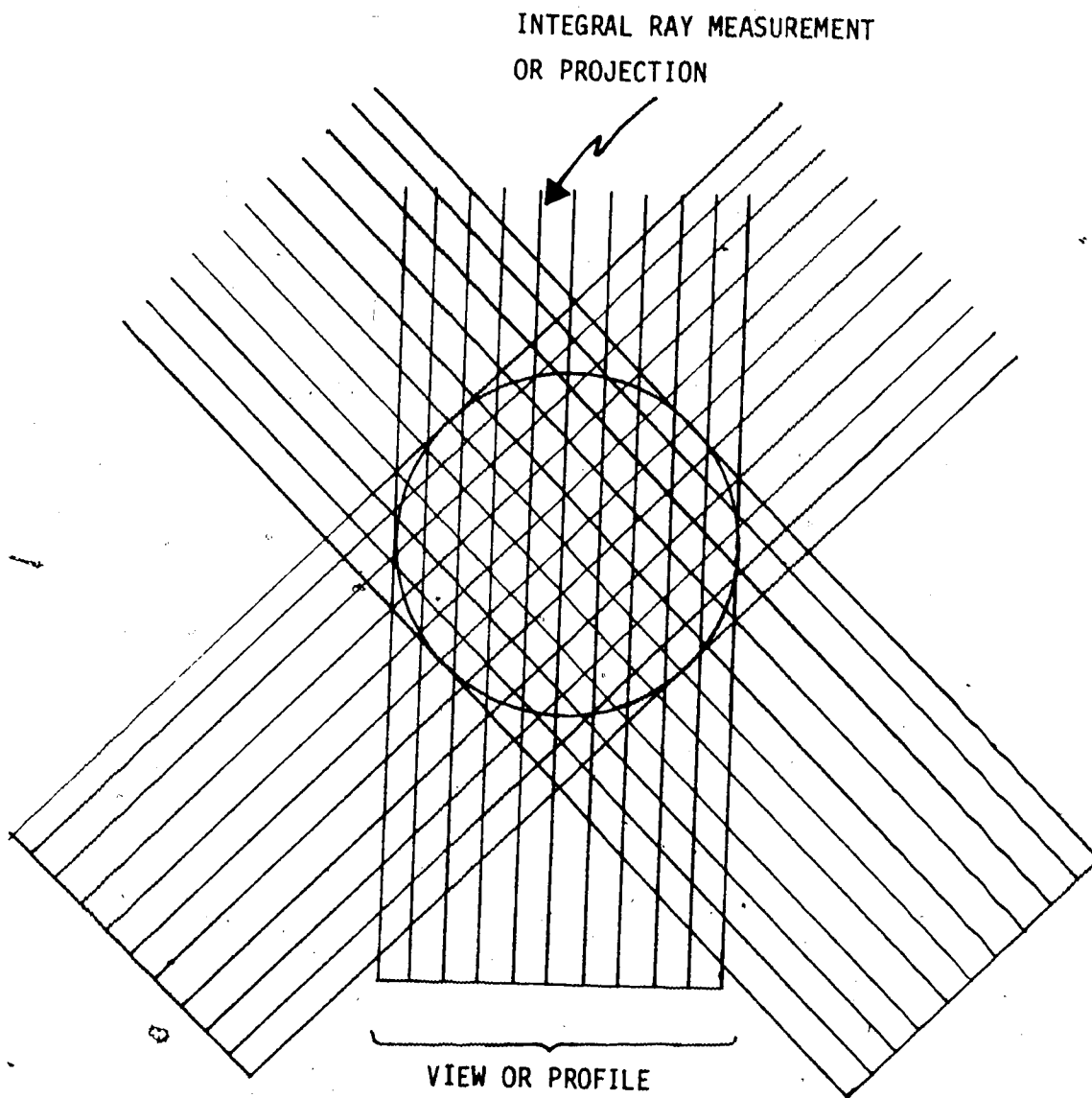


FIGURE 9. PARALLEL BEAM FORMAT

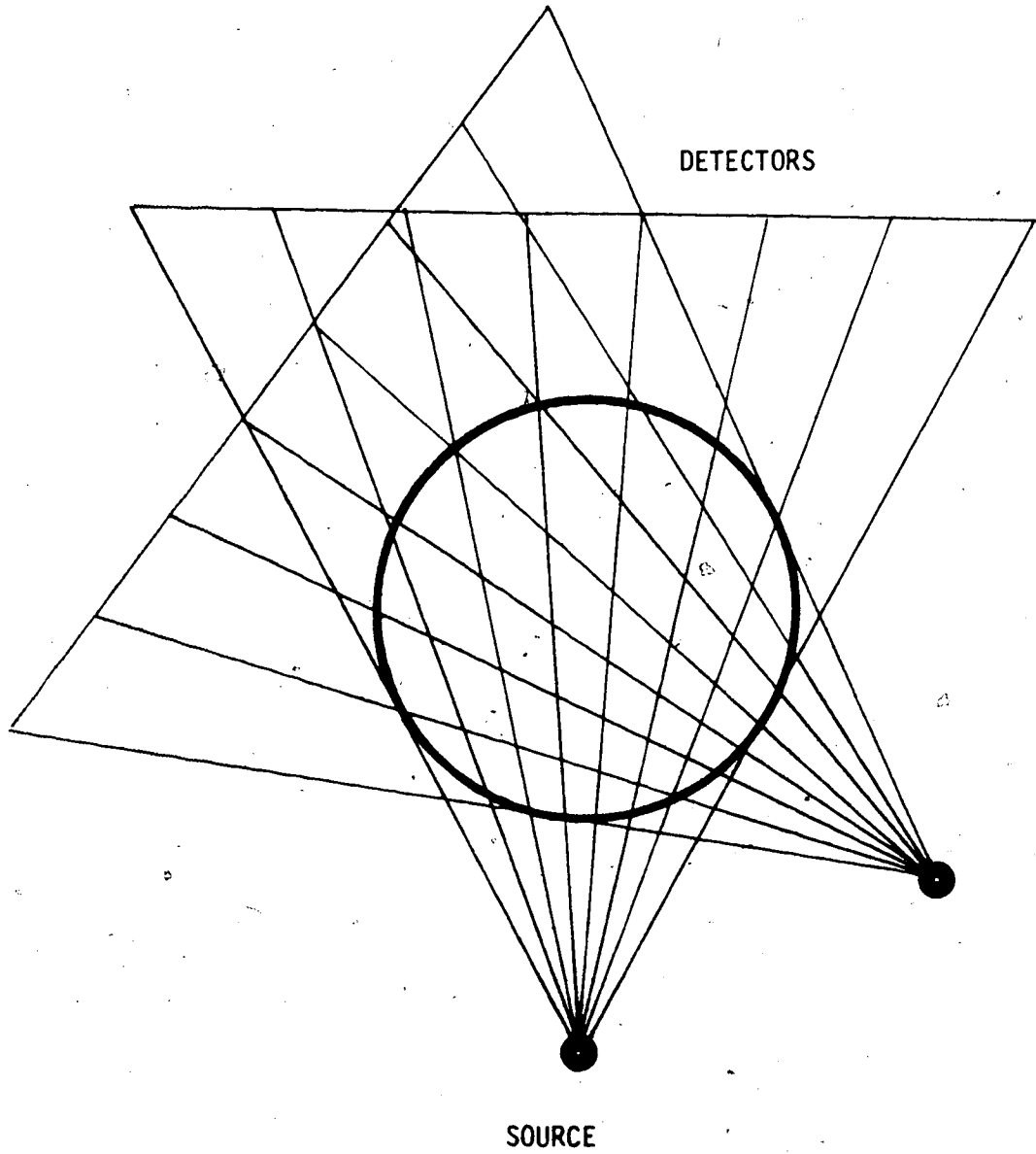
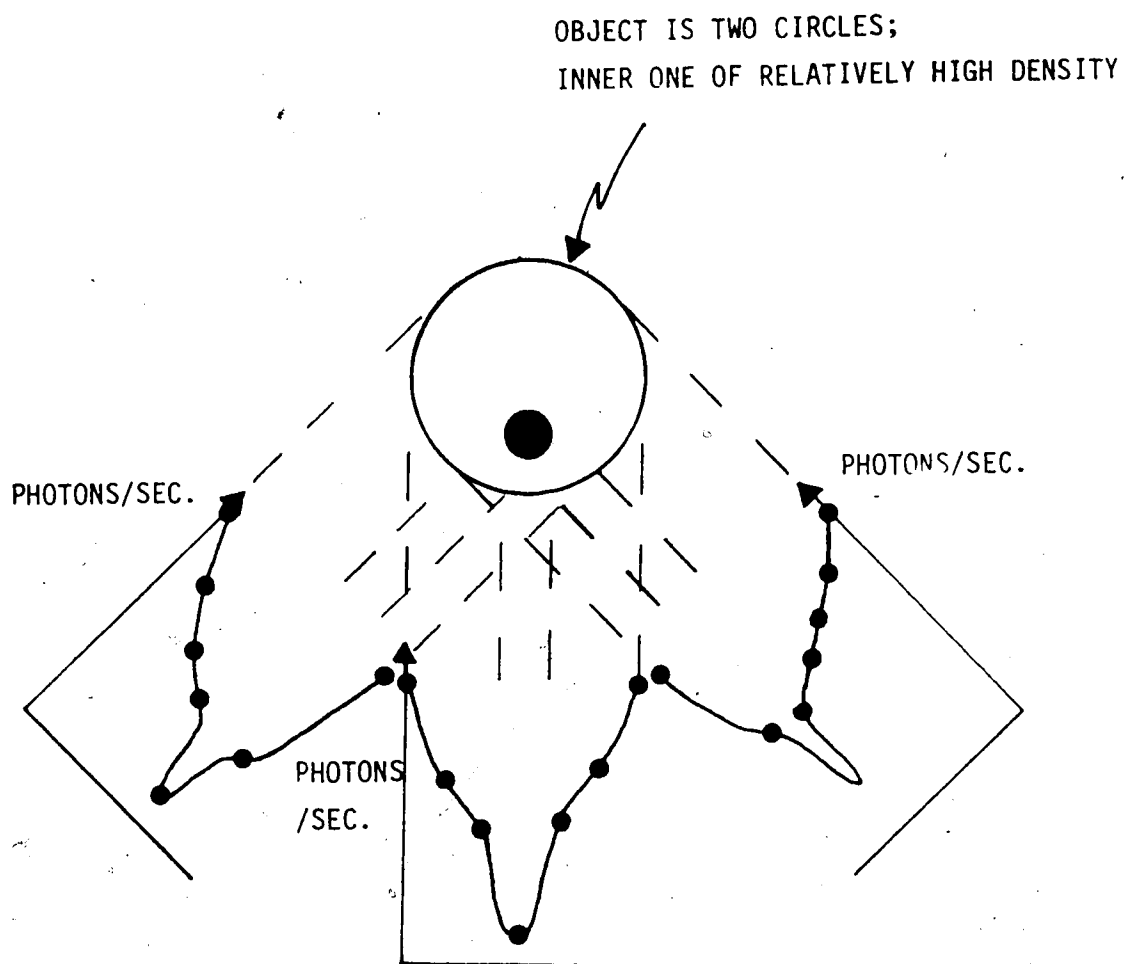


FIGURE 10. ROTATIONAL BEAM FORMAT



illustrative purposes three profiles or projections of an object have been taken (Figure 11) and are then back-projected to reconstruct the object in Figure 12. Each profile is made up of a discrete number of measurements taken at regularly spaced intervals. Reconstruction involves the back-projection of each profile onto a reconstruction matrix. This matrix reconstruction may be performed optically (for example on a screen), using analog electronics or digitally in a computer. The signal intensity according to a given ray sum is applied to all points that make up that ray and this is done for all projections giving an approximation to the original object. As seen in Figure 12 points outside of the original object may receive some of the back-projection intensity resulting in what is known as the "star" artifact. Points within the object also receive components from neighbouring points meaning that subtle differences in density cannot be determined. For these reasons Back-Projection is no longer being used as a technique for reconstruction. However, it does serve as a basis for understanding the reconstruction techniques presently being used.

The technique now used involves measurement of individual profiles and their respective angular orientations and the subsequent storage of this data in a computer. The data is then processed using mathematical algorithms and the reconstructed object is displayed on a plotter using different grey levels to represent the varying



PROFILES ARE MADE UP OF A DISCRETE NUMBER OF MEASUREMENTS

FIGURE 11. BACK-PROJECTION

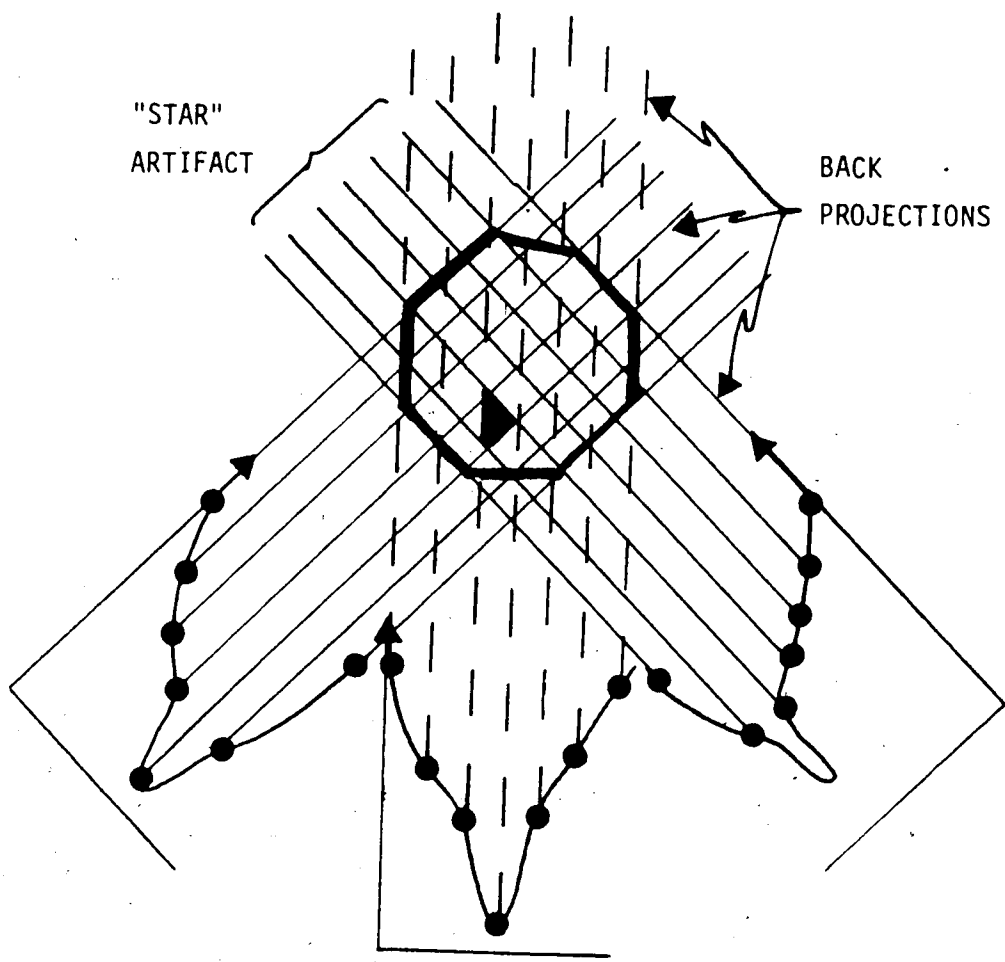


FIGURE 12. IMAGE RECONSTRUCTION USING BACK-PROJECTION

densities. Although the method depicted in Figures 11 and 12 merely sums the individual profiles, mathematical techniques allow for cancellation of back-projections and hence the object can be reconstructed more exactly.

## B. Reconstruction Algorithms

The two main classes of algorithms used for reconstruction are the iterative and analytical techniques.

### Iterative Technique

The iterative technique involves formulating an arbitrary image, calculating the profiles for that image and comparing these profiles to those obtained experimentally. The starting image is usually a blank screen (all ray profiles equal zero) or a circular grey object of uniform density (all ray profiles equal a constant). According to the differences in the measured profiles and those of the arbitrary image the image is modified and the profiles are compared again. This process is repeated until differences between the theoretical and experimental profiles are within acceptable limits. There are three general classes of the iterative technique (7). In the simultaneous correction technique each cell that contributes to a ray is altered and all projections are corrected simultaneously. This technique tends to overcorrect and hence iterations oscillate about the correct value. In the case of the ray-by-ray correction, corrections are made to all points of one ray at which point these corrections are taken into account prior to making

further corrections to a different ray. This technique is found to work best when large angles are taken between consecutive projections to be corrected. The third technique is a point-by-point correction in which each point is corrected for all rays that pass through it and all past changes are embodied into future changes.

In each of the three cases the corrective mechanism can be either additive or multiplicative. Additive, which is the method primarily used, refers to the fact that correction is divided among cells according to their weighting factor. In the multiplicative method, correction is applied to cells according to their present density. In this case a grey starting level is required. The iterative techniques can require a great number of iterations and computations and hence computing time may be a limiting factor.

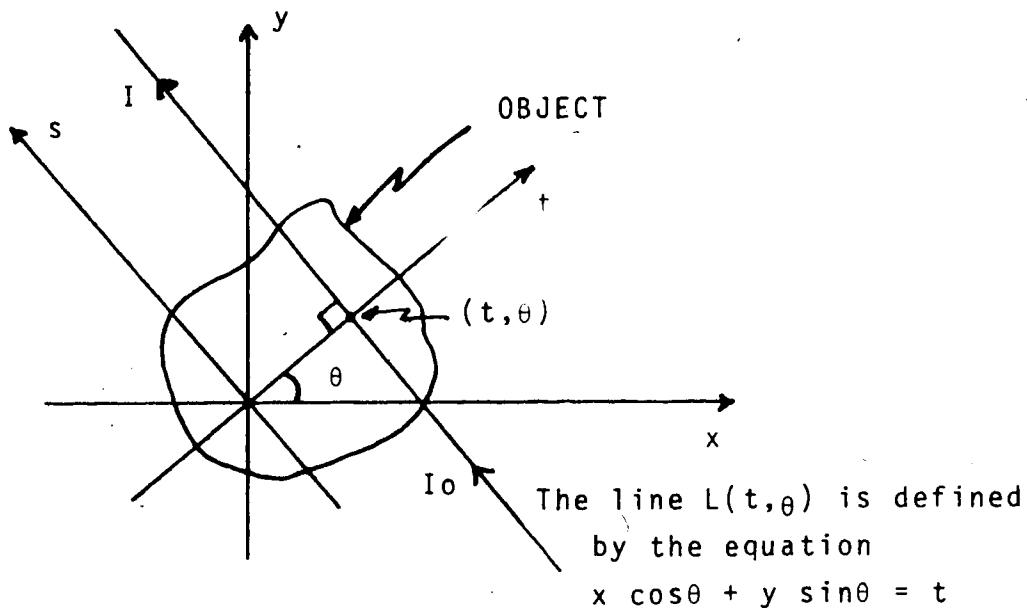
#### Analytical Technique

The Analytical Technique can be subdivided into two major categories: (1) two-dimensional Fourier reconstruction and (2) filtered Back-Projection. Two-dimensional Fourier reconstruction is based on the fact that the Fourier coefficients of the image are equal to the Fourier coefficients of the projections at the same angle. This means that if the Fourier coefficients of the projections are known then the Fourier coefficients of the image are also known and hence by taking their inverse transform the image of the object can be reconstructed. Until the introduction of the Fast Fourier Transform (FFT) and

improvements in high speed computers had taken place, this technique was not practical to use due to the number and complexity of the calculations involved. Mathematical development of this two-dimensional Fourier reconstruction technique is shown on the following pages.

Filtered Back-Projection or the convolution technique is based on this two-dimensional Fourier reconstruction. Papers by Shepp & Logan (33) and Ramachandran & Lakshminarayanan (34) have shown that this Fourier reconstruction may be viewed in the spatial domain as the sum of each ray-integral times a weighting function of the distance from the ray to the point of reconstruction. Thus reconstruction involves prefiltering each ray measurement by a weighting function and then back projecting these filtered ray measurements to reconstruct the object. This allows the image to be reconstructed as each ray measurement is taken rather than having to wait for all measurements to be completed. This method of reconstruction is accurate, simple and greatly reduces computation time over other available methods. The mathematical formulation of the convolution technique from Fourier reconstruction is also shown on the following pages.

ANALYTICAL RECONSTRUCTION TECHNIQUES



$I_0$  is the number of incident photons

$I$  is the number of photons after passing through the object along line  $L(t, \theta)$

In this diagram there are three different coordinate systems. The  $s$ - $t$  coordinates are obtained by rotation of the  $x$ - $y$  cartesian coordinate system while the  $\omega$ - $\theta$  polar coordinate system uses  $\omega$  as the radial component and the angle  $\theta$  as the angular measure.

A line  $L(t, \theta)$  (which is defined by the equation  $x \cos \theta + y \sin \theta = t$ ) is chosen so as to pass through the object. This line depicts a ray integral measurement as would be made during a CT scan. In the parallel beam format a number of parallel ray-integral measurements (profile) would be made along a line  $L(t, \theta)$  at which point

the angle  $\theta$  would be altered and another profile measured. It is due to this pattern of measurement that the s-t coordinate system has been introduced. The use of the polar coordinate system permits convolution algorithms to be used for reconstruction. This aspect will be discussed later in the paper.

First, some definitions:

- (1)  $f(x,y)$  is the linear attenuation coefficient at the point  $(x,y)$ ;
- (2)  $I_0$  is the number of incident photons; and
- (3)  $I$  is the number of photons after passing through the object along line  $L(t,\theta)$ .

The total attenuation of the ray along line  $L(t,\theta)$  is defined to be  $P(t,\theta)$  which is equal to

$$-\ln(I/I_0) = \int_L f(x,y) ds$$

where  $ds$  is an incremental length along  $L(t,\theta)$ .

The one-dimensional Fourier transform of  $P(t,\theta)$  is

$$P(\omega, \theta) = \int_{-\infty}^{\infty} \exp(-i\omega t) P(t, \theta) dt = \int_{-\infty}^{\infty} \int_{-\infty}^{\infty} f(x,y) \exp(-i\omega t) ds dt.$$

Now, consider the transform from the s-t coordinates to the x-y coordinates where

$$\begin{aligned} x &= t \cos\theta + s \sin\theta, & y &= t \sin\theta - s \cos\theta, \\ t &= x \cos\theta + y \sin\theta & \text{and } s &= x \sin\theta - y \cos\theta. \end{aligned}$$

The Jacobian which arises from the transformation is



$$\frac{\partial(s,t)}{\partial(x,y)} = \begin{vmatrix} \frac{\partial s}{\partial x} & \frac{\partial s}{\partial y} \\ \frac{\partial t}{\partial x} & \frac{\partial t}{\partial y} \end{vmatrix} = \begin{vmatrix} \sin\theta & -\cos\theta \\ \cos\theta & \sin\theta \end{vmatrix} = 1.$$

Hence  $dsdt$  which is equal to the magnitude of the Jacobian times  $dx dy$

$$= \left| \frac{\partial(s,t)}{\partial(x,y)} \right| (dx dy) = |1| dx dy = dx dy.$$

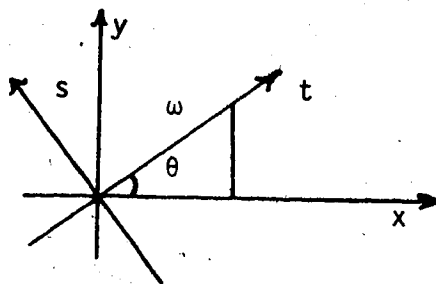
Therefore  $\hat{P}(\omega, \theta)$  may be written as

$$\hat{P}(\omega, \theta) = \iint_{-\infty}^{\infty} f(x,y) \exp(-i\omega (x \cos\theta + y \sin\theta)) dx dy$$

which coincidentally is also the two-dimensional Fourier transform of  $x$  and  $y$  (define as  $\hat{f}(\omega, \theta)$ ).

$$\text{i.e. } \hat{f}(\omega, \theta) = \iint_{-\infty}^{\infty} f(\bar{x}, \bar{y}) \exp(-i\omega (x \cos\theta + y \sin\theta)) dx dy$$

where  $\omega$  is the spatial frequency in the direction of the  $t$  axis.



Hence,  $\cos\theta = x/\omega$  and  $\sin\theta = y/\omega$ .

Now, if we consider the transformation from the  $x$ - $y$  cartesian coordinate system to the  $\omega$ - $\theta$  polar coordinate system the Jacobian arising from this transformation is

$$\frac{\partial(x,y)}{\partial(\omega,\theta)} = \begin{vmatrix} \frac{\partial x}{\partial \omega} & \frac{\partial x}{\partial \theta} \\ \frac{\partial y}{\partial \omega} & \frac{\partial y}{\partial \theta} \end{vmatrix} = \begin{vmatrix} \cos\theta & -\omega \sin\theta \\ \sin\theta & \omega \cos\theta \end{vmatrix} = \omega .$$

Hence,  $dx dy$  which is equal to  $\left| \frac{\partial(x,y)}{\partial(\omega,\theta)} \right| d\omega d\theta$   
 $= |\omega| d\omega d\theta$ .

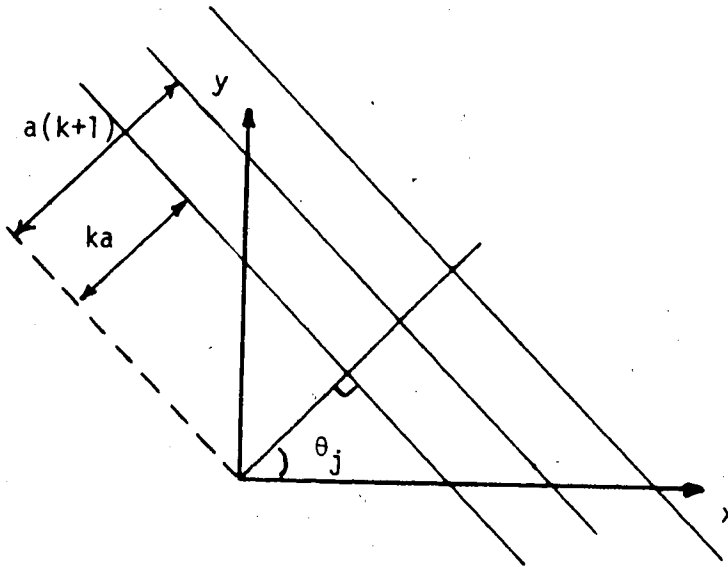
This means that  $f(x,y)$  may be written as

$$f(x,y) = \frac{1}{4\pi^2} \int_0^\pi d\theta \int_{-\infty}^{\infty} P(\omega,\theta) \exp(+i\omega (x \cos\theta + y \sin\theta)) |\omega| d\omega.$$

Thus,  $f(x,y)$  may be uniquely determined by a knowledge of  $P(t,\theta)$  for all lines  $L$ . In reality  $P(t,\theta)$  is known only along a finite number of lines which may be denoted by  $t = t_k = ka$ ,  $k = 0, \pm 1, \pm 2, \dots$  ;

$$j = \frac{j\pi}{n}, \quad j = 0, 1, 2, \dots$$

where  $a$  is the parallel spacing between projections and  $n$  is the number of views.



Rewriting the integrals as finite sums we get

$$\int_0^\pi d\theta \approx \sum_{j=0}^{n-1} \frac{\pi}{n} \quad \text{and} \quad \int_{-\infty}^{\infty} d\omega \approx \sum_{k=-\infty}^{k=\infty} a.$$

By bounding the object to a circle of diameter  $a$

$$\sum_{k=-\infty}^{k=\infty} \text{ can be rewritten as } \sum_{k=-1/a}^{k=1/a}$$

where there are  $2/a$  rays contained in each profile.

Hence,  $f(x,y)$  may be written as

$$f(x,y) = \frac{a}{4\pi n} \sum_{j=0}^{n-1} \sum_{k=-1/a}^{k=1/a} P(\omega, \theta) \exp(-i\omega(x \cos\theta + y \sin\theta)) |\omega|.$$

Consider the Fourier inversion formula

$$f(x,y) = \frac{1}{4\pi^2} \int_0^\pi d\theta \int_{-\infty}^{\infty} \hat{P}(\omega, \theta) \exp(i\omega(x \cos\theta + y \sin\theta)) |\omega| d\omega$$

Substituting in  $t = x \cos\theta + y \sin\theta$  the inner integral may be written as

$$Q(t, \theta) = \int_{-\infty}^{\infty} \hat{P}(\omega, \theta) |\omega| \exp(i\omega t) d\omega.$$

Now if  $f(x,y)$  is a smooth function, then  $P(t, \theta)$  will be a smooth function and hence  $\hat{P}(\omega, \theta)$  will be bandlimited.

i.e. for  $\omega > \Omega$   $\hat{P}(\omega, \theta) \rightarrow 0$ .

If there also exists an even function

$$\hat{\Psi}(\omega) = \int_{-\infty}^{\infty} \Psi(t) \exp(-i\omega t) d\omega$$

which equals  $|\omega|$  for  $\omega < \Omega$

then  $Q(t, \theta)$  can be approximated by

$$Q(t, \theta) \approx \int_{-\infty}^{\infty} \hat{\Psi}(\omega) \hat{P}(\omega, \theta) \exp(i\omega t) d\omega$$

which according to the Convolution theorem is a convolution in the time domain.

$$Q(t, \theta) = 2\pi \int_{-\infty}^{\infty} \Psi(\tau) P(t-\tau) d\tau$$

$$\text{Therefore, } f(x,y) = \frac{1}{2\pi} \int_0^\pi \theta \int_{-\infty}^{\infty} P(\tau, \theta) \Psi(t-\tau) d\tau$$

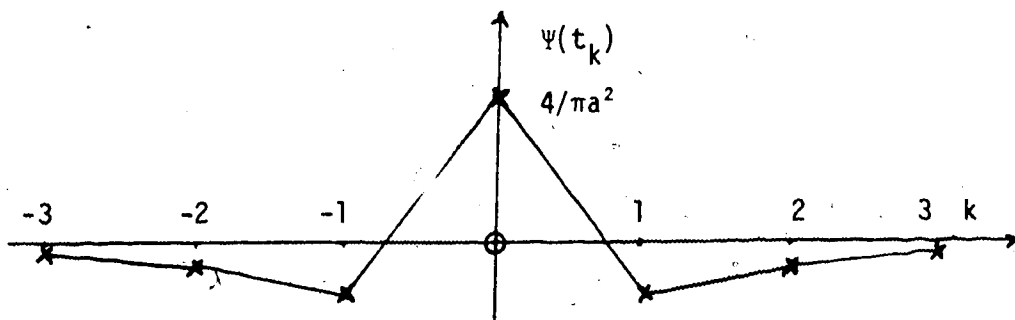
Once again writing the integrals as finite summations we get

$$f(x,y) = \frac{a}{2\pi} \sum_{j=0}^{n-1} \sum_{k=-1/a}^{1/a} P(t_k, \theta) \Psi(x \cos \theta_j + y \sin \theta_j - t_k)$$

Thus  $f(x,y)$  can be written as a summation of the ray integrals times a weighting function  $\Psi$  which is a function of the distance between the line  $L(t_k, \theta)$  and the point of reconstruction  $(x,y)$ . One commonly used weighting function (derived by Shepp and Logan) is

$$\Psi(t_0) = \frac{4}{\pi a^2} ; \Psi(t_k) = -4/(\pi a^2(4k^2-1)) , k = \pm 1, \pm 2, \dots$$

with linear interpolations in the intervals.



Allowing  $\Psi$  to be linear in the intervals is not incompatible with the requirement that for small  $\omega$ ,  $\hat{\Psi}(\omega) \approx |\omega|$  and greatly reduces computational time since the weighting function can be computed and stored and values at intermediate points can be obtained through interpolation.

The Shepp, Logan weighting function  $\Psi(t)$  has the Fourier transform

$$\hat{\Psi}(\omega) = \left| \frac{2}{a} \sin \frac{\omega a}{2} \right| \left( \frac{\sin(\omega a/2)}{\omega a/2} \right)^2$$

$$\text{When } \omega \rightarrow 0, \hat{\Psi}(\omega) \rightarrow \left| \frac{2}{a} \frac{\omega a}{2} \right| \left( \frac{\omega a/2}{\omega a/2} \right)^2 = |\omega| (1)^2 = |\omega|$$

and thus the necessary requirement is met.

### Comparison of Analytical and Iterative Algorithms

Both the iterative and analytical techniques have characteristic advantages and disadvantages. It is generally accepted (7) that analytical methods are faster than are iterative. Use of the convolution technique also allows the image to be reconstructed as measurements are made. In both cases there are problems associated with reconstruction. Due to the digitization involved in analytical methods the projections must be bandlimited. This means that an overshoot phenomenon will occur at sharp edges such as bone-flesh interfaces. Although this effect can be partially corrected by prefiltering, any such gains will be offset by a loss in spatial resolution. Iterative techniques are able to avoid the problems associated with sharp interfaces.

With complete data the two types of algorithms are comparable with respect to the amount of noise in the image. However, in cases where some of the data is missing, the iterative technique will prove to be superior since it merely "smooths" the image while the analytical techniques assume the missing data is the same as the available data.

#### C. Photon Attenuation

The ability of CT to distinguish between narrowly differing densities is dependent on the characteristics of photon attenuation. As photon radiation passes through an absorbing medium it is absorbed exponentially according to the following relationship (35,36);

$$I(S) = I_0 \exp -(\mu(S-S_0))$$

where  $I_0$  is the number of photons at a distance  $S=S_0$  and  $\mu$  is the linear attenuation coefficient. This absorption is due to four processes: the photoelectric process, the Compton process, coherent scattering and pair production. The linear attenuation coefficient ( $\mu$ ) has units of inverse distance and is a measure of the fraction of photons removed per unit length of absorber.  $\mu$  may be converted to either the mass, electronic or atomic attenuation coefficients by dividing by either mass density  $\rho$  ( $\text{gm/cm}^3$ ), electron density  $\rho_e$  ( $\text{electrons/cm}^3$ ) or atomic density  $\rho_a$  ( $\text{atoms/cm}^3$ ). At moderate energies (less than 1.02 Mev) photon attenuation predominantly consists of two contributions: (1) Compton scattering, which is proportional to electron density and (2) photoelectric absorption which is a function of the atomic number of the element (approximately  $Z^4$ ). At the lower edge of the energy spectrum it is the photoelectric effect which is predominant and as such, measured attenuation is representative of the atomic numbers of the elements contained in the object. If either simultaneous or sequential scans at different energies (37) were used it would be possible to obtain measures of both the Compton and photoelectric effects allowing for evaluation of both electron density and atomic number. Hence an in vivo elemental identification is possible using CT (38).

#### Statistical Considerations

Radioactive decay is a statistical process that can be

modelled by a Poisson distribution (39-43). The characteristic of a Poisson process is that the mean and variance are equal. This means that the coefficient of variation (which is equal to the standard deviation divided by the mean) is equal to  $1/\sqrt{\text{mean}}$ . One implication of this is that the higher the associated count rate the lower the coefficient of variation will be. For example; a count rate of 10,000 has an associated coefficient of variation of  $1/\sqrt{10,000} = 1\%$ .

Thus the lower the radioactivity of the source the longer the required counting period in order to maintain the same coefficient of variation. In order that the statistics be maintained and further blurring of the image does not occur (due to measurement over a finite area) the scanner would have to translate more slowly and hence the overall time of the scan would be increased. If the scan takes too long, artifacts due to patient movement become a problem.

#### Dead Time

Radiation detectors and the associated electronics have finite resolving times. After a system records a pulse it is unable to respond to another pulse for a brief period, known as the dead time. As a result the number of pulses recorded by the counting system is less than the actual number of pulses that occurred. This means that the measured statistics of the process have been altered due to the measurement equipment.

In order to rectify this situation it is necessary to



measure the dead time of the system and to use this measurement to correct the measured pulse count. For most applications system dead time is independent of the count rate. Hence, once system dead time has been established, corrections can be made for any count rate.

System dead time ( $p$ ) is determined by measuring (in order):

1. the background count rate ( $B$ ),
2. the count rate resulting from one source ( $n_A$ ),
3. the count rate resulting from two sources (sources A & B) ( $n_S$ ), and
4. the count rate resulting from source B ( $n_B$ ).

If this order of measurement is followed any errors due to accurate repositioning of sources will be eliminated. If the true count rate is  $N$  and  $np < 0.05$  then the following expression is valid (44) ;

$$N = n(1+np)$$

In the cases of the above measurements this results in the following three expressions;

$$N_A + B = n_A(1+n_A p)$$

$$N_B + B = n_B(1+n_B p)$$

$$N_A + N_B + B = n_S(1+n_S p)$$

Adding the first two equations together and subtracting the third equation from the result leads to the following expression (solving for  $p$ );

$$p = (n_A + n_B - n_S - B) / (n_S^2 - n_A^2 - n_B^2).$$

Thus for a measured count rate, ( $n$ ) the fraction of lost

counts is  $n(p)$  and hence  $n(n)(p)$  counts must be added to  $n$  to give the true number of counts  $N$ . This correction is easily performed by a computer.

### Beam Hardening

Absorption of radiation is dependent on the energy of the radiation. As a polyenergetic beam passes through an object the lower energy beams are more severely attenuated than are the higher energy beams. This results in the beam being "hardened" as it is composed of a greater proportion of high energy beams the farther along it is in the object (45-48). Thus in order to determine absolute densities of an object the beam must be either monoenergetic or else non-linear corrections must be applied. Correction for beam hardening may be either material selective or non-material selective. Material selective correction takes into account the type of absorption material and the resultant hardening. This requires knowledge of the types of absorption materials present and the quantities involved and hence an initial reconstruction must first be made. Then the raw data must be manipulated according to the first reconstruction to produce the corrected image. Non-material selective beam hardening merely recognizes that beam hardening has occurred and uses a beam hardening curve to correct the raw data before reconstruction.

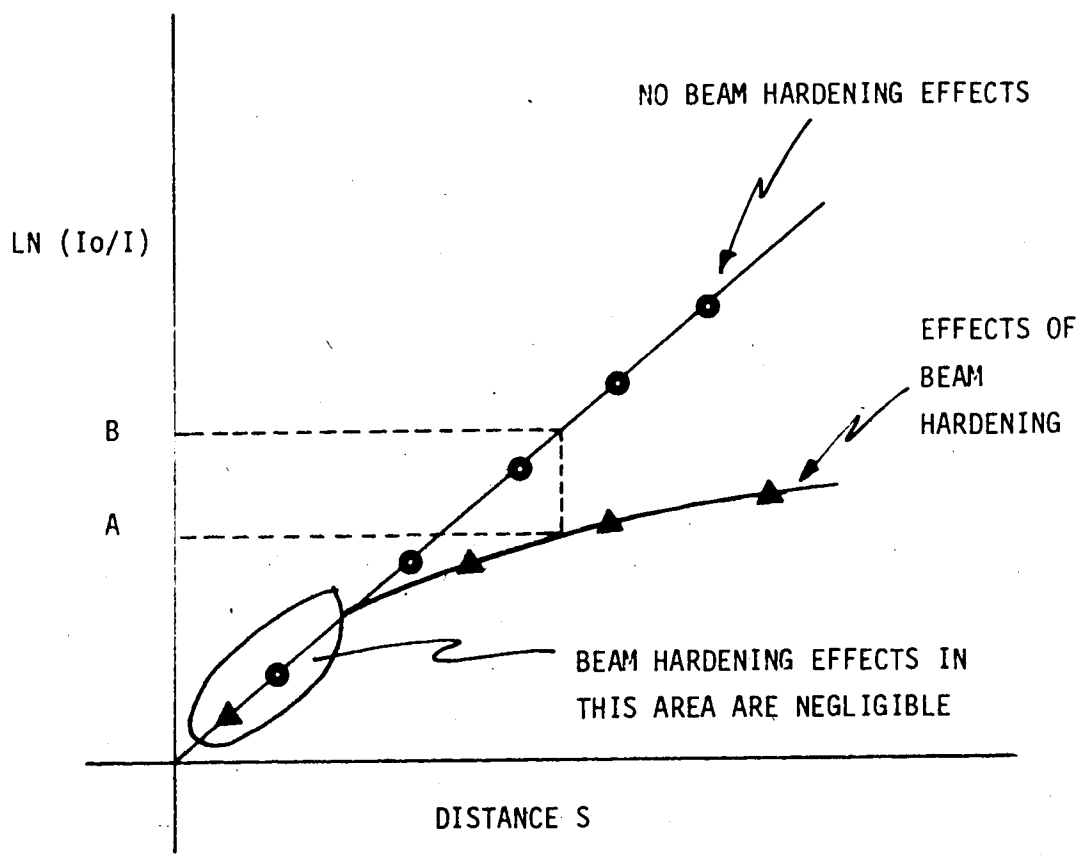
If one measures the amount of beam hardening as a function of distance then these curves may be used to correct raw data. For example, if a measurement of  $\ln(I_0/I)$

= A (Figure 13) is made, the corrected value B, which is the value that would be obtained if there was no beam hardening, is easily obtained from the curve. This procedure can easily be performed for all ray-integral measurements prior to reconstruction. It is interesting to note that the correction required for measurements of relatively low values of  $\ln(I_0/I)$  is small and hence inaccurate corrections for measurements such as through skin (as contrasted to bone) introduces negligible error. Non-material selective correction techniques for beam hardening are obviously not as accurate as are selective techniques however for objects consisting predominantly of one or two absorption materials it does provide a quick and simple correction technique.

#### D. Detector Types

Primary considerations in regards to selection of a detector include resolution, efficiency, energy of radiation, counting rates, and in some applications, size. Energy resolution of a detector is its ability to distinguish between different energy photons. This is often defined as a percentage or ratio of the full width half maximum divided by the primary energy level. Detector efficiency refers to the percentage of rays at a specified energy that will interact with the detector rather than being simply passed through the detector.

Three common detector types are gas, scintillation and



GIVEN A LINEAR ATTENUATION COEFFICIENT  $\mu$   
 $\text{LN}(I_0/I) = \mu \times S$  OR  $I = I_0 \text{ EXP}(-\mu \times S)$

FIGURE 13. BEAM HARDENING CORRECTION

solid state, all of which work on the principle of photons exciting the detector material resulting in the production of ions, optical radiation and electrons respectively. These phenomena are then converted to electronic signals, the magnitude of which are proportional to the photon energy, and the frequency of which are proportional to the number of photons per second striking the detector.

Solid state detectors have better resolution than do the other two types. They are also much more expensive and hence are only used in applications where resolution is critical.

Gas detectors although usually having worse resolution and efficiency than scintillation detectors do have the advantage of generally being more economical and smaller in size. It is for this reason that most fan-beam machines use xenon gas detectors (7) instead of scintillation detectors. Scintillation detectors however are economical, readily available and are easy to use. These factors coupled with reasonable resolution, efficiency, and counting rates have led to the utilization of scintillation detectors for many spectroscopic applications.

#### Scintillation Detector

A scintillation detector is composed of two basic parts : (1) a scintillation crystal and (2) a photomultiplier tube.

##### Scintillation Crystal

The scintillation crystal is a transducer that

converts photons of energy to light pulses of proportional intensity to the energy of the photon. There are both in-organic and organic materials in use for this purpose. Sodium Iodide crystals NaI(Tl) are the most commonly employed crystals for gamma-ray spectroscopy. It is desirable to have a high ratio of counts under the full energy peak relative to the total number of counts and this ratio is approximately four times greater for Sodium Iodide than for example Cesium Iodide crystals CsI(Tl), with the same gamma-ray primary energy. This ratio is also increased by the use of collimators which restrict radiation to the central part of the crystal. Use of a Thallium impurity (0.1 %) acts as a wavelength shifter causing the crystal to emit 2 or more low energy photons (visible light) instead of a single Ultra Violet photon. UV photons are not suitable since they are absorbed by most materials even those transparent to visible light. At low energies, typical resolution for NaI crystals ranges from 6-8 % for crystals under 5 cm diameter to 8-10 % for crystals from 5-10 cm diameter. Thicker crystals provide more efficient light collection and increase crystal efficiency so that the same crystal may be used with higher energy sources. If the crystal is too thin high energy rays may not interact with crystal.

#### Photomultiplier Tube

A photoemissive cathode detects the light pulses

produced by the crystal and in response produces primary electrons. These electrons are electrostatically focused and accelerated by means of a voltage differential to the first dynode in the tube. Upon arrival at the dynode they possess enough energy so that for every primary electron more than one secondary electron is produced. This procedure is continued throughout an arrangement of dynodes (typically 10) until the final stage which is the anode. The voltage at the anode following the passage of a charged particle through the phosphor of the crystal is equal to the charge of the electrons at the anode divided by the capacitance of the anode and is proportional to the intensity of the light impulse over a wide range of photomultiplier gain. Head on type PMT's have a semitransparent photocathode which is in contact with the inside of the glass window. Head-on versus side-on photomultiplier tubes are generally used for scintillation counting due to improved uniformity and collection efficiency.

#### Anode Load

The signal on the anode has a rise time which corresponds to the fluorescence decay time of the crystal. This signal decays through the anode load  $R_L$  (Figure 14) which is the resistor between the anode and the high voltage supply and the parallel combination of the anode to ground capacitance (typically 10 pf) and the output line capacitance to ground (typically 10 pf).

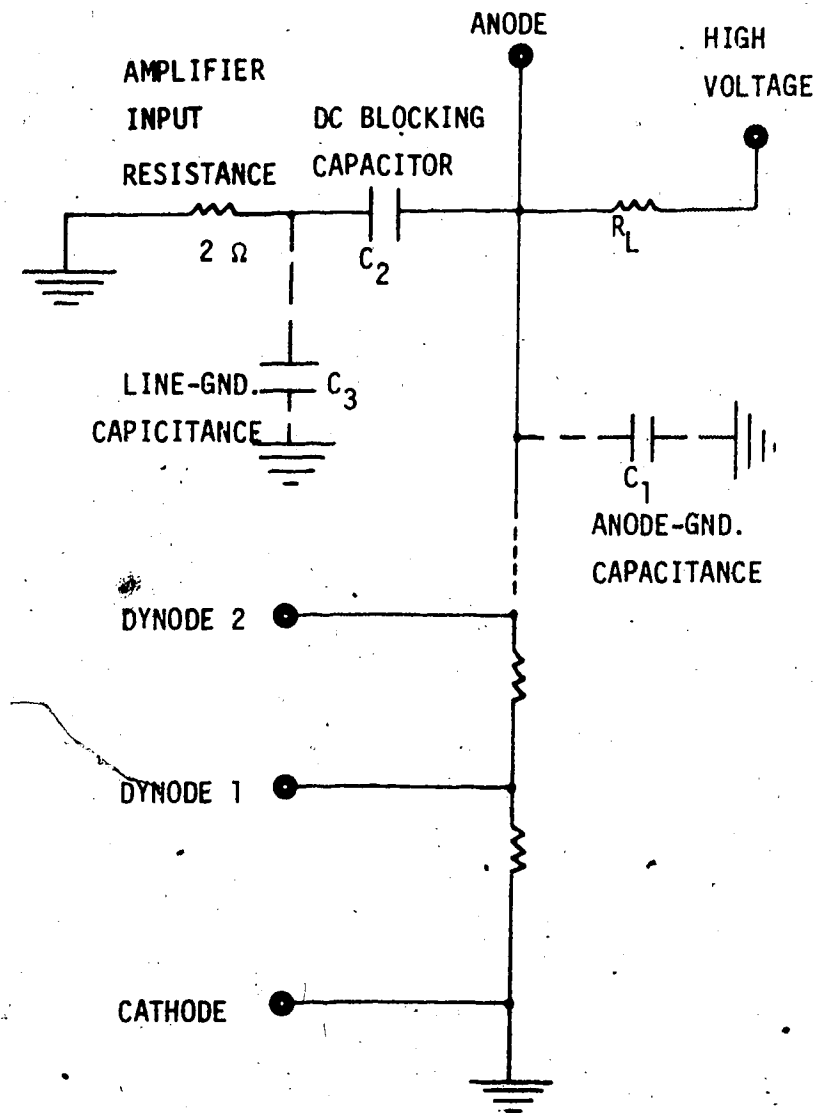


FIGURE 14. PHOTOMULTIPLIER TUBE & RELATED CIRCUITRY



The capacitances are virtually fixed values and are not easily changed and it is only the anode load that is easily altered. The signal on the anode must decay away fast enough so that pulse pileup is not a problem and slow enough so that pulse height is significantly larger than existing noise. Pulse pileup occurs when signals do not have enough time to decay away and the next signal is superimposed on the partially decayed signal.

#### E. Performance Characteristics Of CT Scanners

Prior to this point it has been the component parts of a CT system that have been reviewed. This section examines how some attributes of the overall system are related to these distinct segments.

Resolution of a CT system comprises two distinct, although interrelated types of resolution: spatial resolution and contrast resolution. Spatial resolution of a CT system refers to the minimum size object that can be imaged by the system when that object is part of a periodic structure. Contrast resolution is that percent change in contrast at an interface that can still be imaged given a minimum spatial resolution.

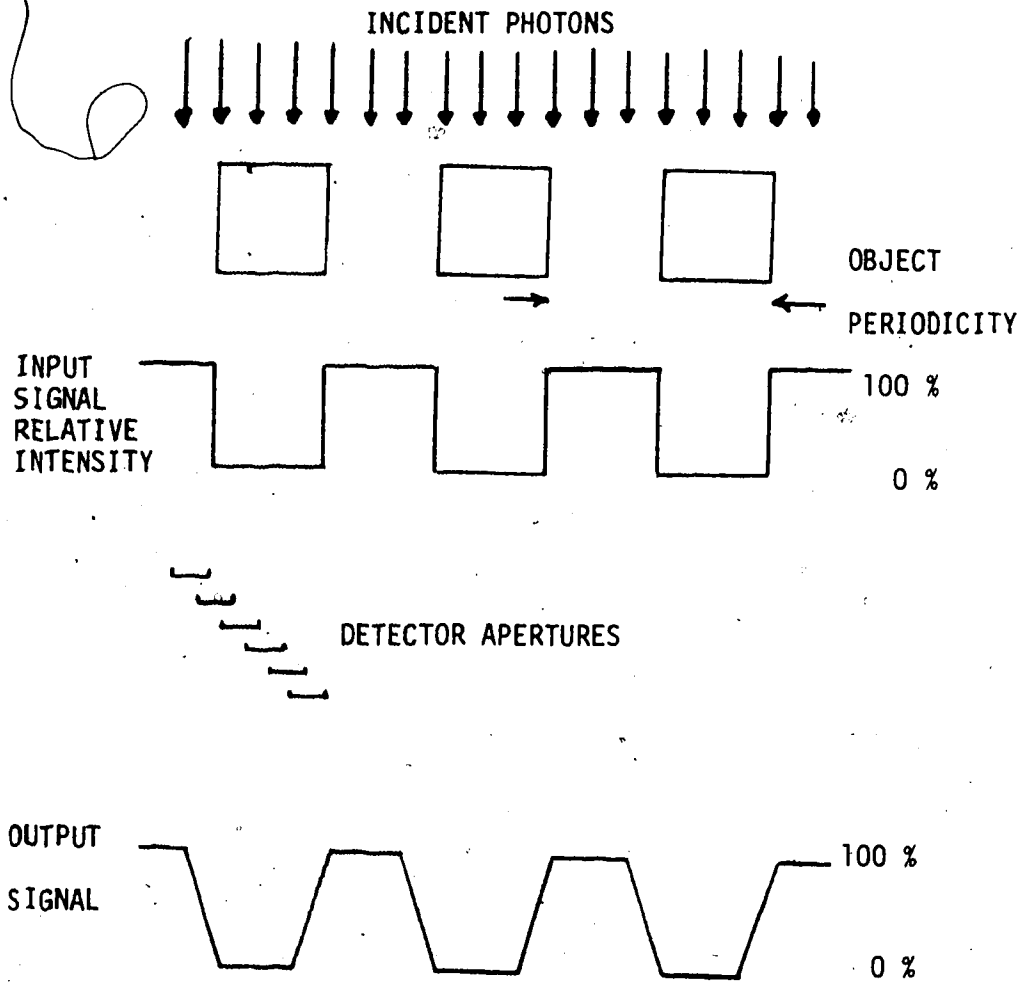
#### Spatial Resolution

Assuming a constant photon flux there are four major factors which affect the spatial resolution of a CT system (49). These are the width of the detector element aperture, the distance between reading or sampling points, the form of

the convolution filter used, and the element size of the display picture (pixel size). In order to examine the spatial resolution of a system it is useful to employ a concept known as the Modulation Transfer Function (MTF). Values of MTF vary from 0 to 1 and are an indication of how well the imaging system transfers the frequency components of the original to the final image. An MTF value of 1 (or 0) means that (all or none) of the frequencies present in the original exist in the final image. Good spatial resolution, then, would be indicated by large values of the MTF extending into the high frequency range.

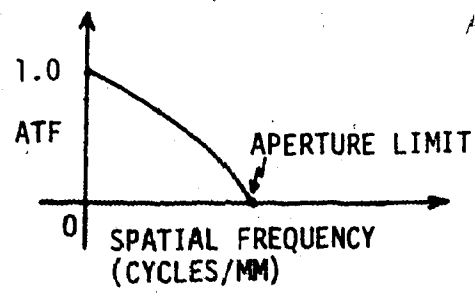
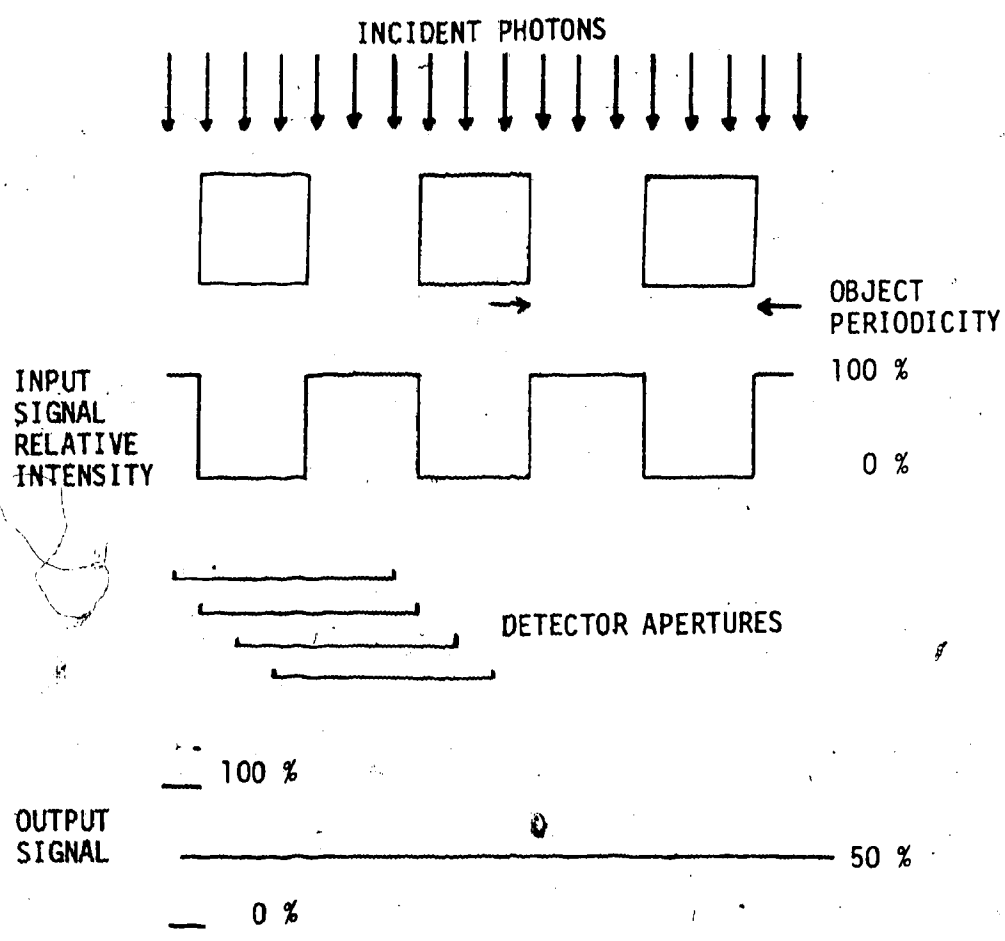
#### Aperture Size

The effect of aperture size can be seen by examining the results obtained by viewing a series of repeating objects through different size apertures while holding all other variables constant. From Figure 15 we see that when the size of the aperture is much smaller than that of the object spacing, the amplitude of the output signal approaches that of the input signal. Thus the aperture limited MTF or the ATF would approach unity. As can be seen from Figure 16, if the aperture size is increased, the amplitude of the output signal becomes smaller than that of the input signal and the value of the ATF is decreased. When the size of the apertures approach twice that of the object periodicity, all information is lost and the ATF approaches zero. The net effect is: the smaller the aperture, given other



WHEN THE OBJECT SPACING IS MUCH GREATER THAN THE DETECTOR APERTURE THE OUTPUT SIGNAL CLOSELY RESEMBLES THAT OF THE INPUT SIGNAL AND THE ATF APPROACHES 1.

FIGURE 15.



WHEN THE OBJECT SPACING IS EQUAL TO THE DETECTOR APERTURE  
THE OUTPUT SIGNAL CONTAINS NO INFORMATION AND THE ATF IS 0.

FIGURE 16.

5

parameters constant, the greater the spatial resolution of the system.

#### Sampling Rate

According to the Nyquist theorem, in order to accurately reconstruct an object that is part of a periodic structure, the sampling rate must be at least twice that of the highest frequency component in the structure. The tradeoff associated with sampling at high frequencies is a resultant increase in the noise of the reconstructed image (33). If the image contains frequencies greater than the Nyquist frequency, aliasing will occur resulting in streaks in the image emanating from such sources as bone edges which contain a number of high frequency components.

#### Convolution Filter

It has been found (49) that the higher the frequency response of the convolution filter used in the reconstruction, the greater the resultant spatial resolution. The problem is that the higher the frequency response of the filter, the greater the resultant noise of the reconstructed image and hence a tradeoff is required.

#### Contrast Resolution

Another area of importance to CT scanners is their contrast resolution. This is measured by examining the system limiting spatial resolution with different contrast media. The limiting factor of CT systems in regards to

contrast resolution is the presence of noise. The signal to noise ratio can be improved by increasing the incident photon fluence rate (reflux). However, increasing radioactivity will result in a corresponding increase in patient dosage. One measure of contrast resolution used for commercial scanners (49) is obtained by multiplying the hole diameter (in mm) by the contrast (in percent) and the square root of the dose (in rads). Inclusion of the dose in this calculation results in a measure of contrast resolution independent of dose rate.

#### F. Commercial CT Scanners

As mentioned previously it is necessary to make alterations to commercial CT scanners before they can be effectively used for measurement of bone mineral density. Having examined some of the theoretical concepts of CT scanning an examination of the differences between a commercial CT scanner and one designed for measurement of bone mineral density will now be given.

Commercial whole body CT scanners are both large and expensive: typically \$600,000 - \$1,000,000 and the source of radiation is virtually always an X-ray tube. These scanners are oriented towards measurement of soft tissues such as the abdomen. In these areas the application of the scanner is generally to locate tumors which will be depicted as an area of density different from that of the surrounding region. Absolute densities are generally not of concern so much as

the ability to distinguish between areas of different densities. Commercial CT scanners are typically fourth generation scanners allowing scans to be performed in under five seconds. Increased speed reduces the problem of movement artifacts, and means less inconvenience to the patient.

In transmission CT the source of radiation may be either an X-ray tube or a radioisotope. An X-ray tube is advantageous over a radioisotope due to a greater photon flux. They do however have the disadvantages of a high initial cost (\$30,000), large physical size and the requirement of a large amount of calibration and adjustment. There is also the possibility of a higher dose rate of radiation with an X-ray tube source.

There are also many problems that actually preclude the use of commercial CT scanners for measurement of bone density. The major problem is manifest in the area of system spatial resolution. Use of a multi-energy X-ray source means that beam hardening may be a major problem and the fact that such scanners are looking at relative rather than absolute density means that the data required for beam hardening correction is often not readily available. This is further complicated by the fact that the detectors used in commercial CT scanners are not operated in a pulse counting mode and hence they cannot provide energy discrimination of detected photons. Sources and detectors are usually not finely enough collimated to provide the initial physical

resolution and the size of the reconstruction matrix usually means that the area associated with an object the size of a bone is too small for an accurate determination of average density of the area. This is due to the fact that the reconstruction matrix of such a system is typically required to cover an area the size of an abdominal cross-section.

Commercial CT scanners could be used for the measurement of bone mineral density. However, they would first require recollimation of the source and detectors and software would have to be altered to correct for beam hardening and to increase the matrix size of the area of analysis. These changes would require a significant disruption of an expensive piece of equipment: a disruption not presently justified given the alternative use of a smaller, radioisotope CT scanner.



#### IV. System Design and Construction

This section will cover five areas of design and construction of the scanner. These include: (1) mechanical operation, (2) radioactive source and detectors, (3) scanner control, (4) adjustments required for a multi-detector system, and (5) data processing. The initial system design and construction were for a generation one CT system. Subsequent to the successful completion of the generation one system the necessary modifications to convert to a generation two system were undertaken.

##### A. Mechanical Operations

The major design requirement insofar as mechanical operation of this device is concerned, is the ability to properly position the source-detector configuration in both the longitudinal and rotational axes.

##### Stand

The stand (Figure 17) was designed to contain the controls such as the microprocessor unit, the power supplies, relays, source and detectors on one portable unit. The ability to position the scanner at different heights was required so as to facilitate measurement of both arms and legs. This was accomplished by mounting the scanner plates on a board with a 12 inch diameter hole cut in the center which slides vertically on ball bushings and is driven by a hand operated ball screw.

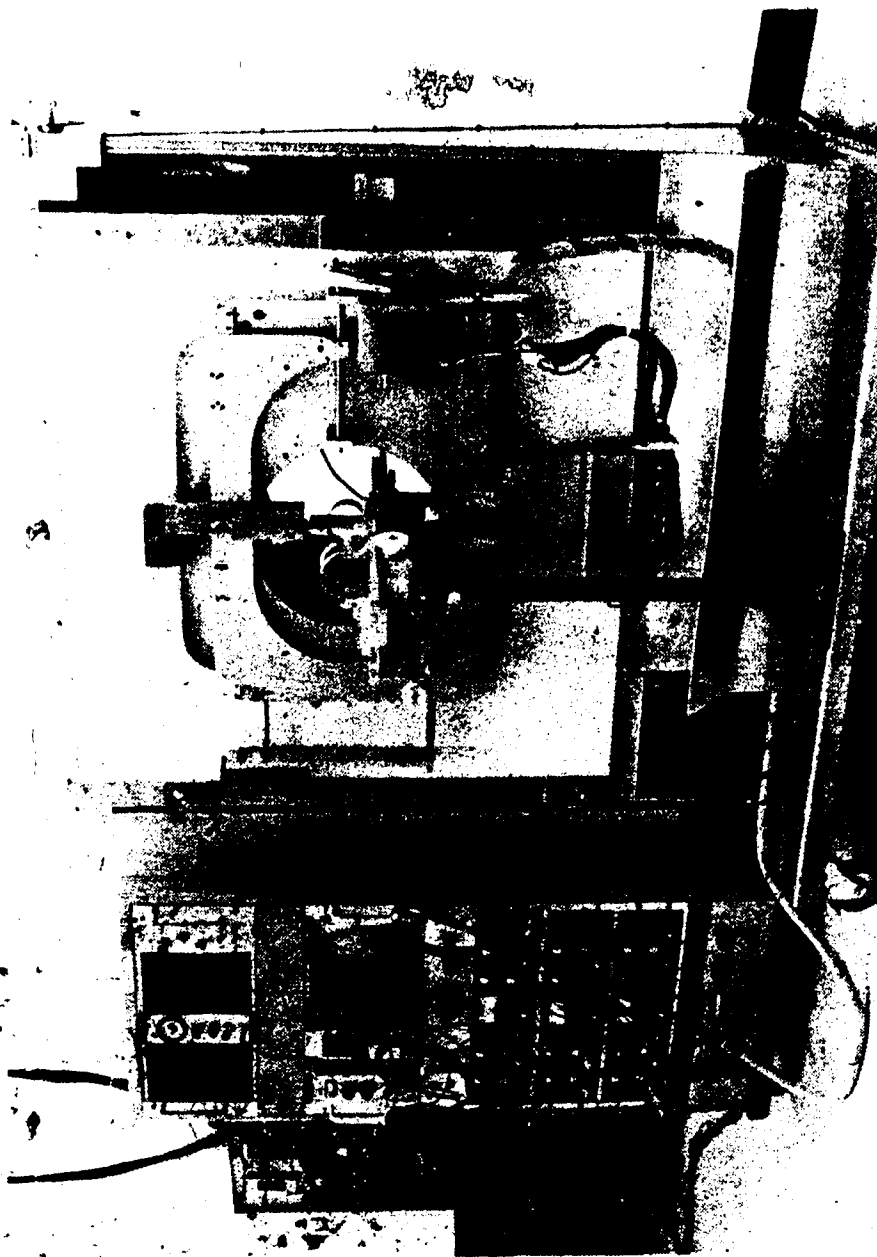


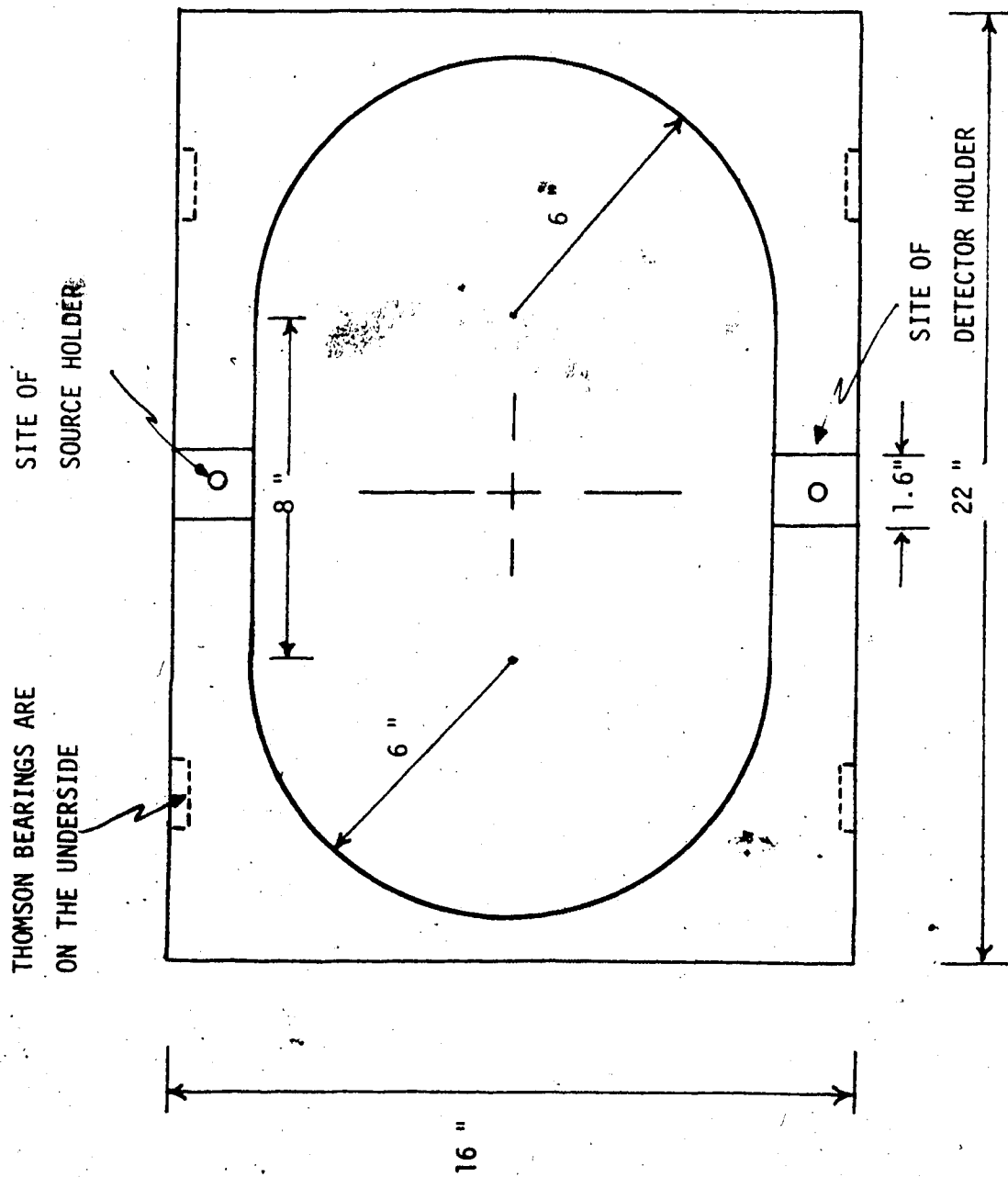
FIGURE 17. CT SYSTEM

### Source-Detector Alignment and Motion

The source and detectors are mounted on the top and bottom edge of one side of a 1/2 inch thick aluminum plate with an elongated 12 inch circular hole cut in the center (Figure 18). The geometry of the source with respect to the detectors is fixed. This first plate is mounted upon a second plate (Figure 19) of 1/2 inch thick aluminum with a 12 inch diameter circular hole cut into it. The top plate is attached to the second plate by means of Thomson bearings mounted on the first plate being guided along case hardened steel rails fastened to the second plate. This arrangement allows the first plate (and hence the source-detector arrangement) to translate linearly with respect to the second plate. The second plate is mounted onto a third plate (Figure 20) which contains a circular bearing with an external gear drive which is used to rotate the source-detector arrangement about the object. These plates and the rotational bearing are mounted onto the stand's board.

### Mechanical Drives

The drive for the translation is a stepping motor mounted on the second plate. This motor is used to drive a belt connected precision ball screw arrangement which is attached to the first plate. Each revolution of the ball screw results in a 2.5 mm motion of the plate. Since, in the half-step mode, the motor makes one revolution every 400 steps the resolution of one step is 2.5 mm/400 steps or



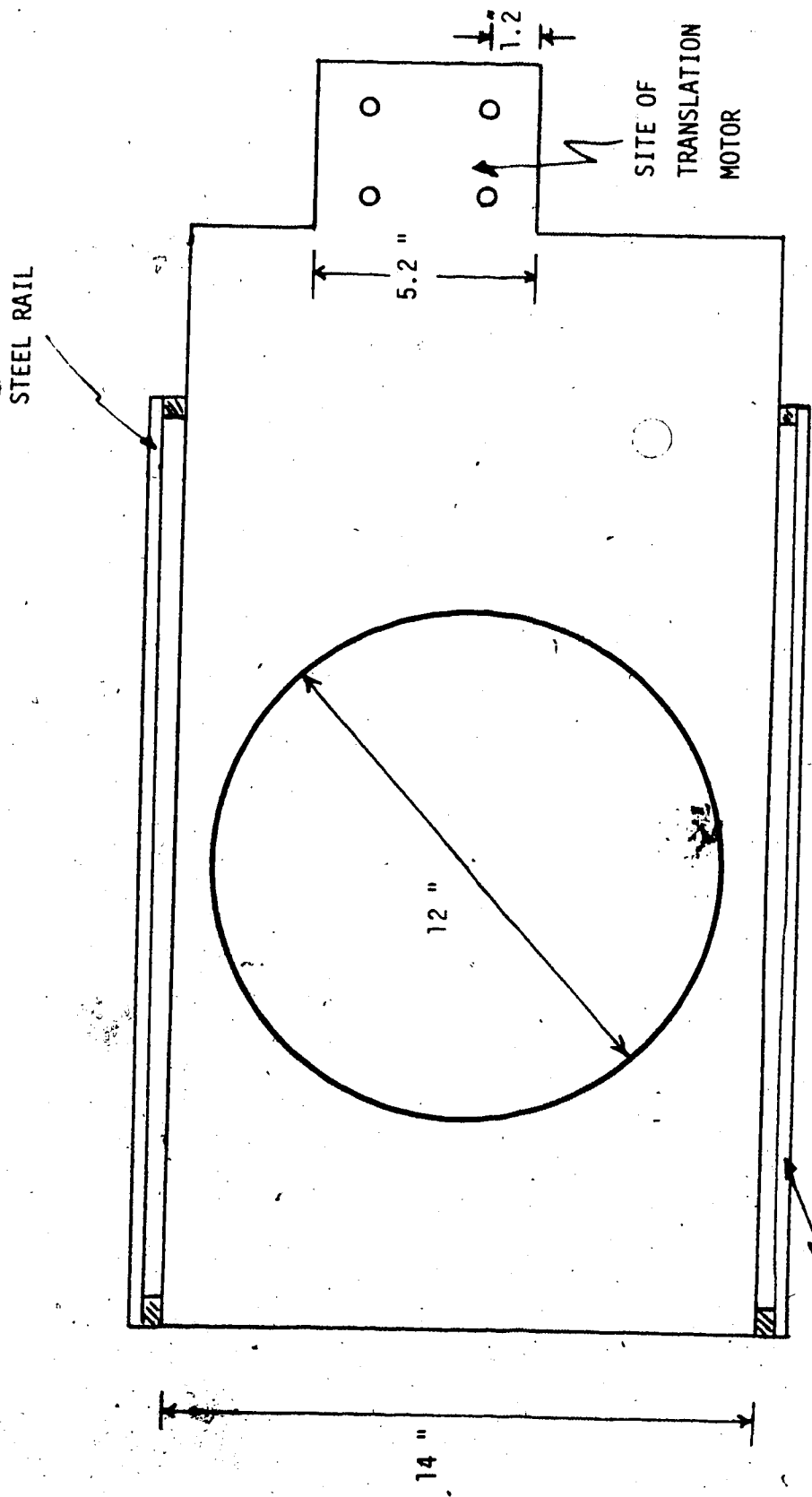
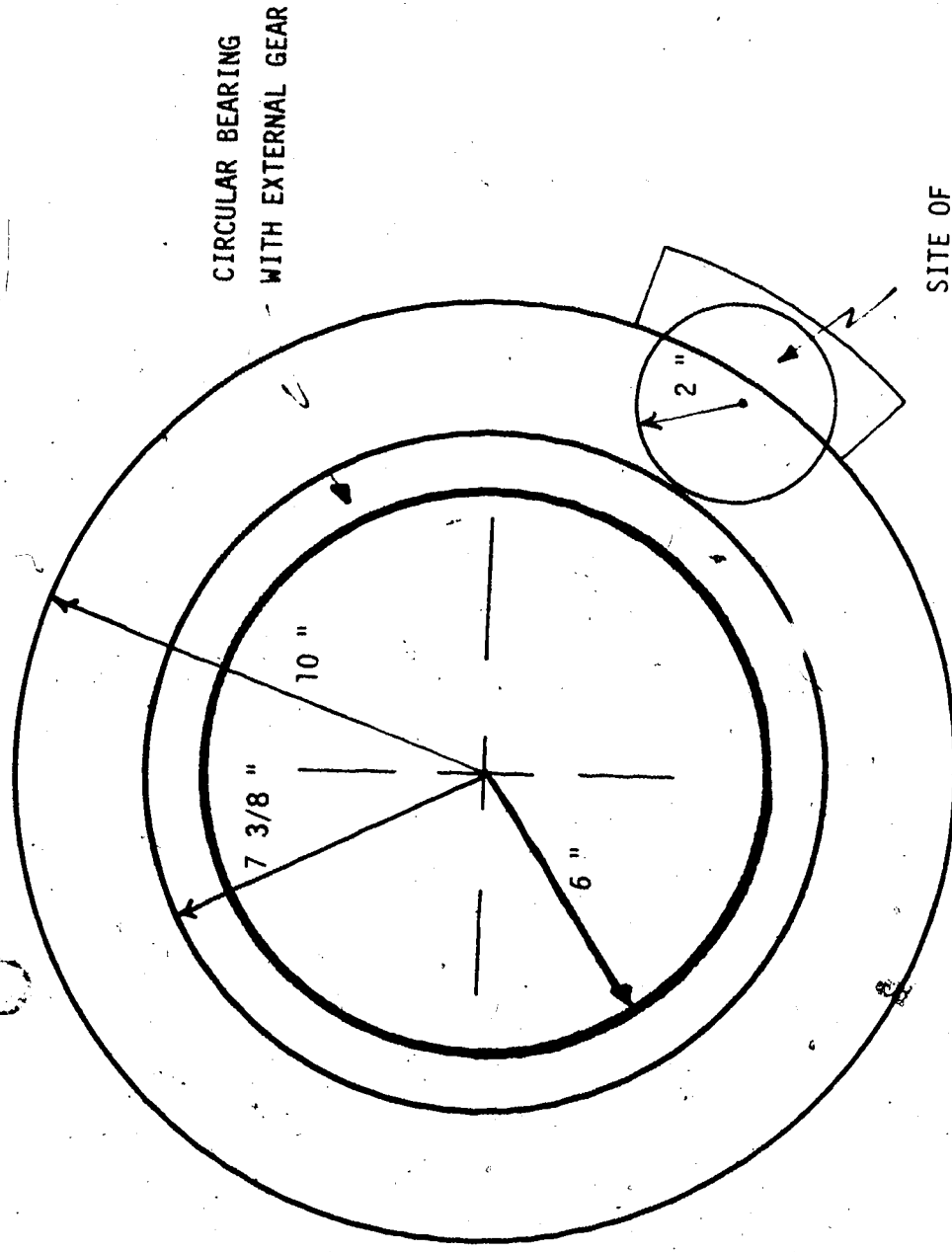


FIGURE 19. PLATE #2



CIRCULAR BEARING  
WITH EXTERNAL GEAR

SITE OF  
ROTATIONAL MOTOR

FIGURE 20. PLATE #3

6.25 um/step. The ball screw is of such a high precision and hence expense that a number of microswitch controlled relays have been installed which shut off power to the stepping motors should the scanner be operated outside its normal scanning range. The plates are rotated by a second stepping motor which drives a worm gear arrangement that is mechanically linked to a spur gear which in turn drives the external gear on the circular bearing. The worm gear was necessary in order to reduce gear backlash caused by the stepping nature of the motors. The gearing ratios mean that approximately 200 steps of 0.9 degrees each are required at the motor shaft to induce a 1 degree rotation of the plates. All of the gearing ratios in the system were known exactly except the gearing ratio of the worm gear arrangement. This ratio was determined by counting the number of motor steps required to rotate the plates 360 degrees as measured by a dial gage with a resolution of 0.0005 inches.

#### B. Radioactive Sources and Detectors

The underlying principle behind any tomographic scanner is the fact that if attenuation of a photon beam can be measured along a sufficient number of pathways through an object then the radiological density at any point within the object can be determined. The radioisotope photon source is 1.5 Curies of Iodine 125 adsorbed to a 2 mm diameter zeolite bead and encapsulated in aluminum. The detectors are 1/2 inch diameter, 1/2 inch thick NaI(Tl) crystals coupled to 13

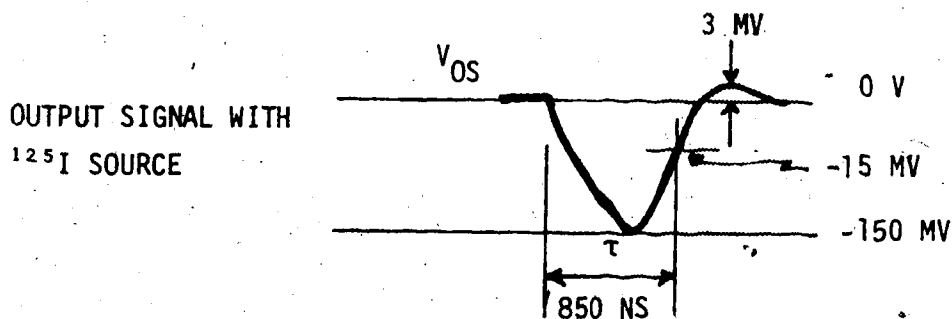
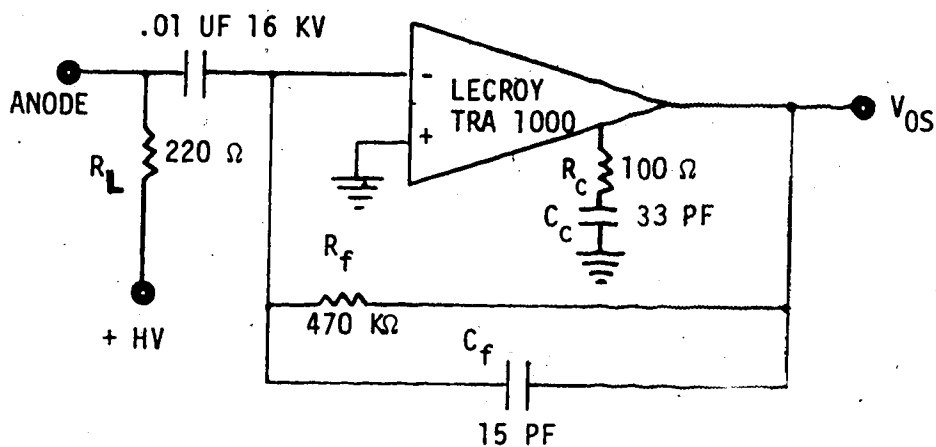
mm diameter photomultiplier tubes with borosilicate windows and bialkali dynodes. The detectors were chosen predominantly on the basis of availability and ease of operation. A radioisotope was selected due to financial constraints and ease of operation. The half-life of Iodine 125 is 60.2 days and the source is replaced every 2-3 half-lives at a cost of approximately \$1400/source. The mechanism of radioactive decay of Iodine 125 is included in the appendix but basically a gamma-ray of approximately 27.5 Kev is produced during the decay process. This energy, being relatively low, has a comparatively large linear attenuation coefficient meaning that subtle differences in density are discernible. At this energy the total attenuation coefficient for NaI is approximately 23 per cm. Hence in a 1/2 inch thick NaI(Tl) crystal only  $2.06 \times 10^{-13}$  of the photons would be passed through the crystal. For Gadolinium 153 with an upper energy of 100 Kev the attenuation coefficient for NaI is 6 per cm. and the number of photons passing through a 1/2 inch crystal would be  $4.91 \times 10^{-4}$  of those incident upon the crystal.

### Signal Processing

From the anode of the photomultiplier the signal is fed into a preamp (Figure 21). Since a NaI(Tl) crystal is used the rise time of the signal corresponds to the fluorescent decay time of Sodium Iodide (250 ns). Using a trial and error technique an anode load of 220 ohms was determined to be suitable in terms of pulse height and pulse pileup. The



PREAMP CIRCUIT USED WITH 8 DETECTORS AND NARROW HV CABLES



NOTE: -15 MV IS THE UPDATING POINT OF THE LECROY 623 DISCRIMINATOR.

DECREASING  $R_f$  SHORTENS PULSE WIDTH AND SLIGHTLY DECREASES PULSE HEIGHT.

I.E. IF  $R_f$  IS CHANGED FROM 3.3 KΩ TO 220 Ω: V -300 MV TO -150 MV

$\tau$  2.2 US TO 0.85 US

$V_{OS}$  +18 MV TO + 3 MV

DECREASING  $C_c$  AND  $C_f$  WILL DECREASE  $\tau$  BUT ALSO WILL CAUSE OSCILLATION.

THEREFORE,  $C_c$  AND  $C_f$  WERE CHOSEN AS SMALL AS POSSIBLE WITHOUT OSCILLATION.

FIGURE 21. PREAMP CIRCUIT

preamp then shapes the signal, increases its amplitude and transforms the impedance. The preamp used is a Le Croy TRA 1000 preamp and is able to provide a signal of sufficient amplitude so that a linear amplifier is not required. This particular preamp was chosen because of its low input noise (30 pA/ sqrt (Hz) r.m.s.) and its frequency response (20 MHz at 1 mV/uA gain). The output of the preamp goes into a Le Croy Model 623 8-channel discriminator which provides an output pulse for every input pulse over a preset energy. Thus lower energy pulses are discriminated against and only pulses above a certain energy are counted. From the discriminators the output pulses are sent to a CAMAC 50 M Hz Scaler which counts the number of pulses received in a given interval. This counting interval can be set by the HP 2100 computer which is interfaced to the CAMAC.

### C. Scanner Control

The drive motors are two Slo-Syn model M092 FC09 stepping motors with nominal torque ratings of 200 oz inches. A stepping motor translates an electrical pulse into a precise mechanical motion of the shaft. This motion is in fixed, repeatable increments permitting accurate positioning of the motor shaft. The motors can move in either 0.9 degree or 1.8 degree increments per input pulse. The position of the shaft is to within 3 % accuracy and this error is noncumulative from step to step. These motors require a DC power supply and associated electronic drives which contain

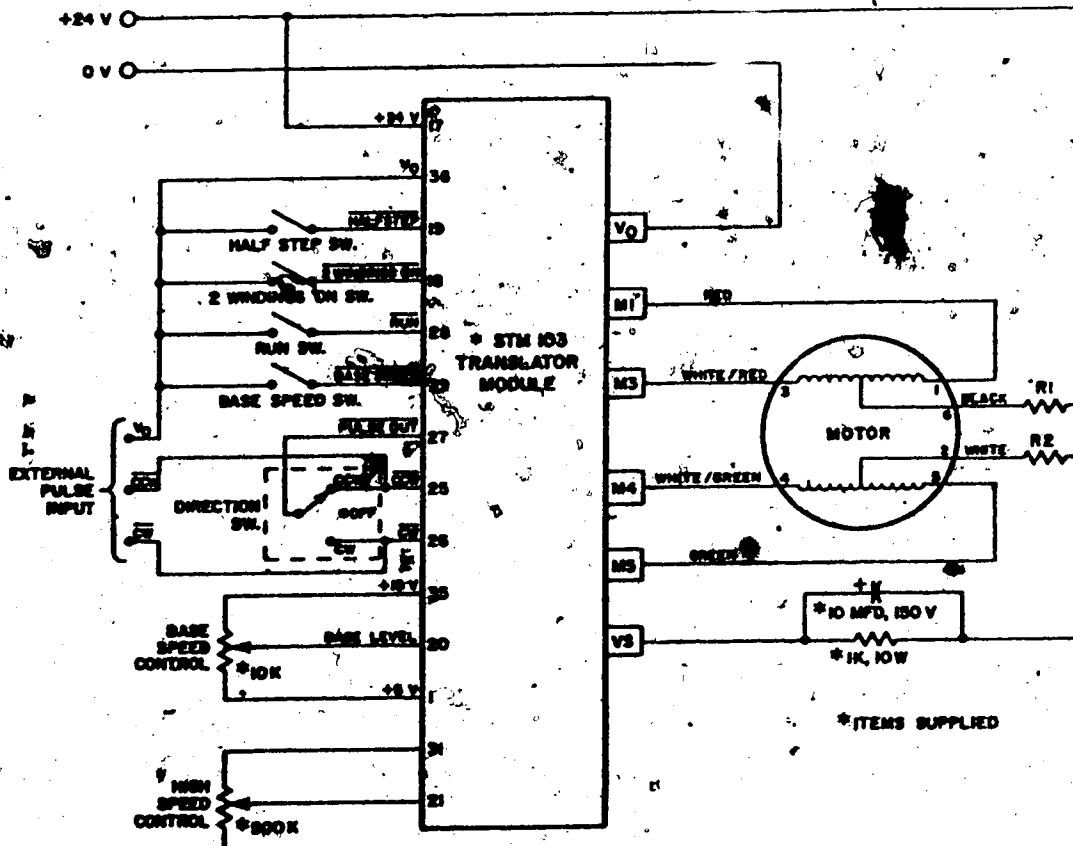
the required circuitry to convert pulses into the proper switching sequences for the motor. The power supplies are 2 Slo-Syn MPS3000 24 V DC while the electronic drives are 2 Slo-Syn STM103 3000 step per second motor controllers (Figure 22). These controllers have internal oscillators that can be used to drive the motors in either direction and either in the half-step (0.9 degrees per step) or the full-step (1.8 degrees per step) modes. They are also able to receive pulses from external logic devices such as microprocessors and minicomputers. In the scanner external logic sources include a Motorola microprocessor unit (MPU) and a monostable multivibrator which is used to provide single stepping capability.

The control system for this scanner was designed keeping in mind available equipment and computing facilities (Figure 23). A Motorola MEK 6800 D2 microprocessor unit (MPU) provides the central clock for the system. It is used to control the two stepping motors which provide the rotational and translational motions, as well as to signal the computer when to collect data from the scalars. All MPU software programs have been assembled and are contained in the appendix.

#### Timing Considerations

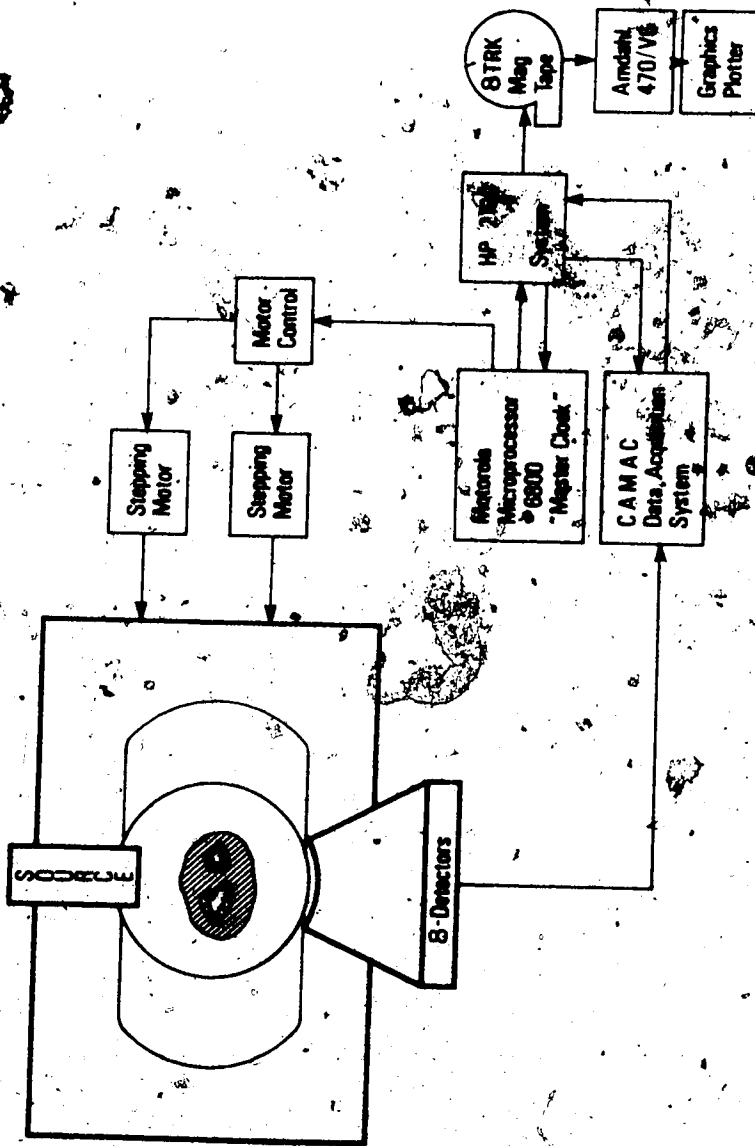
Since the microprocessor unit is used to control the stepping motors and hence scanner position it is also necessary that the MPU clock be used to determine when data from the detectors should be collected. Upon receipt of a

STEPPING MOTOR AND TRANSLATOR CIRCUIT DIAGRAM



CONNECTION DIAGRAM

FIGURE 22.



General System Philosophy: Data Acquisition

FIGURE 23. SYSTEM BLOCK DIAGRAM

signal from the MPU the HP must respond quickly to the signal and collect data since the scanner is continually moving. Although it was hoped that this could be accomplished with the HP running under its normal multi-user operating system it was found necessary to operate the HP in a stand alone mode while operating the CT system. This was due to the fact that under the multi-user system the time from a data-ready signal from the MPU until data was actually collected from the scalers was variable over too great a range. The stand-alone mode allows data to be collected within 4 microseconds (2 HP clock pulses) of a signal from the MPU.

#### MPU Control

The Motorola MPU is the basic D2 kit with the only additions being that of 1/2 K of Ram (M6810) and 2 of EPROM (Intel P2708). Program development and EPROM loading were done on an AMI microcomputer development center.

The choice of the 8 bit Motorola as the control processor was based upon:

1. availability of parts,
2. price, and
3. facilities for EPROM programming.

Although the trend is toward 16 bit and 32 bit microprocessors it was felt that the 8 bit microprocessor was sufficient for this particular application and this combined with the aforementioned constraints led to the selection of the M 6800.

To facilitate insertion and removal of the object to be scanned the scanner must begin and end operation in a "park" position which may not coincide with the actual scanning path. The sequence of events which occur during a scan are as follows:

1. the MPU determines the park to start distance and direction and sends the appropriate pulses to the motor controllers;
2. a signal is sent to the HP signifying that a scan is to begin;
3. a signal is returned from the HP to the microcomputer unit signifying that the HP is ready and that a scan may begin;
4. a signal is sent from the MPU to the HP signifying that a scan has been started and that acceleration of the translational motor has begun;
5. a second signal sent to the HP from the MPU signifies that acceleration has ceased and that translation velocity has been reached;
6. all translation pulses are sent to the motor controllers from the MPU;
7. pulses are sent from the MPU throughout the scan to the HP signifying when to collect data from the detectors;
8. after translation is complete the MPU decelerates the translational motor, determines the required rotation and sends the appropriate pulses to the motor;
9. the pattern (2-8) is repeated until the appropriate

number of rotations and translations have been performed;

10 at which point the appropriate pulses are sent to the motors so that the scanner is returned to the park position.

Acceleration and deceleration of the stepping motors is required since motor torque decreases with increasing speed. Thus in order to ensure that all pulses sent to the motor result in a step while at the same time operating at the maximum allowable speed, acceleration and deceleration of the motors is needed. This is accomplished by the microprocessor which uses a subroutine ASD (see appendix) provide a series of pulse trains at varying frequencies.

#### MPU Based PIA

The microprocessor unit (MPU) is interfaced to the motor controllers and the HP by an on-board integrated circuit (M 6820 PIA - peripheral interface adapter). The PIA contains an 8-bit bidirectional data bus for communication with the MPU, two bidirectional 8-bit buses (output registers) for interface to peripherals, two programmable control registers, two programmable data direction registers and four individually-controlled interrupt input lines; two of which are usable as peripheral control outputs. The MEK 6800 D2 kit contains two PIAs, one of which is used to interface the keyboard. The second PIA appears to the MPU as four memory locations located at \$8004 - \$8007.



(where "\$" denotes a hexadecimal number). The output register (OR) and data direction register (DDR) of port A (one 8-bit bus used for interfacing) are located at \$8004 and the control register (CR) is located at \$8005 while the corresponding registers for port B are located at \$8006 and \$8007. The contents of the control registers determine the operation mode of the interrupt lines and whether an output register or data direction register is to be addressed. This latter feature is required since the OR and DDR share the same address location. The data direction register determines whether the corresponding interface lines to the output register are inputs (DDR=0) or outputs (DDR=1).

To control the scanner 6 lines of the PIA port A are used. Two lines are needed for each of the two stepping motors (bidirectional) and two lines are used in a handshake mode between the HP and the MPU. The MPU is initialized by a subroutine (PIA) which first sets control register A (CRA) permitting DDRA to be addressed. DDRA is then set to \$1F (bit 7 is the most significant bit) so that lines 0-4 of ORA are outputs while lines 5-7 of ORA are inputs. Control register A is then reset so that ORA can be addressed. The normal state of the output register is set equal to \$1F (only bits 0-4 may be set by the MPU). Signals to the translation motor are sent along lines 3 and 4 (\$0F and \$17) while signals to the rotational motor are sent

along lines 0 and 1 (\$1D and \$1E). A signal to the HP is sent on line 2 (\$1B) and a signal from the HP is received on line 5. Bits 0-4 are active on the positive transition meaning that subsequent to the normal state of the output register the desired signal must be stored in ORA and then the normal state must again be stored in ORA at which point the message is transmitted. This pattern was used since it was found necessary to initialize the output register at the start of an scan in order to be certain of the contents of the register. The signal from the HP is level sensitive and responds to a positive signal in bit 5.

#### Acceleration - Deceleration Ramp

When operating the stepping motor from the internal oscillator, the translator module automatically accelerates and decelerates the motor to prevent the motor from missing steps or overshooting when stopping. This ramping of the pulse rate is also necessary when operating the translator module from pulses supplied by an external source (in this case the MPU). When using the internal oscillator, acceleration and deceleration times to a high speed are independantly adjustable from 50 milliseconds to 1 second. The acceleration and deceleration ramps are used during the transition from a preset although adjustable base speed to a preset although adjustable high speed.

In order that the number of steps and time for

acceleration and deceleration be kept to a minimum known quantity a suitable MPU controlled ramp had to be found. The base speed of the control module was set to zero and using the internal oscillator a suitable ramp for a high speed of 1500 Hz was obtained through trial and error. It was found that the same ramp was suitable for use with both stepping motors. The upper speed of 1500 Hz was selected since it had been decided that the maximum speed of the motors during a rotation or a translation would be at approximately that frequency. Once a suitable ramp had been obtained these pulses were then measured with an Ortec ratemeter (which converted the pulse frequency to a proportional voltage); the output from which was displayed on a storage oscilloscope. Thus acceleration via the internal oscillator produced a ramp on the oscilloscope representative of the accelerating ramp used. The next step was to mimic this ramp using the MPU as the pulse source. A subroutine (ASD - acceleration, speed, deceleration) was developed that produces twelve ramps of varying lengths and frequencies. As a test of the MPU generated ramp the MPU output was also measured with the Ortec ratemeter and displayed on the oscilloscope and the resultant waveform was compared with that obtained from the internal oscillator of the control module. Once a close approximation had been found the MPU based ramp was tested on the scanner.

The frequencies, corresponding ramp lengths, and type and direction of motion are loaded by ASD from RAM and must be set in RAM prior to calling ASD. These parameters may be set so that ASD can be used for only acceleration or deceleration or to preset the scanner location. A count of all pulses sent during subroutine ASD is made. A number of smaller subroutines are used in conjunction with ASD. These include various acceleration and deceleration subroutines which set the parameters in RAM so that ASD may be used to accelerate to or from a certain speed. There are three deceleration subroutines (DECEL, DECEL32, DECEL5) which are used to decelerate the scanner from speeds of less than 1500 Hz, less than 400 Hz and less than 100 Hz respectively. The respective lengths of these three ramps are 200 steps, 32 steps and 5 steps. The upper speed limit of acceleration is variable up to 1500 Hz merely by setting the ramp length parameter contained in two RAM locations. For a normal scan (with a top speed of 1318 Hz) the frequencies and ramps are loaded from two subroutines (F and INIT) contained in EPROM into the RAM locations. The frequencies vary from 20.2 Hz to 1115 Hz and the corresponding ramp lengths vary from 1 to 42 pulses. The same ramp is used for acceleration and deceleration with two hundred steps being required in both cases. The number of pulses at a maximum frequency of 1422 Hz can be varied from 0 to over 4 million and hence ASD is

suitable for presetting scanner position.

Another minor subroutine R8D initializes parameters in RAM and then calls ASD resulting in a 25.7 degree rotation of the scanner. This is the rotation required between translations in a normal scan using the 8-detector holder.

#### Translation

Once the motor has been accelerated up to the desired speed a subroutine (TRANSL) is called. This subroutine makes use of a number of parameters previously loaded into RAM which determine the delay between motor pulses and the number of motor pulses per signal to the HP. A signal to the HP signifies that data is to be collected from the scalars.

#### Start

At the start of every translation of a scan an MPU based subroutine (START) is called. This routine (which uses the handshake arrangement between the MPU and the HP) sends a signal to the HP (signifying that a translation is desired) and in return waits for a signal from the HP (prior to allowing the MPU program to continue). An additional signal is sent to the HP prior to the start of the ramp.

#### Program Location

The MPU contains two EPROMs (1024 x 8 bit) located at \$6000-\$63FF and \$C000-\$C3FF. The EPROM located at \$C000 contains all subroutines such as ASD and TRANSL

(see flowchart in appendix) while the main body of the control programs are located in the EPROM at \$6000. Since the subroutines are rarely altered this means that most changes to the system control programs can be made by altering just one of the EPROMs. The RAM contained in the MPU is static RAM (128 x 8 bit) and is located at addresses \$0000 through \$03FF. The reason that many of the control parameters are loaded by the subroutines from RAM is that this theoretically makes it possible to alter the control parameters from the keyboard. At present however, most of the RAM parameters are loaded into RAM from the main control programs (which are stored in EPROM) at the same time as the main control program is run. This is due to the fact that the control parameters are at present seldomly changed.

#### Reproducibility of Measurements

Bone mineral changes are significant along the longitudinal aspect of the extremities. Consequently, for a valid quantification of changes in time in a given individual, it is important to be able to reproduce the site of the scan (50). To achieve this required positioning accuracy a MPU controlled scout scan system was developed which locates the desired measurement site.

The scout scan involves measurement of 26 single profiles at different points axially about the measurement site. Reconstruction of these profiles (see Figure 24) yields an X-ray like image which depicts the relative sizes



FIGURE 24. SCOUT SCAN

and orientations of the bone(s) (femur vs. radius, ulna): This information when compared to the same information obtained from previous scans of the same patient permits accurate location of the desired measurement site.

The anatomical criteria used to define the scan site are the distances from the distal tips of the radius and ulna axially along the bones. At present, sites two millimeters to either side of the measurement site are also being evaluated. These three sets of data are then interpolated in order to provide a reconstructed area identical to those previously measured.

#### Single Stepping

In order to provide the desired accuracy for initial positioning of the scanner it was necessary to provide some means for single stepping both the rotational and translational drive motors. This was accomplished by use of a 74123 retriggerable monostable multivibrator (51) as shown in Figure 25.

#### HP/Microprocessor Interfacing

The microprocessor unit both sends and receives positive signals of + 5 volts while positive signals sent from the HP are +12 volts. In order to sink the required current (12 mA) to provide a low signal to the HP the output from the PIA is tied into two inverters before being connected to the HP (Figure 26). Positive signals from the HP are converted to +5 volts by use of a resistor-zener diode divider circuit (Figure 27).



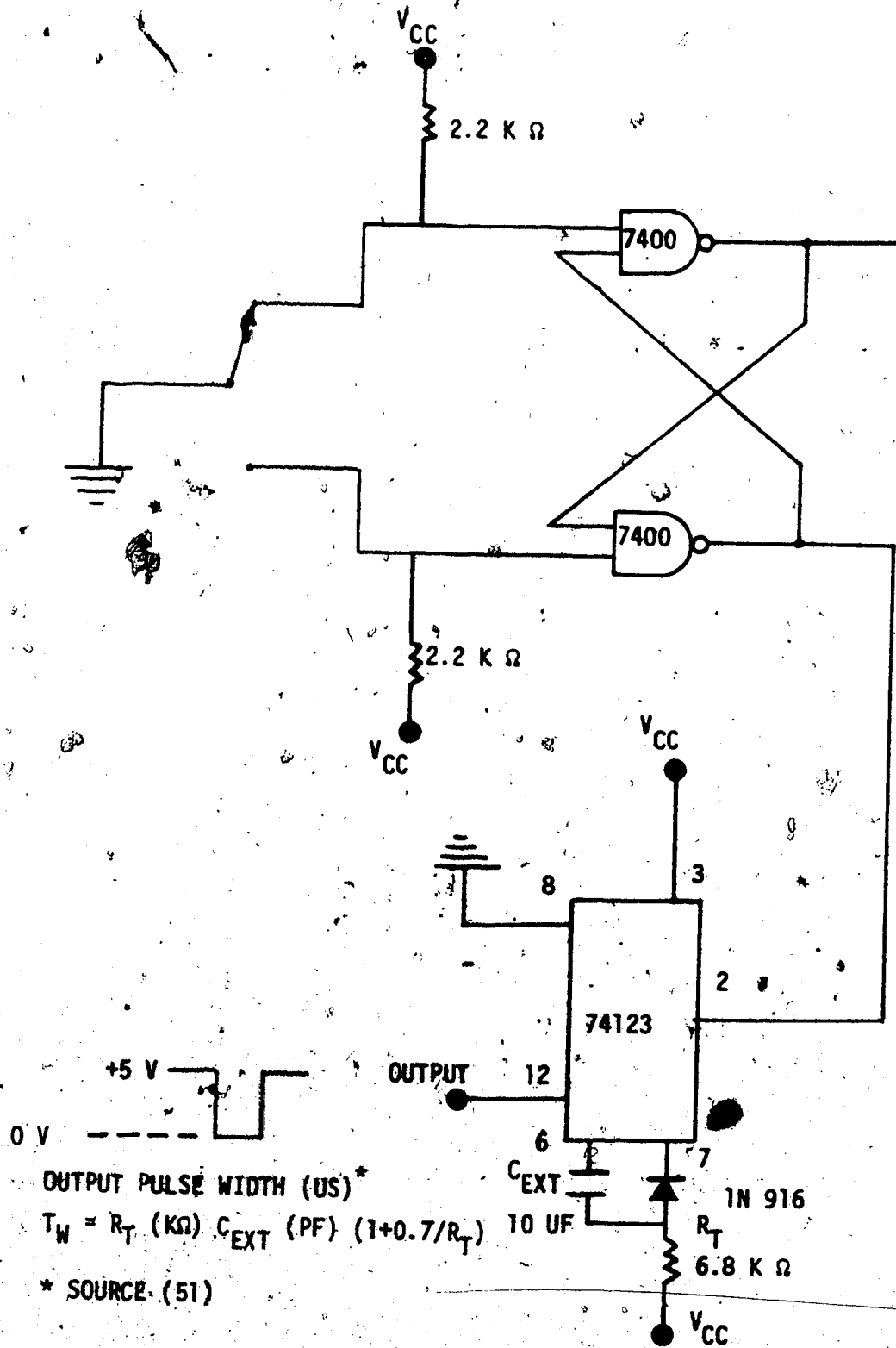


FIGURE 25. SINGLE STEPPING CIRCUITRY

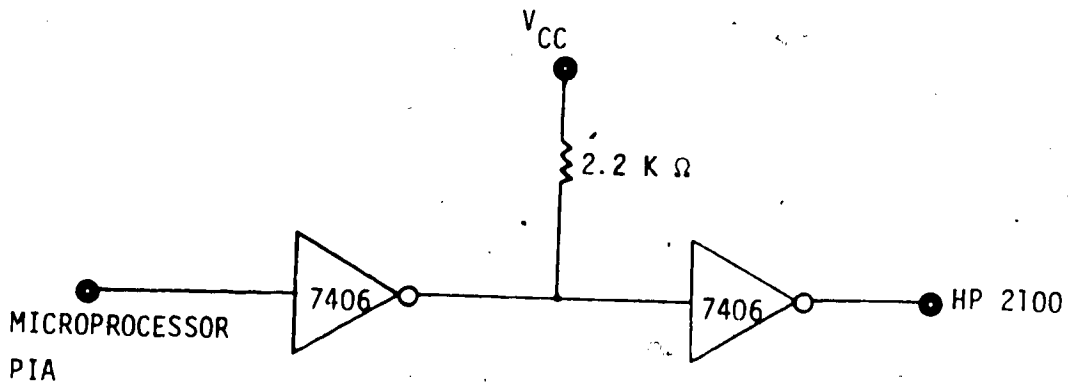


FIGURE 26. CURRENT SINK

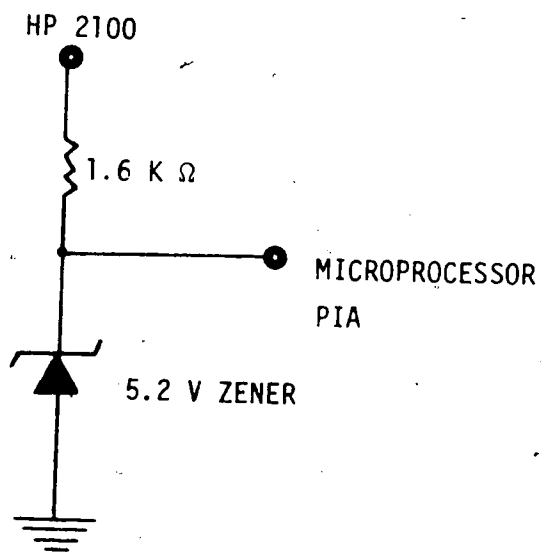


FIGURE 27. VOLTAGE DIVIDER

#### D. Multidetector System

Upon completion and subsequent testing of the generation one system the modifications necessary to change the system to a generation two configuration were undertaken. This chapter will describe the problems encountered in making these modifications.

The principle of the multidetector system is to collimate a single radioactive source so that an array of photons is produced which subtend a solid angle emanating from the source. The detectors are also collimated so that scattering of rays between detectors is reduced. Linear scans are made in exactly the same fashion as for the single-detector systems however the angle of each rotation is  $n$  times greater where  $n$  is the number of detectors (this assumes the detectors are spaced at the desired angular increments). Thus the number of linear translations and the number of rotations can be greatly reduced decreasing the time required for a scan. This reduction in scan time is significant in that errors caused by patient movement can be reduced. In this particular scanner moving from a generation one system to an eight-detector generation two system reduced the normal scan time from approximately 5 minutes to approximately 1.5 minutes. Although the order of data collection in a multi-detector system is different from that of a single detector system the reconstruction algorithm used is exactly the same.

### Physical Limitations

In order for radiological attenuation of the object to be determined the detectors must be allowed to measure what is known as an "open" or unattenuated count rate during a scan. This means that in the multi-detector system, for each translation, all source-detector alignments must be totally clear of the object at some point in the translation. Given a finite translational pathlength this means that either one or both of the object size and the angle of the detector arc must be restricted. In this arrangement it is always possible to scan larger objects by not using the outer detectors in an array and effectively reducing the angle of the detector array. This would mean that the rotational angle between translations would have to be reduced.

Another limitation is the size of the detectors. The fact that these detectors can only be packed together within limits means that in order to have a desired angle between detectors the source-detector distance cannot be less than a certain minimum. This distance is of utmost importance since the photon flux impinging on the detectors follows the inverse square law meaning that the further the source-detector distance the worse the available statistics given the same radioactive source and counting interval. Other considerations in regards to the detector geometry include scan time, count rates and available channels for signal processing. The final result, an 8 detector unit similar to the one depicted in Figure 28, is a compromise

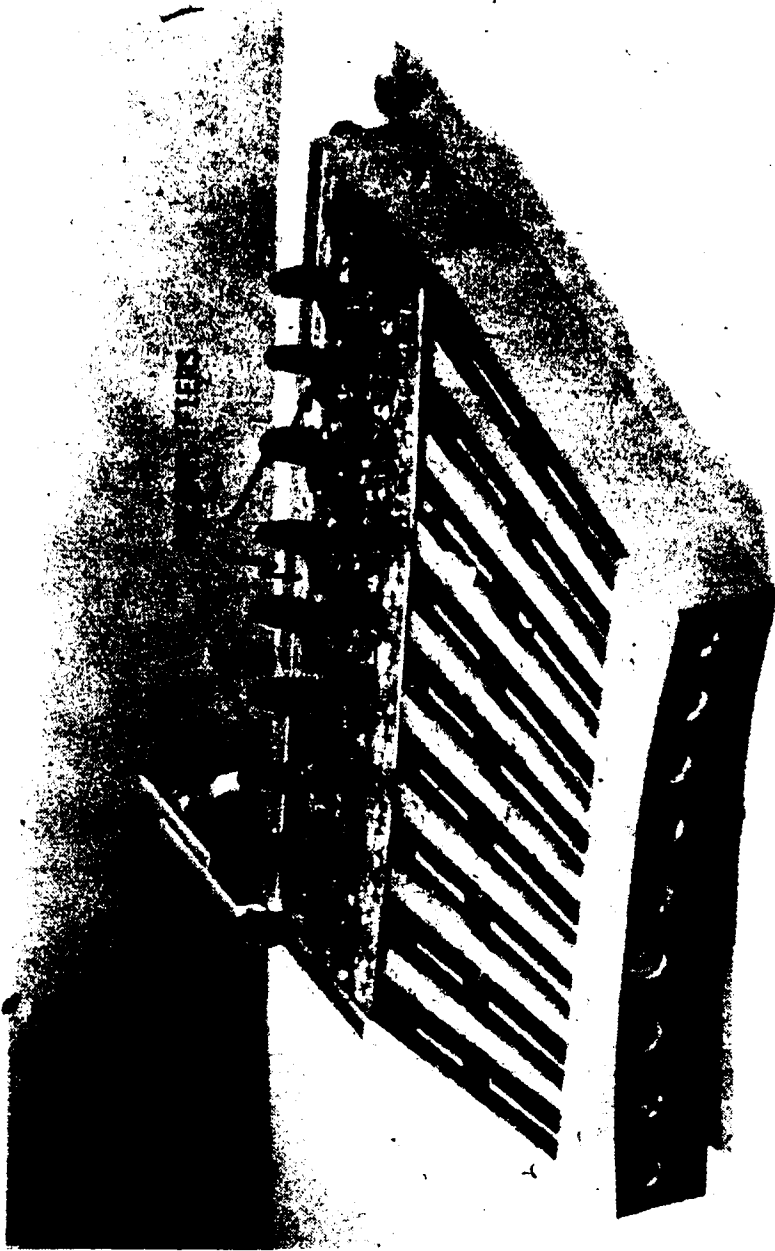


FIGURE 28. DETECTOR HOLDER

between the aforementioned factors.

### Intervals and Subintervals

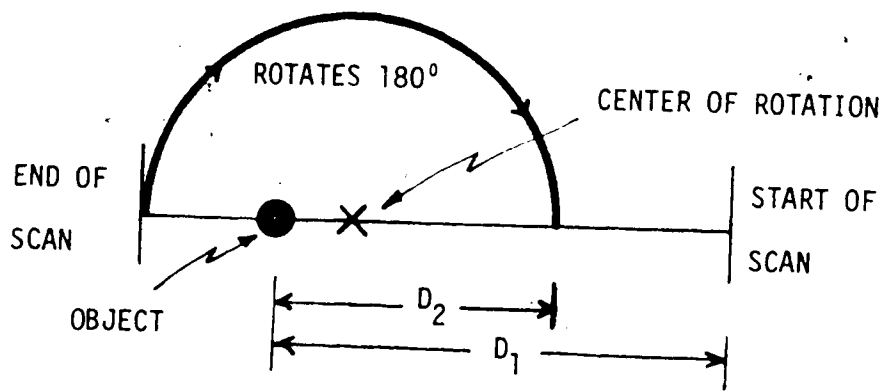
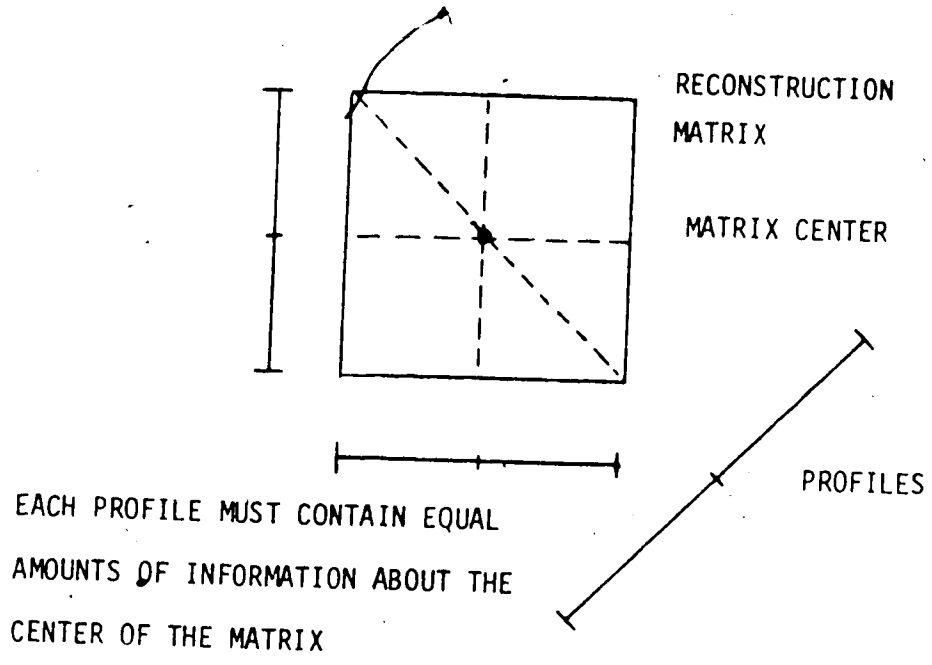
In the case of the multidetector system the translation of the scanner is perpendicular in direction to at most one of the source-detector orientations. Thus, while during a translation one detector may move a distance of "A" perpendicular to its orientation, the other detectors will move distances somewhat different than "A" perpendicular to their own orientations. The reconstruction algorithm requires that all the detector spacings have to be the same distance apart and therefore some means of correction has to be applied. This is done by measuring subintervals; each interval or ray-integral measurement consisting of a number of subintervals. Thus while the detector that is aligned perpendicular to the direction of motion will have intervals consisting of a specified number of subintervals the other detectors' intervals will be made up of more subintervals. The number of subintervals per interval varies from detector to detector according to their respective angular deviation from the line perpendicular to the direction of translation. Interpolation between subintervals is typically required in order to accurately define an interval. In this particular system 8 subintervals are measured for every interval of the detector aligned perpendicularly to the direction of motion. Thus while in a normal scan some 1024 subintervals are measured per detector per translation they are later compressed on the HP to 128 intervals prior to

reconstruction.

### Centering

The reconstruction matrix requires that each profile consist of equal amounts of data collected about the center of the reconstruction matrix. This is due to the fact that the convolution algorithm weights all ray measurements according to their distance from the point of reconstruction. In the case of the multidetector scanner each detector has a different starting point so it is impossible for all of them to collect equal amounts of data about the center of the scanner. In order to compensate for this, offsets must be calculated and applied to the collected data from each detector.

This problem is most easily seen by examining the case of a single detector scanner. Assume that the scanner moves a distance  $D_1$  from the start of a scan to an object  $O$  before completing the scan (Figure 29). Then, if the scanner is rotated through 180 degrees and started once again the distance from the start of the scan to the object  $O$  is now  $D_2$ . In order that equal amounts of data be collected about both sides of the object the data will have to be offset by an amount equal to  $(D_1 - D_2)/2$ . Thus if equal amounts of data have been collected about both sides of the object  $D_1$  is equal to  $D_2$  and no offsets are required. These calculations are aided by a special microcomputer program (Cent) which is a high resolution measurement. An object of high density and small physical size (i.e. a wire) is placed approximately in



IF THE PROFILE IS TO CONTAIN EQUAL AMOUNTS OF DATA ABOUT BOTH SIDES OF THE OBJECT THE POSITION OF THE DATA WILL HAVE TO BE OFFSET BY  $(D_1 - D_2)/2$ .

FIGURE 29. CENTERING CONSIDERATIONS

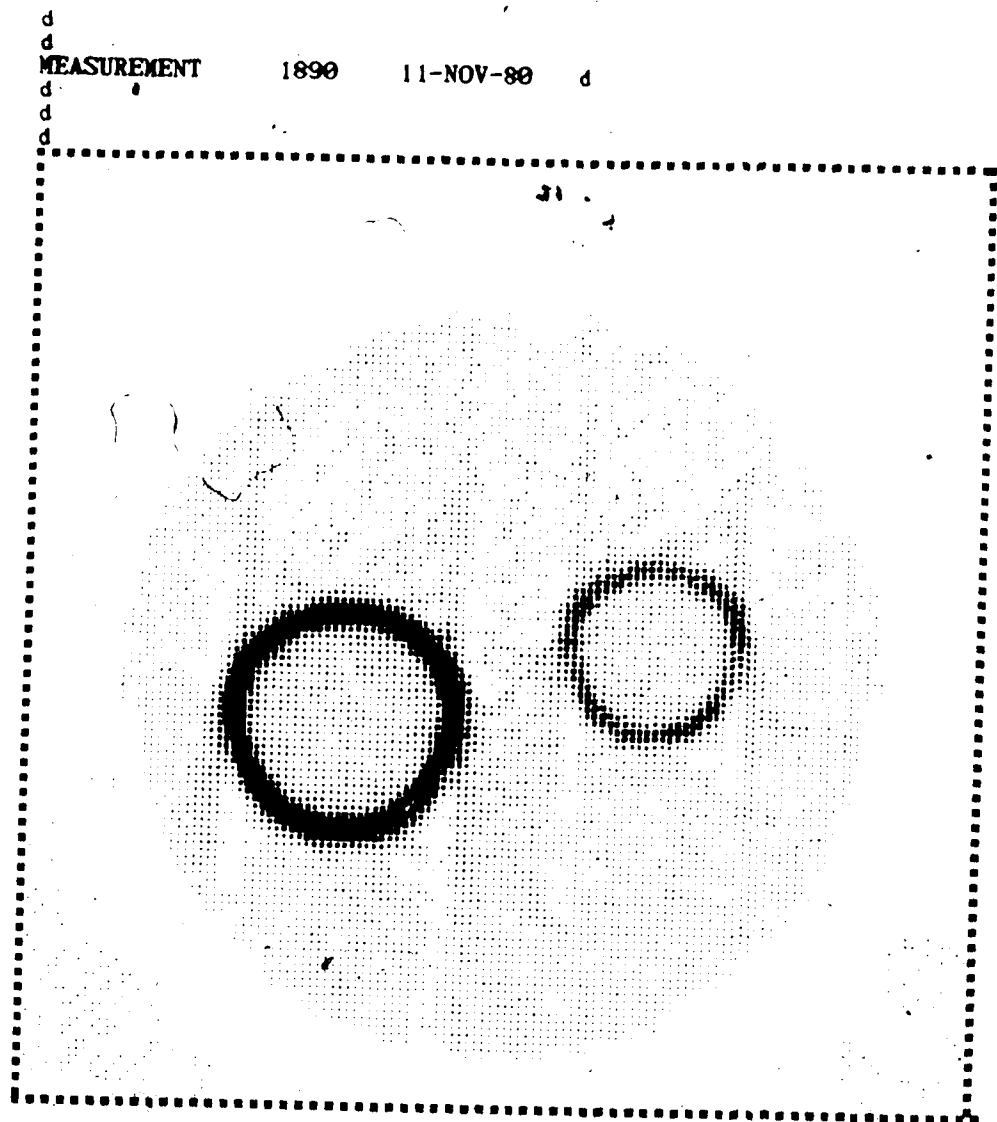


the middle of the scan path. The scanner is then translated at low speed and data is collected every two motor steps. The scanner is then rotated through 180 degrees and the scan is repeated. Looking at Figure 29 we see that information so obtained will allow one to calculate the offsets for each detector. This procedure must be repeated every time the mechanics of the scanner (such as the source) are altered.

With an aluminum-plexiglass model, centering errors of 100 motor steps or 0.625 mm, per detector are noticeable (Figure 30). In the case of a circular object the centering artifact appears on the image as two circles of slightly different radii being joined.

#### E. Data Processing

Data for one translation is stored in the HP 2100 and during a rotation is transferred to magnetic tape. This is then processed and analyzed on the University Computer (Amdahl 470/ V7) and hard copies of the image are obtained on the associated electrostatic plotter printer. The reconstruction program uses the convolution technique with the filter function proposed by Shepp and Logan to produce a 256 x 256 reconstruction matrix. Prior to reconstruction both dead time and a non-material selective beam hardening correction are made on the Amdahl as is an interpolation between ray measurements and angles. The interpolation takes the 128 data points per projection and interpolates between them in order to produce 256 data



PLEXIGLASS PHANTOM WITH TWO CIRCULAR ALUMINUM TUBES

FIGURE 30. CENTERING ARTIFACTS

points per projection and also interpolates between projections to produce 112 instead of the normal 56 projections. Although these interpolations do increase computation time and have a smoothing effect on the image the increased matrix size is needed in order that the analysis program has enough pixels with which to work. Interpolation between the angles is necessary to remove angular artifacts from the image. It has been shown (7) that if there are  $N$  ray-integral measurements made per projection, then for the data to be complete there should be  $M$  projections, where  $M = (\pi/4)N$ . Thus if there are 128 ray-integral measurements made there should be  $128(\pi/4)$  or approximately 100 projections made in order for the data to be complete. Hence if the number of angles were not interpolated to produce 112 projections instead of 56 projections, angular artifacts would be present in the reconstructed image. The interpolation between measurements is to produce 256 ray-integral measurements so that reconstruction on a  $256 \times 256$  matrix can be performed easily. It should be noted that it is not necessary to reconstruct on a matrix the same size as there are number of ray-integrals per profile; however, reconstruction is facilitated if this is the case.

In order to use a Grinnell CRT display, which is tied into the HP system it is necessary to either reconstruct the matrix on the HP 2100, which takes about 30 minutes (for a  $128 \times 128$  matrix), or else to load the Amdahl reconstructed

matrix onto magnetic tape and to subsequently load the matrix into the HP.

#### Open Count

Although the open count rate is measured for all detectors during each translation the statistics associated with such counts are of limited accuracy due to a short counting period. For this reason an open count rate is made at the start of the day. This count is made over a period of several minutes (using the Scout Scan program) so that the coefficient of variation associated with the measurement is low. This open count ( $I_0$ ) is then used throughout the day to calculate the ray-integral measurements ( $\ln(I_0/I)$ ).

#### Pixel Size and Grey Levels

The pixel size of the system is determined by dividing the scan length by the number of pixels in one side of the reconstruction matrix. The maximum size object that can be scanned is 76.8 mm and the size of the reconstruction matrix is 256 x 256. Hence the pixel size of the system is 76.8 mm/256 or 0.3 mm. Each pixel level in the reconstructed matrix is defined by a two's complement 16 bit number and hence there are 32,768 possible positive pixel levels. Although the system pixel size is 0.3 mm corresponding to a 256 x 256 matrix the hard copy imaging system is not able to resolve points of that size. As a result a 128 x 128 matrix with 32 grey levels is used with a corresponding pixel size of 0.6 mm. Since there are four times as many pixels in the actual reconstruction matrix as in the image matrix, four of

the actual pixels are averaged together to produce one of the image pixels. The Grinnell display system is able to reproduce matrices of size 512 x 512 with 256 grey levels and hence the system limiting pixel size for this display mode (CRT) is 0.3 mm.

### Analysis Program

While the image depicting the bones may be aesthetically pleasing it is really the parameters contained in subsequent analysis programs that are of clinical value. The image's main function is to ensure that the scan was done properly and that no artifacts due to such factors as patient movement have been introduced. Once an image of the bone has been reconstructed, an analysis program is used to identify such parameters as area, total mineral content and average density. These parameters are defined for total bone, trabecular bone and the cortical or compact bone (Table 1).

The analysis program first defines where the cortical bone begins and strips away the surrounding fleshy material (Figure 31). This is done by defining a cortical bone density level (8000 is normally used) and defining all levels of material outside of those pixels with levels greater than or equal to 8000 as being zero. The radius and ulna are then separated and each bone is analyzed separately. Each bone is then separated into a number of shells by essentially moving the cortical bone contour in, one pixel at a time. Trabecular bone was initially defined

MEASUREMENT: 596 13-MAR-80  
 RADIUS EVALUATION LEVEL 8000

	SHELL		REST BONE		REST AREA	
	DENSITY [G/CCM]	SM [%]	DENSITY [G/CCM]	SM [%]	DENSITY [G/CCM]	SM [%]
0	0.0	0.0	0.0	0.0	0.0	0.0
1	0.9161	0.0078	0.85	0.0	0.5374	65.01
2	1.2343	0.0148	1.20	0.1115	0.5534	67.42
3	1.4802	0.0206	1.39	0.2095	0.5582	70.38
4	1.5982	0.0256	1.60	0.2867	0.5408	72.56
5	1.5921	0.0281	1.76	0.3503	0.4984	72.90
6	1.4603	0.0267	1.83	0.3777	0.4356	70.78
7	1.2573	0.0253	2.01	0.3521	0.3674	66.84
8	1.0512	0.0247	2.35	0.3300	0.3042	61.90
9	0.8709	0.0207	2.37	0.3176	0.2495	56.35
10	0.7063	0.0183	2.59	0.2623	0.2076	51.51
11	0.5664	0.0147	2.60	0.2282	0.1797	48.14
12	0.4715	0.0135	2.87	0.1810	0.1670	47.34
13	0.4059	0.0152	3.75	0.1624	0.1622	47.79
14	0.3710	0.0163	4.38	0.1774	0.1586	47.82
15	0.3742	0.0145	3.87	0.1860	0.1541	47.19
16	0.3983	0.0133	3.34	0.1625	0.1518	47.45
17	0.3875	0.0138	3.58	0.1462	0.1490	48.45
18	0.3479	0.0136	3.90	0.1409	0.1447	49.28
19	0.3233	0.0152	4.69	0.1530	0.1432	50.99
20	0.3108	0.0156	5.06	0.1509	0.1394	50.90
21	0.2817	0.0169	5.53	0.1436	0.1348	51.02
22	0.2499	0.0179	6.74	0.1460	0.1317	50.91
23	0.2554	0.0159	7.02	0.1468	0.1261	48.11
24	0.2970	0.0200	7.95	0.1156	0.1144	43.06
25	0.2514	0.0215	9.56	0.1199	0.1090	44.73
26	0.2250	0.0215	9.56	0.1032	0.0992	41.90
					0.0942	37.29

TOTAL BONE		TRABECULAR BONE		COMPACT BONE	
AREA	3.0366 [CM*2]	REL. AREA	61.1737 [%]	ABS. THICKNESS	0.2142 [CM]
TOT. MIN. CONTENT	2.5102 [G/CM]	TOT. MIN. CONTENT	0.9128 [G/CM]	REL. THICKNESS	21.7863 [%]
AV. DENSITY (BD)	0.8266 [G/CCM]	AV. DENSITY (TBD)	0.4914 [G/CCM]	AV. DENSITY (CBD)	1.3549 [G/CCM]

TABLE 1.

MEASUREMENT 596 13-MAR-80

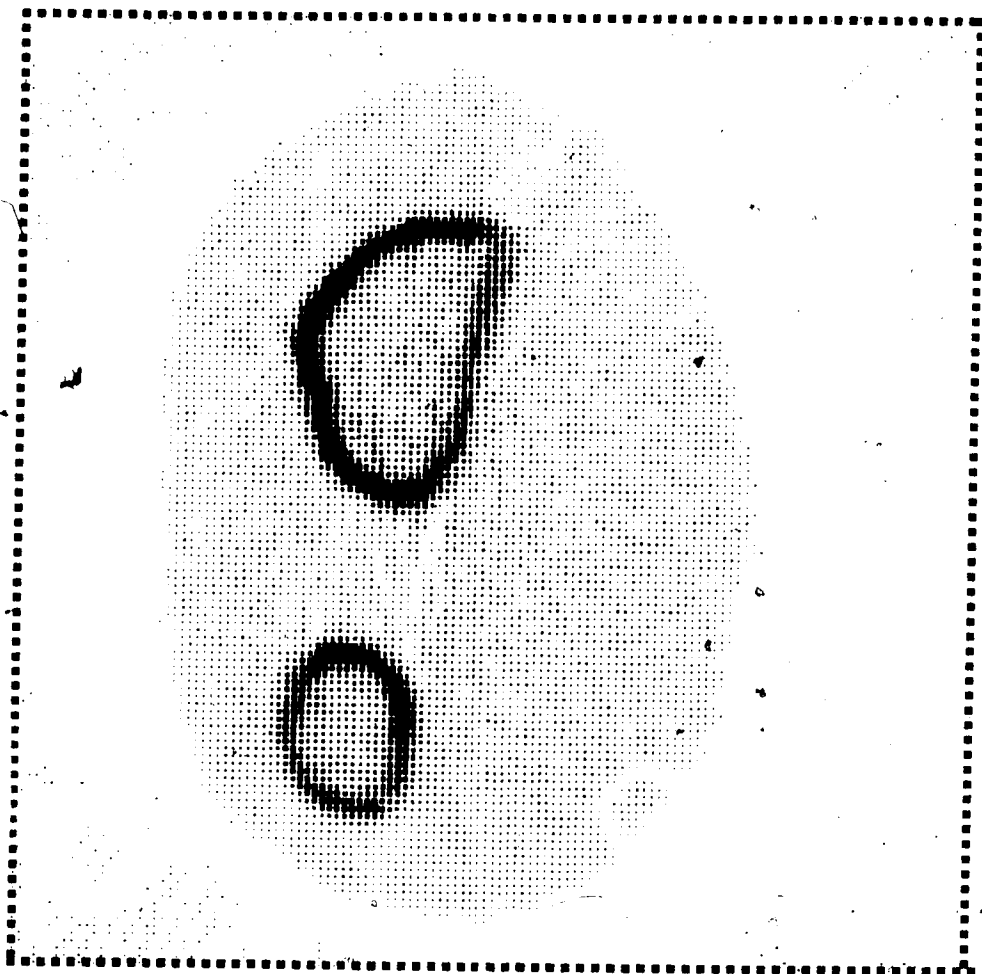


FIGURE 31. NORMAL RADIUS-ULNA

as that area of bone which comprised the inner 50 percent of the total bone area. It was felt that this arbitrary definition of trabecular bone may not be applicable to all patients. The criteria now used involves first calculating the average densities for all shells. Trabecular bone is then defined as the inner area of bone bordered by the maximum change in adjacent shell densities. The CT attenuation coefficients are converted to bone density (g/ccm) by dividing  $\mu$  by the average mass attenuation coefficient for bone. Due to the fact that a non-material selective beam hardening correction is applied (as contrasted to a material selective correction (48)) these measures of density are only valid for longitudinal studies. Cross-sectional (i.e. population) studies require absolute values for bone density and this necessitates material selective corrections.



## V. System Evaluation

The scanner was evaluated in terms of: (1) spatial resolution, (2) precision, (3) accuracy and (4) radiological dosage. The results of these evaluations are discussed in this section and a technique for measuring contrast resolution is suggested.

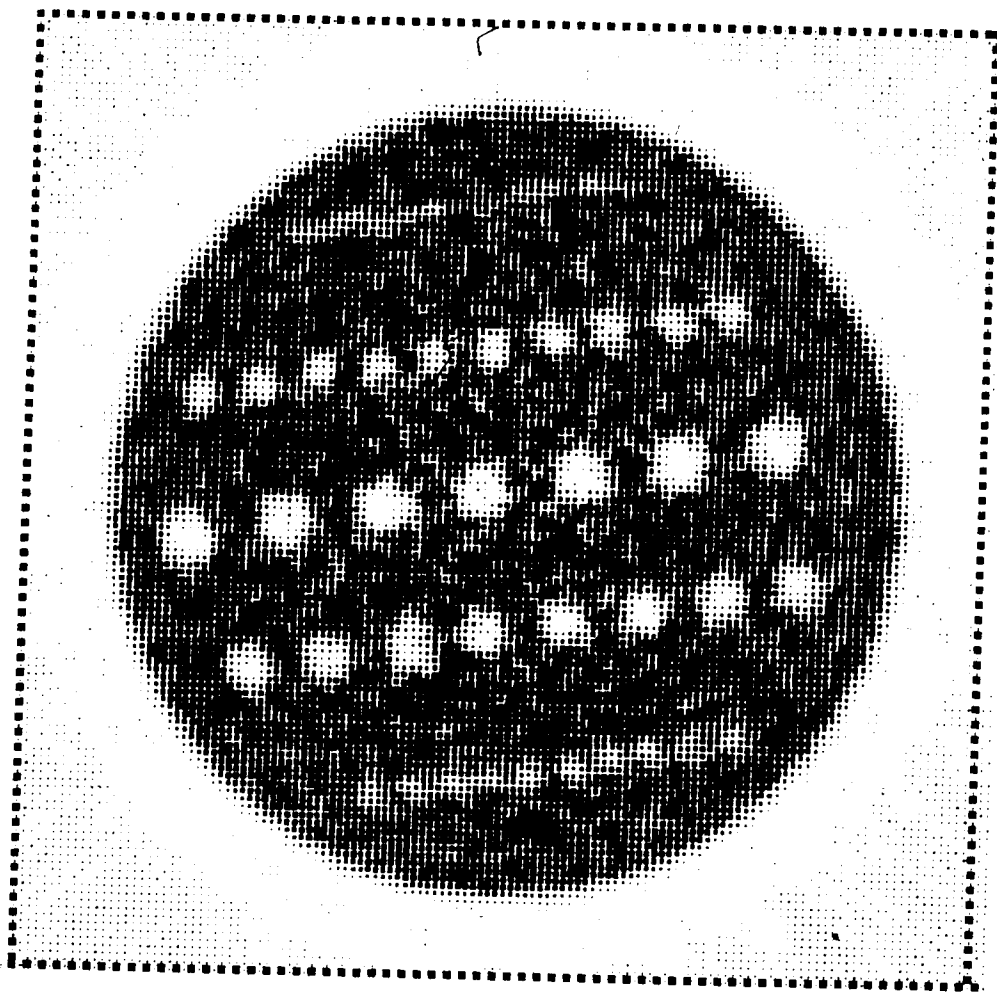
### A. Spatial Resolution

Physical resolution of the system was evaluated using a 2 1/2 inch diameter circular plexiglass model with periodic structures of various size holes drilled into it. These holes are drilled so that the space between holes is equal to the hole diameter. The model was subsequently scanned at three different speeds and the holes were left open to the air. Motor pulses during the three speeds of translations were sent at 1318 Hz, 330 Hz and 82.4 Hz and data from the CAMAC scalers was collected every 12 motor pulses in all three instances. Since these speeds are ratios of 16:4:1 respectively the resultant subinterval counts obtained during the scan were in the ratios of 1:4:16 respectively. Since coefficient of variation (C.V.) is inversely proportional to the square root of the number of counts this means that the C.V.s associated with each of the ray-integral measurements were improved by a factor of two with each decreasing speed of scan. The open count rates of the source for detectors 1 through 8 were; on a subinterval basis: (1) 374.42, (2) 349.92, (3) 334.08, (4) 345.49, (5)

389.56, (6) 369.65, (7) 405.93, and (8) 379.45. Thus the C.V. associated with an average 8 subinterval per interval open count measurement is  $1/\sqrt{(2948.49)} = 1.84\%$ . At the medium speed (interval C.V. = 0.92 %) the spatial resolution has been improved whereas a further decrease in the interval C.V. to 0.46 % (low speed) had no apparent impact on the spatial resolution of the system.

It should be noted that one limit of the system in regards to spatial resolution is the spatial resolution of the imaging system. In this case although the reconstructed matrix is of size 256 x 256 with a 0.3 mm pixel size, the hard copy image matrix is only of size 128 x 128 with a corresponding pixel size of 0.6 mm. To further complicate matters, the image display has a magnification effect of 1.6 times that of the object. Using the Grinnell display system one can display a matrix size of 512 x 512 and hence it is possible to view the system limited resolution on the video screen and yet essentially the same results were obtained as with the hard copy display. At high speed (Figure 32) the system spatial resolution was limited to 1/8 of an inch while at medium speed (Figure 33) the spatial resolution is improved to one sixteenth of an inch (approximately 1.5 mm). However, a further decrease in speed to low speed (Figure 34) had little or no effect on the spatial resolution. This is evidence that beyond a certain level statistics are no longer the limiting factor in regards to spatial resolution.

MEASUREMENT 319 17-JAN-80



HOLE DIAMETERS (INCHES) ARE (TOP TO BOTTOM)  $1/32$ ,  $3/32$ ,  $5/32$ ,  
 $1/8$  AND  $1/16$ .

FIGURE 32. HIGH SPEED RESOLUTION

MEASUREMENT 318 17-JAN-80

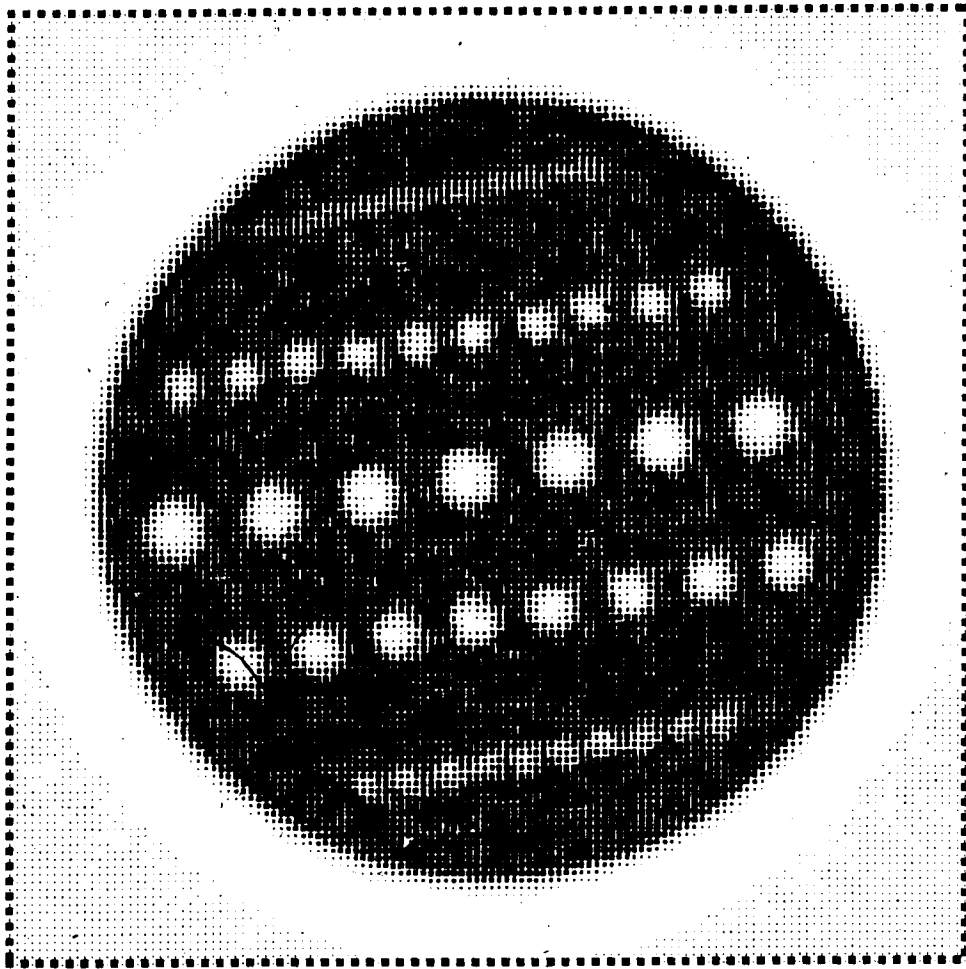


FIGURE 33. MEDIUM SPEED RESOLUTION

MEASUREMENT 317 17-JAN-80 d

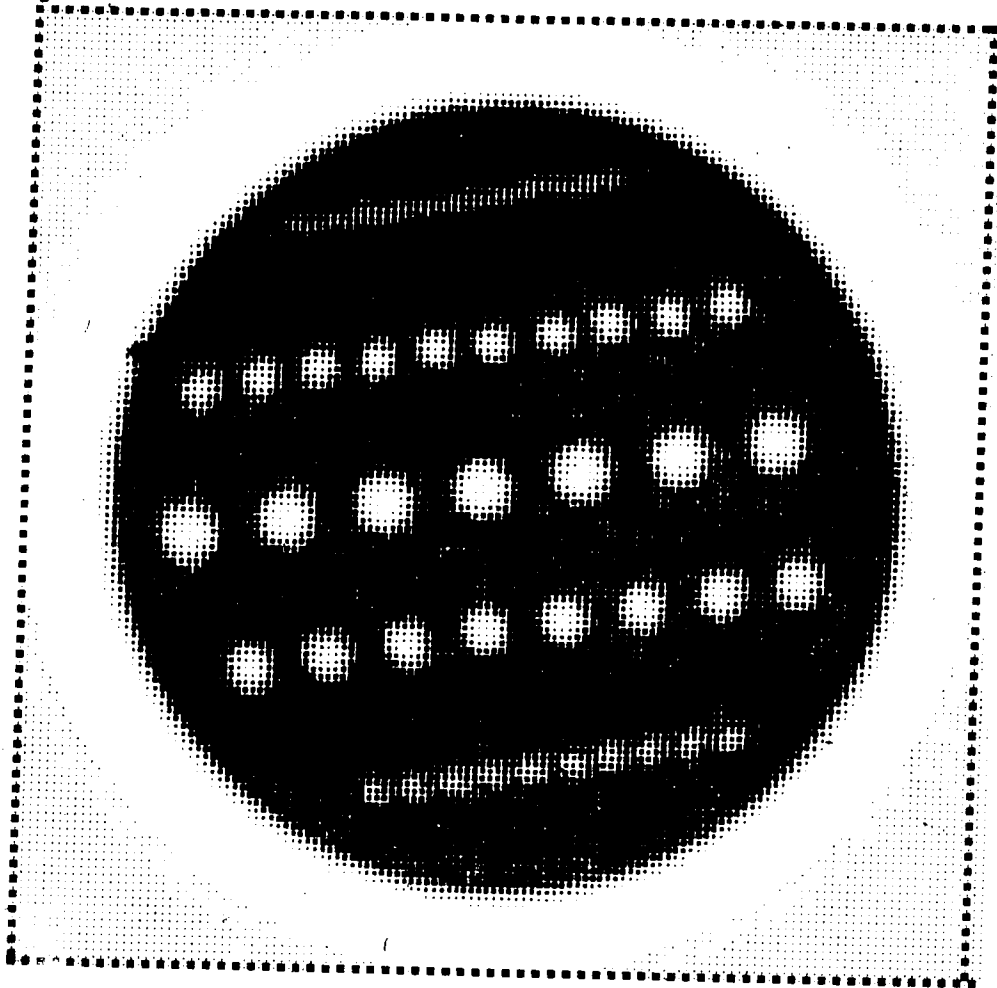


FIGURE 34. LOW SPEED RESOLUTION

## B. Precision

The critical factor for the overall precision of the system is not so much the precision associated with the machine as with the ability to remeasure the patient at exactly the same site since both the amount of trabecular bone and its density vary significantly at sites axially along the arms or legs. This means that precision of the system is predominantly a function of the ability to determine the site of measurement. To reduce these errors in precision due to repositioning use of the scout scan was instituted.

A number of repeat scans were made on a 40 year old male normal (52). Each scan involved repositioning the arm using the scout scan and making three measurements on the arm. The first measurement was made at the site selected by the scout scan while the other two measurements were made at sites two millimeters of either side. These three measurements were then interpolated to produce the same area of bone for analysis purposes as was used in prior analyses. The data obtained from these measurements (Table 2) shows that a precision of better than  $\pm 1\%$  is achievable for both cortical and trabecular bone density.

## C. Accuracy

Accuracy of the scanner is a difficult quantity to define since it relates to a "correct" value being obtained. For measurements of bone this means that the bone would have

PRECISION EVALUATION

Measurement Number	Scan * Number	Bone Area (Pixels)	Trabecular Bone Density	Cortical Bone Density
1	1	3362	0.503	1.301
	-	-	-	-
2	1	3577	0.491	1.250
	2	3293	0.519	1.333
3	1	3552	0.501	1.250
	2	3248	0.522	1.328
4	1	3389	0.509	1.275
	2	3155	0.535	1.370
5	1	3586	0.497	1.237
	2	3308	0.510	1.330

With the above scans interpolated so as to produce a bone area of 3362 the results are as follows

1	3362	0.503	1.301
2	3362	0.512	1.313
3	3362	0.514	1.299
4	3362	0.512	1.286
5	3362	0.507	1.292

These interpolated results, when considering a normal distribution, result in standard deviations of 0.884 % for trabecular bone density and 0.847 % for cortical bone density.

\*Note: Although three scans were made during each measurement only those two scans that were used in the interpolation are included.

TABLE 2.

to be removed and "ashed" to determine the true mineral content. Obviously, this is only possible to perform with cadavers and consequently the sources of data are limited.

To circumvent these problems a solution of di-Potassium Hydrogen Phosphate ( $K_2HPO_4$ ) was used (53). The solution was mixed to a known concentration and placed inside a plexiglass cylinder (Figure 35). CT measurements were made on a number of different concentrations and the resultant linear attenuation coefficients of the image were compared to the known values of the dilute solution. Results of these tests are shown in Table 3 and Figure 36. These results show that although the absolute values may not be entirely accurate, the percentage change in value is quite accurate. Since the mineral content present in bone does vary tremendously from person to person it is measures of percentage changes that are of clinical importance rather than absolute values of mineral density. One reason that the absolute values are of limited accuracy is that the linear attenuation coefficients for the solution are calculated on the basis of a single energy which does not coincide exactly with the energy spectrum of Iodine 125.

#### D. Radiation Dose

Calculations of a theoretical radiological dose (as performed on the following pages) show that the total radiation dose received during the course of a scout scan and three adjacent scans is 0.9 rads.



MEASUREMENT 861 3-JUN-80

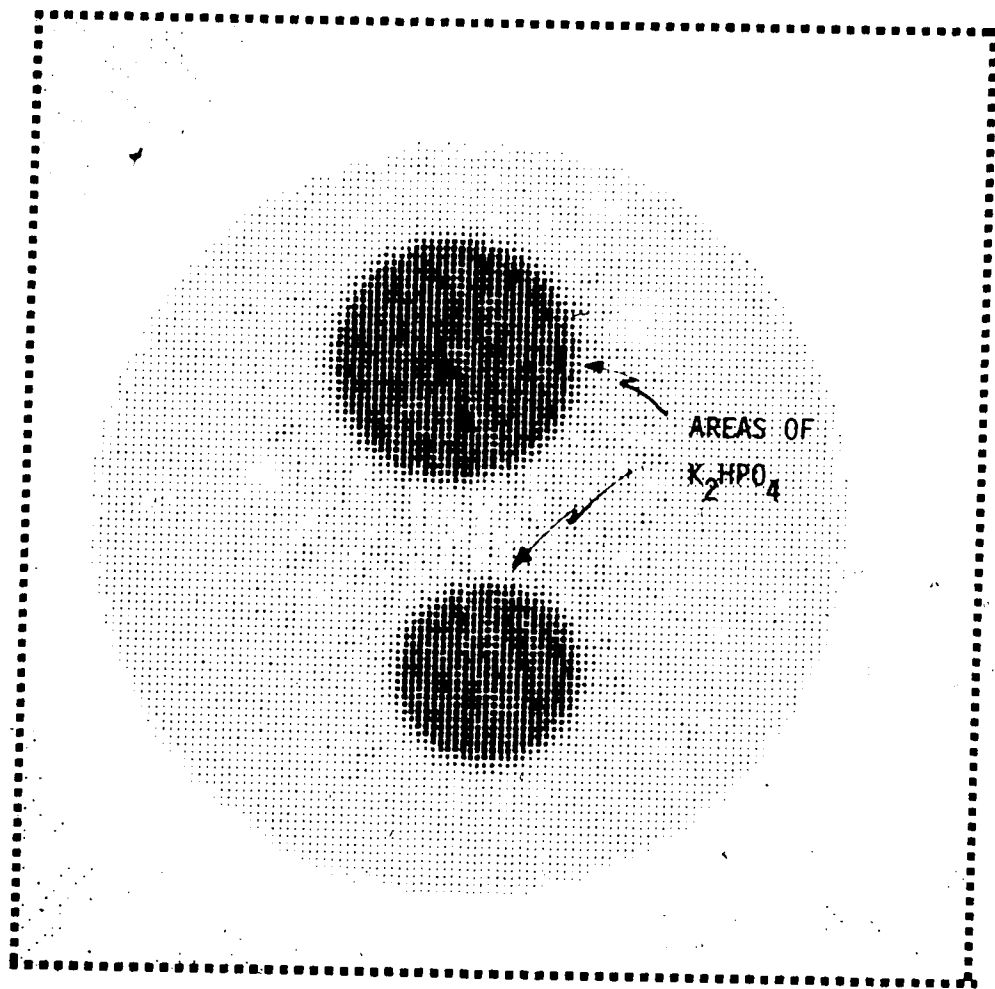


FIGURE 35. TEST CYLINDER

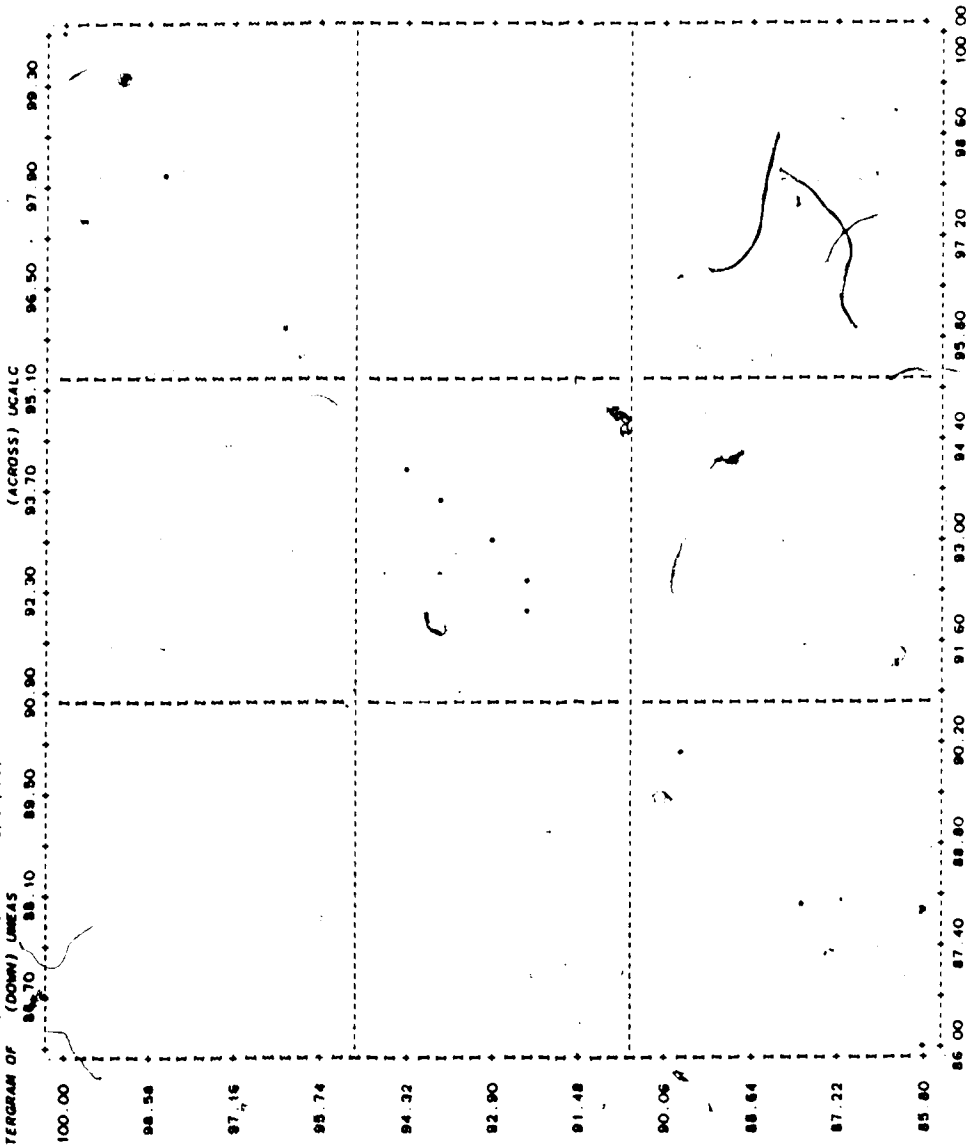
ACCURACY EVALUATION

Measured Linear Attenuation Coefficient (per cm.)	Percent of Maximum Measured Linear Attenuation Coefficient	Calculated Linear Atten. Coefficient (per cm.)	Percent of Maximum Calculated Linear Attenuation Coefficient
1.882	100	1.709	100
1.852	98.4	1.675	98.0
1.814	96.4	1.641	96.0
1.776	94.4	1.606	94.0
1.765	93.8	1.598	93.5
1.747	92.8	1.589	93.0
1.739	92.4	1.581	92.5
1.735	92.2	1.572	92.0
1.690	89.8	1.538	90.0
1.654	87.9	1.504	88.0
1.615	85.8	1.470	86.0

A linear regression of the percent calculated linear attenuation coefficient was run against the percent measured linear attenuation coefficient (using the SPSS package) and found to have a correlation of  $r=0.9987$  and a significance of  $p < 0.0001$

TABLE 3.

FILE NONAME (CREATION DATE = 10/27/80)  
SCATTERGRAM OF

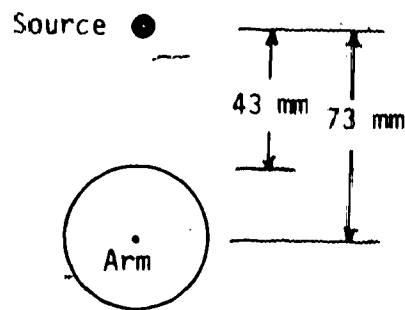


100.00  
98.58  
97.16  
95.74  
94.32  
92.90  
91.48  
90.06  
88.64  
87.22  
85.80

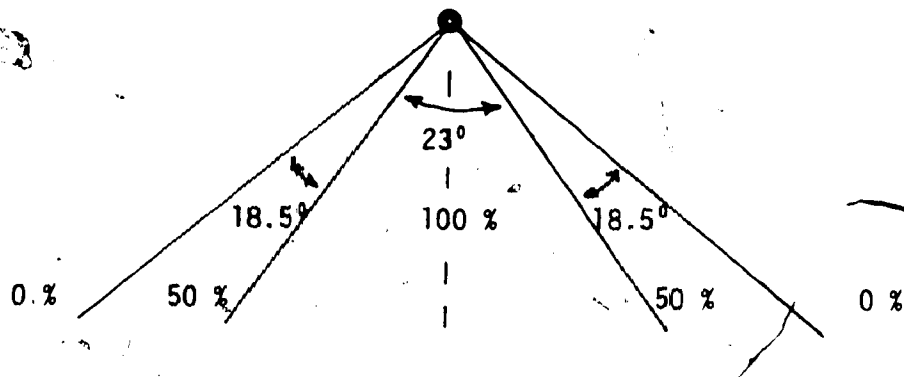
FIGURE 36. SYSTEM ACCURACY

Radiological Dose

Assume that an arm of diameter 60 mm is placed in the center of the scan area. This results in a distance of 43 mm from the source to the nearest point on the arm.



At a distance of 43 mm the source-collimator configuration was found to produce the following approximate intensity distribution.



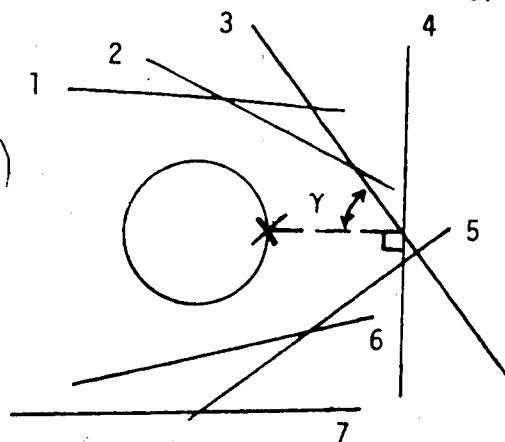
The scanner moves a distance of 106.2 mm in 12.89 sec resulting in an average speed of 8.24 mm / sec. The area irradiated at 100 % intensity consists of a length L, where  $L = 2 \tan (23^\circ/2) (43 \text{ mm}) = 17.5 \text{ mm}$ . The area irradiated at an average intensity of  $1/2(100\% + 50\%) = 75\%$  consists

of 2 lengths, each one of length  $L_1$ , where

$$L_1 = 1/2 (2 \tan (60^\circ/2) 43 \text{ mm} - 17.5 \text{ mm}) = 16.08 \text{ mm.}$$

Thus the total length irradiated at effectively 100% is  
 $17.5 (100\%) + 2(16.08)(75\%) = 41.61 \text{ mm}$  which at a speed of  
 $8.24 \text{ mm / sec}$  means an effective (100%) irradiation time of  
 $41.61 \text{ mm} / 8.24 \text{ mm/sec} = 5.05 \text{ seconds.}$

This is the irradiation time for one translation. However,  
 each scan consists of 7 translations made at varying angles.



The rotation between angles is  $25.71^\circ$  and the approximate "hotspot" (area subjected to maximum radiation) is that point on the arm perpendicular to translation number 4 (denoted by point X).

Thus at  $\gamma = 90^\circ$  the irradiation is 100% while at  $\gamma = 0^\circ$  the irradiation is 0%. Hence irradiation is proportional to  $\sin \gamma$ .

Translation 1	$\gamma = 90^\circ - 3(25.71^\circ) = 12.87^\circ$	$\sin \gamma = 0.22$
Translation 2	$\gamma = 90^\circ - 2(25.71^\circ) = 38.58^\circ$	$\sin \gamma = 0.62$
Translation 3	$\gamma = 90^\circ - 1(25.71^\circ) = 64.29^\circ$	$\sin \gamma = 0.90$
Translation 4	$\gamma = 90^\circ$	$\sin \gamma = 1.00$
Translation 5	$\gamma = 64.29^\circ$	$\sin \gamma = 0.90$
Translation 6	$\gamma = 38.58^\circ$	$\sin \gamma = 0.62$
Translation 7	$\gamma = 12.87^\circ$	$\sin \gamma = 0.22$

Therefore, for one scan the total irradiation time (100% intensity) at the hotspot is  $4.48 (5.05 \text{ sec}) = 22.62 \text{ seconds}$ .

A new source of 1.5 Ci  $I^{125}$  was measured using an ionization chamber at a distance of 0.5 meters (so that the entire chamber was irradiated) and found to have a dose rate of 11 mr/min. Using the inverse square law the dose rate at 43 mm would be  $11 \text{ mr/min} (500/43)^2 = 1487 \text{ mr/min} = 24.79 \text{ mr/sec}$ . This means that the total dose per scan at the hotspot is  $24.79 \text{ mr/sec} (22.62 \text{ sec}) = 560 \text{ mr}$ . Since the speed of the scout scan is the same as for a normal scan the effective (100%) irradiation time is 5.05 sec leading to a dose of  $5.05 \text{ sec} (24.79 \text{ mr/sec}) = 125 \text{ mr}$ . Assuming adjacent measurements produce a 50 % increase in dose the total exposure dose for 1 scout scan and 3 adjacent scans is  $1.5(560 + 125) = 1027.5 \text{ mr} \approx 1 \text{ r (roentgen)}$ . At 30 KeV this is approximately equal to an absorbed dose of 0.9 rad.

Although these theoretical calculations do provide a rough estimate of dose there are a number of associated problems. One major problem is the assumption that absorption of radiation is only significant at the surface. Although this may be true for denser objects with high linear attenuation coefficients it is not true for skin. The linear attenuation coefficient of skin is approximately 0.45/cm (for 30 KeV) which means that some 1.5 cm of skin must be traversed before the intensity of the radiation is down by a factor of 2. Since there is a limited amount of skin at the forearm, radiation passing through skin only will have a significant effect on the dose rate whether or not it directly impinges upon the area of consideration. Although most rays do pass through some bone and thereafter do not contribute appreciably to skin dose it should be realized that there is an element of variation from person to person.

Another area of concern is the effects of scattered radiation from the bones and their effect on the dose at a particular point. It is relatively complicated to account for scatter on a theoretical basis and as such the use of Thermo-Luminescent Detectors (TLD's) has been suggested.

### Thermo-Luminescent Detectors

TLD's are capsules of powder or crystals that react chemically when exposed to radiation. After exposure to radiation the powder is removed from the capsules and heated up. When heated the powder produces photon flashes the number and intensity of which are proportional to the radiation exposure.

It is presently being proposed that a number of holes be drilled in a plexiglass phantom and filled with TLD powder. Subsequent to making a number of measurements on the phantom the powder is to be removed and tested to determine the radiation exposure. The plexiglass phantom will contain aluminum tubes to simulate the radius and ulna and will be made in the approximate size and shape of a human forearm. Measurements of dose performed in this manner should produce a profile of the radiation dose throughout a human forearm.

#### E. Contrast Resolution

Contrast resolution could be measured by examining the limiting spatial resolution with differing contrast media in the holes. One possible contrast media is di-Potassium Hydrogen Phosphate ( $K_2HPO_4$ ) mixed in a water base. If solutions of varying concentration were placed in the 1/16 th of an inch diameter holes then the system limited contrast resolution would be defined by comparing the smallest linear attenuation coefficient of the imageable solutions with that of plexiglass. The major difficulties in



these measurements will be placing the proper concentration solutions in the holes and ensuring that no air bubbles are present. Measurements of contrast resolution have not been made due to these difficulties and the limited usefulness of such measurements.

## VI. System Limitations and Future Plans

Four of the major limitations at present are: (1) statistical limitations due to the use of a radioisotope photon source, (2) a lengthy scanning time due to use of a second (versus a third or fourth) generation CT scanner, (3) a lack of flexibility in regards to scanner control, and (4) an inability to view the image immediately after scanning due to limited processing facilities. This chapter will explore these limitations and will suggest ways to reduce or eliminate them.

### A. X-Ray Tube

Subject to appropriate funding present plans include the purchase of a mini-X-ray tube. As a result of physical considerations photon flux is more limited in the case of a radioisotope source than for an X-ray tube. Although use of an X-ray tube may result in higher radiation dose rates it will also facilitate a reduced scan time and hence the net radiation exposure may not be radically altered. With the aid of filters the X-ray tube will also allow a greater selection of photon energies to be used. This may allow the scanner to perform elemental identifications through the use of differential energy scans and to be used for scans of areas of high radiological attenuation such as the knee. The use of filters may also reduce the problems of beam hardening caused by the multi-energy X-ray radiation. Although beam hardening will be a problem, so long as the

"raw" data is available, it is possible to correct for.

### B. System Three

Present plans include the construction of a generation three system. This improvement will result in a substantial decrease in scan time hence reducing movement artifacts, improving patient comfort and reducing the dose of radiation.

### C. Control System

The major constraint at present is that the control programs are "locked" into EPROMs. In order to alter any of the scan parameters, such as speed, scan length, distance between projections and/or the angle between profiles, a new program must be written into the EPROMs. To circumvent this problem it is proposed that the EPROMs be programmed with a number of basic subroutines and that all control parameters be loaded into the MPU from external sources. One of the subroutines contained in the EPROMs would be a program that reads data into the MPU via the PIA (M6820). Data to be read into the MPU would be loaded into the HP 2100 from either the console or a series of programs contained on magnetic tape. This data will be subsequently transferred from the HP 2100 into a memory module contained in the CAMAC system. The transfer of data from the HP to the memory module (4000 16 bit words) will free the HP to perform other functions subsequent to loading the CAMAC. Control parameters will be

loaded from the memory module to the 512 bytes of RAM (M6810) contained in the MPU. Direct interrupts will also be provided between the MPU and the HP 2100 computer. The read program which is the subroutine that reads data from the memory module to the microprocessor unit has been assembled and is included in the appendix.

#### D. Processing Facilities

A new 32 bit minicomputer has been ordered (SEL 32/57) and delivery is expected for the fall of 1980. Purchase of an array processor dedicated to the reconstruction is also being considered and appears likely at this point in time. The resultant upgrading of computing facilities will allow the image to be displayed on the Grinnell imaging system at the same time or shortly after a scan is performed. This means that the validity of the scan can be checked immediately and should another scan be required the patient will still be present.

## References

1. Bocage EM: Patent No. 536,464; Paris France 1921 (Quoted in 'History of Tomography' by J Massiot, 1974 Medica Mundi, 19(3), 106-115).
2. Radon J: Ueber die Bestimmung von Funktionen durch ihre Integralwerte laengs gewisser Mannigfaltigkeiten. Ber Verh Saechs Akad Wiss 69:262-277, 1917.
3. Bracewell RN: Strip integration in radioastronomy. Australian Journal of Physics 9:198-211, 1956.
4. Cormack AM: Representation of a function by its line integrals with some radiological applications. Journal of Applied Physiology 34:2722-2727, 1963.
5. Hounsfield GN: Computerized transverse axial scanning (tomography): Part 1. Description of system. British Journal of Radiology 46:1016-1022, Dec. 1973.
6. Health Research Group, Washington D.C.: Computerized axial tomography (CAT) scanners is fancier technology worth a billion dollars of health consumer's money? U.S. Department of Commerce - National Technical Information Service, HRP-0019236, 1977.
7. Brooks RA, Di Chiro G: Principles of computer assisted tomography (CAT) in radiographic and radioisotopic imaging. Phys. Med. Biol. 21:681-732, 1976.
8. Rügsegger P, Elsasser U: Computerassistierte Photonenabsorptionsmessung zur Quantifizierung der Spongiosadichte. Premier Symposium CEMO, La Chaux-de-Fonds, Oct. 5-8, 1975.

9. Snyder W, et al: Report of the Task Group on Reference Man, ICRP 23. Oxford, Pergamon Press, 1975.
10. Overton TR, Silverberg DS, Rigal WM, Friedenbergl L: University of Alberta bone mineral analysis system - performance and clinical application. (In) Proceedings of International Conference On Bone Mineral Measurement, ed. RB Mazess, Chicago, DHEW Publication No. (NIH) 75-683, 1973.
11. Elsasser U: Quantifizierung der Spongiosadichte an Rohrenknochen mittels Computertomographie. Diss. ETH, Zurich, 1977.
12. Guyton A: Textbook of Human Physiology. Philadelphia, Saunders, 1971.
13. Heaney RP: Bone physiology and calcium homeostasis. (In) Textbook of Medicine, ed. by PB Beeson and W McDermott, Philadelphia, Saunders, 1971.
14. Sodeman WA, Sodeman WA: Pathologic Physiology, Philadelphia, Saunders, 1967.
15. Frost HM: Treatment of osteoporoses by manipulation of coherent bone cell populations, (In) Clinical Orthopaedics and Related Research, JB Lippincott Co., 1979.
16. Brown DM: Rickets and osteomalacia. (In) Current Therapy 1977, ed. by HF Conn, Philadelphia, Saunders, 1977.
17. Henry JB: Clinical chemistry: clinico pathologic correlations in bone diseases. (In) Clinical Diagnosis, ed. by I Davidsohn and JB Henry, Philadelphia, WB

- Saunders Co., 1974.
18. Saville PD: Osteoporosis. (In) Current Therapy 1977, ed. by HF Conn, Philadelphia, Saunders, 1977.
  19. Cameron JR, Sorenson J: Measurement of bone mineral in vivo: An improved method. Science 142:230-232, 1963.
  20. Cameron JR, Mazess RB, Sorenson J: Precision and accuracy of bone mineral determination by direct photon absorptiometry. Invest. Radiol. 3:141-150, 1968
  21. Smith DM, Johnstone CC, Yu P: In vivo measurement of bone mass, its use in demineralization states such as osteoporosis. Journal of American Medical Association 291:325-329, 1972.
  22. Goldsmith NF, Johnstone JO, Ury H, Vose G, Colbert C: Bone-mineral estimation in normal and osteoporotic women. Journal of Bone and Joint Surgery 53A1:83-100, Jan. 1971.
  23. Lewellen TK, Nelp WB: Total body calcium analysis using the  $^{40}\text{Ca}(n,\alpha)^{37}\text{Ar}$  Reaction. NASA Technical Report contract number NAS9-13029.
  24. Webber CE, Kennett TJ: Bone density measured by photon scattering: A system for clinical use. Dep't of Nuclear Medicine, McMaster University Medical Centre.
  25. Hinderling Th, Rügsegger P, Anliker M: C.T. reconstruction from hollow projections: an application to in vivo evaluation of artificial hip joints. Journal of Computer Assisted Tomography 3(1):52-57, Feb/1979.
  26. Brooks RA, DiChiro G : Theory of image reconstruction in

- computed tomography. *Radiology* 117:561-572, December 1975
27. Shepp LA, Kruskal JB, Logan BF: Computerized tomography: the new medical x-ray technology. Bell Laboratory Publication 07974, Murray Hill, New Jersey, 1974.
  28. Ledley RS: Introduction to computerized tomography. *Computerized Biological Medicine* 6:239-246, 1976.
  29. McCullough EC, Payne JJ: X-ray transmission computed tomography. *Medical Physics* 4(2), Mar./Apr. 1977.
  30. Bates RHT, Peters TM: Towards improvements in tomography. *New Zealand Journal of Science* 14:883-896.
  31. Bracewell RN, Riddle AC: Inversion of fan-beam scans in radio astronomy. *Journal of Astrophysics* 150:427-434, 1967.
  32. Peters TM, Lewitt RM: Computed tomography with fan beam geometry. *Journal of Computer Assisted Tomography* 1(4), 1977.
  33. Shepp LA, Logan BF: Reconstructing interior head tissues from x-ray transmissions. Bell Laboratories Report, Murray Hill, New Jersey, 1974.
  34. Ramachandran GN, Lakshminarayanan AV: Three-dimensional reconstruction from radiographs and electron micrographs: application of convolutions instead of Fourier transforms. *Proc. Natl. Acad. Sci. U.S.* (68), 2236-2240.
  35. Stanton L: *Basic Medical Radiation Physics*, New York, Meredith Corporation, 1969.



36. Siegbahn K: Alpha-, Beta- And Gamma-Ray Spectroscopy, Amsterdam, North-Holland Publishing Co., 1966.
37. Larsson S, Bergstrom M, Dahlqvist I, Israelsson A, Lagergren C: A method for determining bone mineral content using Fourier image reconstruction and dual source technique. *Journal of Computer Assisted Tomography* 2:347-351, July 1978. *Journal of Computer Assisted Tomography* 2:184-188, 1978.
38. Latchaw RE, Payne JT, Gold LHA: Effective atomic number and electron density, as measured with a computed tomographic scanner: computation and correlation with brain tumour histology. *Journal of Computer Assisted Tomography* 2:199-208, 1978.
39. Chesler DA, Riederer SJ, Pelc NJ: Noise due to photon counting statistics in computed x-ray tomography. *Journal of Computer Assisted Tomography* 1(1):64-67, 1977.
40. Gore JC, Tofts PS: Statistical limitations in computed tomography. *Phys. Med. Biol.* 23:1176-1182, 1978.
41. Riedler SJ, Pelc JN, Chesler DA: The noise power spectrum in computed x-ray tomography. *Phys. Med. Biology* 23(3):446-454, 1978.
42. Tretiak OJ: Noise limitations in x-ray computed tomography. *Journal of Computer Assisted Tomography* 2:477-480, 1978.
43. Brooks RA, Di Chiro G: Statistical limitations in x-ray reconstruction tomography. *Medical Physics* 3:237-240,

- 1976.
44. Evans RD: The Atomic Nucleus, New York, McGraw-Hill, 1955.
  45. Brooks RA, Di Chiro G: Beam hardening in x-ray reconstructive tomography. Phys. Med, Biol. 21:390-398, 1976.
  46. Sandrik JM, Judy PF: Effects of the polyenergetic character of the spectrum of iodine 125 on the measurement of bone mineral content. Department of Radiology, University of Wisconsin Medical Center, Madison Wisconsin.
  47. Kijewski PK, Bjarngard BE: Correction for beam hardening in computed tomography. Medical Physics 5(3), May/June 1978.
  48. Ruegsegger P, Hangartner Th, Keller HU: Standardization of C.T. images by means of a material selective beam hardening correction. Journal of Computer Assisted Tomography 2:253-262, July 1978.
  49. General Electric: CT/T technology continuum, Milwaukee, GE Medical Systems Division, 1979.
  50. Ruegsegger P, Niederer P, Anliker M : An extension of classical bone mineral measurements. Annals of Biomedical Engineering 2:194-205, 1974
  51. Lancaster D: TTL Cookbook, Indianapolis, HW Sams & Co., 1974.
  52. Hangartner Th, Ridley JD: Internal communication.
  53. Ridley JD: Internal communication.

54. Hangartner Th: Internal communication.
55. Medical Internal Radiation Dose Committee of the Society of Nuclear Medicine: MIRD Pamphlet No. 10, Iodine-125 electron capture decay.

$^{125}_{53}\text{I}$  DECAY MECHANISM  
 $^{53}$

---

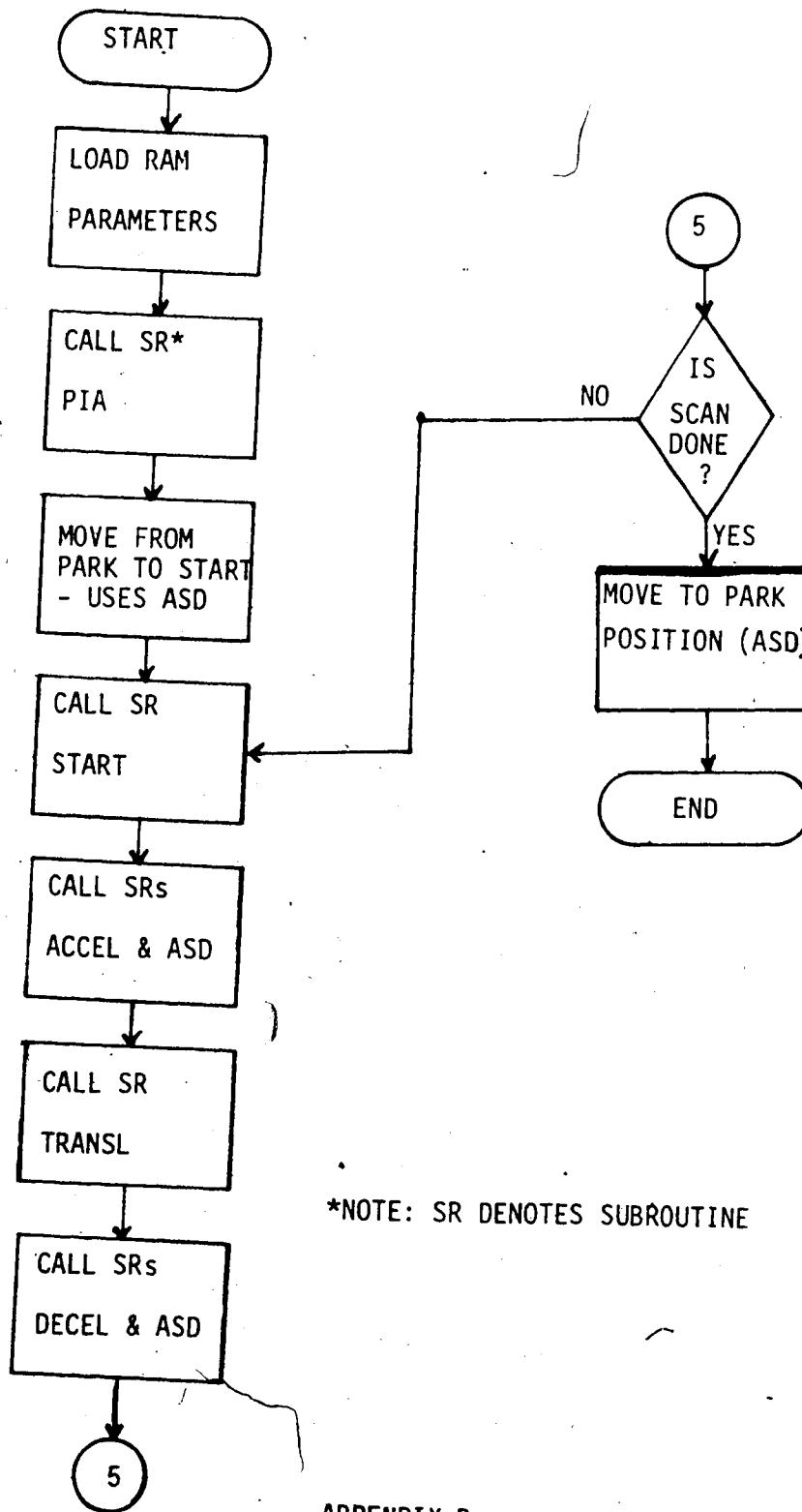
$^{125}_{53}\text{I}$  decays via electron capture to  $^{125}_{52}\text{Te}$  and in doing

so gives off a 35.4 KeV gamma ray. This gamma ray will:

- 1) appear on the outside .0666 times per disintegration;
- 2) cause a k alpha-1 x-ray .7615 times per disintegration (27.4 KeV);
- 3) cause a k alpha-2 x-ray .3906 times per disintegration (27.2 KeV);
- 4) cause a k beta-1 x-ray .2056 times per disintegration (30.9 KeV);
- 5) cause a k beta-2 x-ray .0426 times per disintegration (31.8 KeV);
- 6) cause an L x-ray .2226 times per disintegration (3.7 KeV).

Thus in general the original gamma ray energizes an electron in the k shell causing it to move out of its orbit. This gap is filled by a loose electron which, in falling into the k shell, gives off an x-ray of approximately 27.5 KeV. The associated half-life is 60.2 days.

NORMAL SCAN



\*NOTE: SR DENOTES SUBROUTINE

APPENDIX B.

\*\*\* APPENDIX C - CONTAINS ALL MAIN PROGRAMS AND ALL SUBROUTINES (EXCEPT READ) \*\*\*

Motorola M68SAM Cross-Assembler

```

00001      8004      EQU      $8004
00002      8004      EQU      $8004
00003      8005      EQU      $8005
00004      0000      EQU      $0000
00005      NAM      DETB
00006      6000      ORG      $6000
00007
00008
00009
00010
00011
00012
00013
00014
00016
00017
00018
00019
00020
00021
00022
00023
00024
00025
00026
00027      6000      86      OF
00028      6002      97      2C
00029      6004      86      07
00030      6006      97      2D
00031      6008      86      0C
00032      600A      97      32
00033      600C      86      08
00034      600E      97      33
00035      6010      86      04
00036      6012      97      34
00037      6014      86      05
00038      6016      97      35
00039      6018      BD      C278
00040
00041
00042
00043
00044
00045      601B      86      17

* REVISED APR 24, 1980
* THIS PROGRAM WILL BE USED TO PERFORM
* A MULTI-DETECTOR SCAN USING 8 DETECTORS.
* USING A 1:1 PULLEY RATIO THE TRANSLATION
* IS 16992 STEPS. (106.2 MM).
* 1 MM = 1600 STEPS.
* BE SCANNED WITH THIS ARRANGEMENT IS 76.8 MM DIAMETER.
* THE SCANNER WILL COLLECT 1416 DATA. FROM THE
* PARK POSITION THE SCANNER MUST MOVE BACK (-)
* 1447 STEPS (+200 FOR ACCEL.) BEFORE
* STARTING THE SCAN.
* MOTOR PULSES ARE SENT EVERY 466 CYCLES
* (APPROX. 760 US) AND DATA PULSES ARE SENT TO
* THE HP EVERY 12 MOTOR PULSES. THE SCANNER IS TO
* ROTATE 25.71 DEG. AFTER EACH TRANSLATION & IS
* TO PERFORM 7 TRANSLATIONS & 6 ROTATIONS.
* EACH TRANSLATION TAKES APPROX. 13 SECONDS
LDA A #50F
STA A M+44
LDA A #07
STA A M+45
LDA A #12
STA A M+50
LDA A #08
STA A M+51
LDA A #04
STA A M+52
LDA A #05
STA A M+53
JSR PIA
* MOVE FROM PARK TO START POSITION
* ONE GROUP OF 1647 PULSES
* MAKES USE OF THE R21 RAMP
* 1647=400 + 1247*1
LDA A #517
; TRANSLATIONAL DIRECTION
; TRANSLATIONAL DIRECTION
;# OF TRANSLATIONS
;# OF MOTOR STEPS / HP SIGNAL
; DETERMINES DELAY IN TRANSLATION
; DETERMINES DELAY IN TRANSLATION
; DETERMINES DELAY IN TRANSLATION
; CALLS INIT AND F AS WELL

```

```

00046 601D 97 00 STA A M
00047 601F CE 04DF LDX #1247
00048 6022 DF 2A STX M+42
00049 6024 CE 066F LDX #1647
00050 6027 DF 25 STX M+37
00051 6029 BD C000 JSR ASD
00052 602C BD C29B ST JSR START
00053 602F C6 1B LDA B #1B ; TELL HP RAMP IS BEGINNING
00054 6031 F7 8004 STA B ORA
00055 6034 BD C28C JSR DELAY
00056 6037 C6 1F LDA B #1F
00057 6039 F7 8004 STA B ORA
00058 BEGIN ACCELERATION
00059 603C BD C1F5 JSR ACCEL
00060 603F BD C000 JSR ASD
00062 * SCAN - UP PROVIDES A MOTOR PULSE EVERY 466 CYCLES & A HP PULSE
00063 * EVERY 12 MOTOR PULSES
00064 * HP PULSE IS SENT EVERY M+46 MOTOR PULSES
00065 6042 CE 4260 LDX #16992 ; PULSES REQUIRED FOR SCAN
00066 6045 BD C280 JSR TRANSL
00067 * DELAY BETWEEN PULSES = 4*68 + 42 + 8*12 + 56 = 466 CYCLES
00068 6048 BD C208 JSR DECEL
00070 604B 7A 002D DEC M+45 ; IS SCAN FINISHED?
00071 604E 27 0C BEQ JMPE
00072 6050 BD C28D JSR R8D
00073 6053 96 2C LDA A M+44
00074 6055 88 18 EOR A #18
00075 6057 97 2C STA A M+44
00076 6059 7E 602C JMP ST
00078 * MOVE BACK TO PARK POSITION
00079 * MUST MOVE BACKWARD 15744 PULSES
00080 * SHOULD MOVE BACK 15745
00081 * HOWEVER SCAN APPEARS TO BE OUT
00082 * ONE PULSE AT SOME POINT
00083 605C 86 17 JMPE LDA A #17
00084 605E 97 00 STA A M
00085 6060 CE 3BFO LDX #15344
00086 6063 DF 2A STX M+42
00087 6065 CE 3D80 LDX #15744
00088 6068 DF 25 STX M+37
00089 606A BD C000 JSR ASD
00090 * ROTATE BACK TO PARK POSITION
00091 * MUST ROTATE BACK 31080 PULSES
00092 606D CE 77D8 LDX #30680 ; 30680*M+12 PULSES
00093 6070 DF 2A STX M+42
00094 6072 CE 7968 LDX #31080
00095 6075 DF 25 STX M+37

```

```

00096 6077 86 1D
00097 6079 97 00
00098 607B BD C000
00099 607E 3F
00103 6090
00104
00105
00106
00107
00108
00109
00110
00111
00112
00113
00114
00115
00116 6090 86 OF
00117 6092 97 2C
00118 6094 86 02
00119 6096 97 2D
00120 6098 86 02
00121 609A 97 32
00122 609C 86 01
00123 609E 97 33
00124 60A0 86 13
00125 60A2 97 34
00126 60A4 86 08
00127 60A6 97 35
00128 60A8 BD C278
00130
00131
00132
00133
00134 60AB 86 OF
00135 60AD 97 00
00136 60AF CE 0060
00137 60B2 DF 2A
00138 60B4 CE 00F0
00139 60B7 DF 25
00140 60B9 BD C000
00141 60BC BD C298 ST1
00142 60BF C6 1B
00143 60C1 F7 8004
00144 60C4 BD C28C
00145 60C7 C6 1F

LDA A #S1D
STA A M
JSR ASD
SWI
ORG $6090
* NAM CENT
* THIS IS A PROGRAM WHICH WILL BE USED TO CENTER
* THE SCANNER. IT'S USE WILL BE REQUIRED WHENEVER ANY OF
* THE MECHANICS OF THE SYSTEM (SUCH AS THE SOURCE)
* ARE CHANGED. USING A 1:1 RATIO ON THE PULLEYS
* THE TRANSLATIONAL MOTION IS 6500 STEPS
* PULSES ARE SENT TO THE HP EVERY 2 MOTOR PULSES
* (EVER 6.79 MS OR EVERY 4172 CYCLES).
* THE TRANSLATION TAKES 22. SEC. AT WHICH POINT THE
* SCANNER IS ROTATED THROUGH 180 DEG. AND THEN THE TRANSLATION
* IS PERFORMED ONE ADDITIONAL TIME AND THE SCANNER IS ROTATED
* BACK. PRESET FROM THE PARK POSITION IS +3600 -32 FOR ACCEL = 3568 STEPS
LDA A #S0F
STA A M+44
LDA A #02
STA A M+45
LDA A #02
STA A M+50
LDA A #01
STA A M+51
LDA A #19
STA A M+52
LDA A #08
STA A M+53
JSR PIA
* MOVE FROM PARK TO START POSITION
* ONE GROUP OF 3568 PULSES
* MAKES USE OF THE R21 RAMP
* 3568 = 400 * 9
LDA A #S0F
STA A M+168
LDX M+168
STX M+168
LDX #3568
STX M+37
JSR ASD
JSR START
LDA B #S1B
STA B ORA
JSR DELAY
LDA B #S1F

: # OF ROTATIONS
: PULSE TO HP EVERY 2 STEPS
: DETERMINES DELAY BETWEEN STEPS
: DETERMINES DELAY BETWEEN STEPS
: DETERMINES DELAY BETWEEN STEPS
: CALLS INIT AND F AS WELL
: TRANSLATION DIRECTION
: TELL HP RAMP IS BEGINNING

```



```

00146 60C9 F7 8004      STA B  ORA
00147
00148
00149
00150
00151
00152 60CC BD C1F5      JSR  ACCEL
00153 60CF CE 0020      LDX  #32
00154 60D2 DF 25        STX  M+37
00155 60D4 BD C000      JSR  ASD
00156 60D7 CE 1964      LDX  #6500      ;PULSES REQUIRED FOR SCAN
00157 60DA BD C2B0      JSR  TRANSL
00158
00159
00160 60DD BD C242      JSR  DECC32
00161
00162
00163
00164
00165
00166
00167
00168 60E0 96 2D        LDA  A  M+45
00169 60E2 81 02        CMP  A  #02
00170 60E4 27 04        BEQ  K5
00171 60E6 86 1D        LDA  A  # $1D
00172 60E8 97 00        STA  A  M
00173 60EA 7A 002D K5   DEC  M+45
00176 60ED CE 8C2A      LDX  #35882     ;35882*M+12
00177 60F0 DF 2A        STX  M+42
00178 60F2 CE 8DBA      LDX  #36282
00179 60F5 DF 25        STX  M+37
00180 60F7 BD C000      JSR  ASD
00181 60FA 96 2D        LDA  A  M+45
00182 60FC 27 09        BEQ  JMPE1
00183 60FE 96 2C        LDA  A  M+44
00184 6100 88 18        EOR  A  # $18
00185 6102 97 2C        STA  A  M+44
00186 6104 7E 60BC      JMP  ST1
00188
00189
00190 6107 86 17        * MOVE BACK TO PARK POSITION
00191 6109 97 00        * MUST MOVE FORWARD 3568 STEPS
00192 610B CE 0DFO      JMPE1 LDA A # $17
00193 610E DF 25        STA  A  M
00194 6110 CE 0C60      LDX  #3568
00195 6113 DF 2A        STX  M+37
                                LDX  #3168
                                STX  M+42
                                ; CHANGE TRANSLATION DIRECTION

```

\* SCAN - UP PROVIDES A MOTOR PULSE EVERY 2086 CYCLES & A HP PULSE  
 \* EVERY 412 CYCLES (EVERY 2 MOTOR PULSES)  
 \* HP PULSE IS SENT EVERY M+46 MOTOR PULSES  
 \* ACCELERATE UP TO SPEED  
 \* DELAY BETWEEN PULSES = 98 + 12 + 19\*104 = 2086 CYCLES  
 \* DECEL.  
 \* THIS IS A PROGRAM DESIGNED TO OBTAIN A SUITABLE RAMP  
 \* FOR ROTATION OF 180 DEGREES.  
 \* IT MAKES USE OF A GENERAL SUBROUTINE ASD (ACCELERATION, SPEED, DECELERATION  
 \* 35882 PULSES ARE  
 \* REQUIRED AT MAX. FREQ. WE WILL USE 35882 GROUPS  
 \* 1 PULSE

```

00196 6115 BD C000      JSR   ASD
00201                   * NAM SSCAN
00202 6140              * ORG   $6140
00203                   * (SCOUT SCAN)
00204                   * THIS SCAN IS USED TO AID IN ACCURATE REPOSITIONING
00205                   * OF THE ARM. THE SCANNER WILL ROTATE 90 DEGREES. PRESET
00206                   * A DISTANCE OF +3125 - 200 (FOR ACCEL.) STEPS FROM THE PARK POSITION
00207                   * AND THEN START MEASUREMENTS. THERE WILL BE 26 MEASUREMENTS
00208                   * EACH CONSISTING OF A SINGLE SCAN OF 7848 STEPS AND 654 INTERVALS
00209                   * (760 US / STEP). THERE IS A 2 SEC. DELAY BETWEEN EACH MEASUREMENT
00210                   * TO ALLOW THE ARM POSITION TO BE ADJUSTED. THE SCANNER IS THEN SET
00211                   * BACK TO THE PARK POSITION AND IS ROTATED BACK TO ITS ORIGINAL POSITION
00212 6140 86 OF       LDA A #50F
00213 6142 97 2C      STA A M+44
00214 6144 86 1A      LDA A #26
00215 6146 97 2D      STA A M+45
00216 6148 86 OC      LDA A #12
00217 614A 97 32      STA A M+50
00218 614C 86 08      LDA A #08
00219 614E 97 33      STA A M+51
00220 6150 86 04      LDA A #04
00221 6152 97 34      STA A M+52
00222 6154 86 05      LDA A #05
00223 6156 97 35      STA A M+53
00224 6158 BD C278    JSR   PIA
00225                   * 90 DEGREES=18141 STEPS
00226 615B CE 454D    LDX   #17741
00227 615E DF 2A      STX   M+42
00228 6160 CE 46DD    LDX   #18141
00229 6163 DF 25      STX   M+37
00230 6165 BD C000    JSR   ASD
00231                   * MOVE FROM PARK TO START POSITION
00232                   * ONE GROUP OF 2925 PULSES
00233                   * MAKES USE OF THE RAMP
00234                   * 2925 = 400 + 2525*1
00235 6168 86 OF       LDA A #50F
00236 616A 97 00      STA A M
00237 616C CE 090D    LDX   #2525
00238 616F DF 2A      STX   M+42
00239 6171 CE 086D    LDX   #2925
00240 6174 DF 25      STX   M+37
00241 6176 BD C000    JSR   ASD
00242 6179 BD C29B    JSR   START
00243 617C C6 1B      LDA B #51B
00244 617E F7 8004    STA B ORA
00245                   * TELL HP RAMP IS BEGINNING

```

```

00246 61B1 BD C28C      JSR   DELAY
00247 6184 C6 1F        LDA B  #31F
00248 6186 F7 8004      STA B  ORA
* BEGIN ACCELERATION
00250 6189 BD C1F5      JSR   ACCEL
00251 618C BD C000      JSR   ASD
00252
00253
00254
00255 * SCAN - UP PROVIDES A MOTOR PULSE EVERY 1010 CYCLES & A HP PULSE
00256 618F CE 1EAB      * EVERY 12 MOTOR PULSES
00257 6192 BD C2B0      * HP PULSE IS SENT EVERY M+46 MOTOR PULSES
00258 LDX #7848             * PULSES REQUIRED FOR SCAN
00259 JSR  TRANSL
* DELAY BETWEEN PULSES = 152 + 42 + 68*4=466 CYCLES
* DECELERATION
00260 6195 BD C208      JSR   DECEL
00261 6198 7A 002D      DEC  M+45
00262 619B 27 18        BEQ  JMPE2
00263 619D 96 2C        LDA A  M+44
00264 619F 88 18        EOR A  #318
00265 61A1 97 2C        STA A  M+44
00266
00267 * 2 SECOND DELAY BETWEEN MEASUREMENTS
00268 61A3 CE B89C      LDX #47260
00269 61A6 78 0029      ASL  M+41
00270 61A9 78 0029      ASL  M+41
00271 61AC 78 0029      ASL  M+41
00272 61AF 09           DEX
00273 61B0 26 54        BNE  MC1
00274 61B2 7E 6179      JMP  ST2
00275
00276 *MOVE BACK TO PARK POSITION
00277 *MUST MOVE FORWARD 2925
00278 61B5 86           JMPF2 LDA A #317
00279 61B7 97 00        STA A  M
00280 61B9 CE 0900      LDX #2525
00281 61BC DF 2A        STX M+42
00282 61BE CE 0860      LDX #2925
00283 61C1 DF 25        STX M+37
00284 61C3 BD C00C      JSR   ASD
00285
00286 * ROTATE BACK 90 DEGREES
00286 61C6 CE 454D      LDX #17741
00287 61C9 DF 2A        STX M+42
00288 61CB CE 46DD      LDX #18141
00289 61CE DF 25        STX M+37
00290 61D0 86 1D        LDA A #31D
00291 61D2 97 00        STA A  M
00292 61D4 BD C000      JSR   ASD
00293 61D7 3F           SWI

```

```

00296 61E0      ORG     $61E0
00297          NAM     BD2TM
00298          * THIS PROGRAM WILL BE USED TO PERFORM
00299          * A MULTI-DETECTOR SCAN USING 8 DETECTORS.
00300          * USING A 1:1 PULLEY RATIO THE TRANSLATION
00301          * IS 16992 STEPS (106.2 MM) IT WILL COLLECT 1416 DATA. FROM THE
00302          * PARK POSITION THE SCANNER MUST MOVE BACK
00303          * 1447 STEPS +32 FOR ACCEL.) DEF( STARTING THE SCAN.
00304          * MOTOR PULSES ARE SENT EVERY 1862 CYCLES
00305          * (APPROX. 3030.6 US) AND DATA PULSES ARE SENT TO
00306          * THE HP EVERY 12 MOTOR PULSES. THE SCANNER IS TO
00307          * ROTATE 25.71 DEG. AFTER EACH TRANSLATION & IS
00308          * TO PERFORM 7 TRANSLATIONS & 6 ROTATIONS.
00309          LDA     A     #30F          ; TRANSLATIONAL DIRECTION
00310          STA     A     M+44
00311          LDA     A     #07
00312          STA     A     M+45          ;# OF TRANSLATIONS
00313          LDA     A     #12
00314          STA     A     M+50          ;# OF MOTOR STEPS / HP SIGNAL
00315          LDA     A     #07
00316          STA     A     M+51          ; DETERMINES DELAY IN TRANSLATION
00317          LDA     A     #84
00318          STA     A     M+52          ; DETERMINES DELAY IN TRANSLATION
00319          LDA     A     #01
00320          STA     A     M+53          ; DETERMINES DELAY IN TRANSLATION
00321          * MOVE FROM PARK TO START POSITION
00322          * ONE GROUP OF 1479 PULSES
00323          * MAKES USE OF THE R21 RAMP
00324          * 1479=400 + 1079*1
00325          JSR     PIA
00326          LDA     A     #317          ; CALLS INIT AND F AS WELL
00327          STA     A     M
00328          LDX     #1079
00329          STX     M+42
00330          LDX     #1479
00331          STX     M+37
00332          JSR     ASD
00333          JSR     START
00334          LDA     B     #1B
00335          STA     B     ORA
00336          JSR     DELAY
00337          LDA     B     #31F
00338          STA     B     ORA
00339          JSR     ACCEL
00340          LDX     #32
00341          STX     M+37
00342          JSR     ASD
00343          61E0 86 OF
00344          61E2 97 2C
00345          61E4 86 07
00346          61E6 97 2D
00347          61E8 86 0C
00348          61EA 97 32
00349          61EC 86 07
00350          61EE 97 33
00351          61F0 86 54
00352          61F2 97 34
00353          61F4 86 01
00354          61F6 97 35
00355          61F8 BD C278
00356          61FB 86 17
00357          61FD 97 00
00358          61FF CE 0437
00359          6202 DF 2A
00360          6204 CE 05C7
00361          6207 DF 25
00362          6209 BD C000
00363          620C BD C29B ST3
00364          620F C6 1B
00365          6211 F7 8004
00366          6214 BD C28C
00367          6217 C6 1F
00368          6219 F7 8004
00369          621C BD C1F5
00370          621F CE 0020
00371          6222 DF 25
00372          6224 BD C000

```

```

00347 * SCAN - UP PROVIDES A MOTOR PULSE EVERY 1862 CYCLES & A HP PULSE
00348 * EVERY 12 MOTOR PULSES
00349 * HP PULSE IS SENT EVERY M+46 MOTOR PULSES
00350 6227 CE 4260 LDX #16992 ;PULSES REQUIRED FOR SCAN
00351 622A BD C280 JSR TRANSL
00352 * DELAY BETWEEN PULSES = 84*(1*12+8)+42+7*12+6 = 1862 CYCLES
00353 * DECELERATION
00354 622D BD C242 JSR DEC32
00355 6230 7A 002D DEC M+45 ;IS SCAN FINISHED?
00356 6233 27 0C BEQ JUMP3
00357 6235 BD C28D JSR R8D
00358 6238 96 2C LDA A M+44
00359 623A 88 18 EOR A #$18 ;CHANGE TRANSLATIONAL DIRECTION
00360 623C 97 2C STA A M+44
00361 623E 7E 620C JMP ST3
00363 *MOVE BACK TO PARK POSITION
00364 *SHOULD MOVE BACK 15577
00365 *HOWEVER APPEARS TO BE OUT ONE PULSE
00366 6241 86 17 JUMP3 LDA A #$17
00367 6243 97 00 STA A M
00368 6245 CE 3848 LDX #15176
00369 6248 DF 2A STX M+42
00370 624A CE 3CDB LDX #15576
00371 624D DF 25 STX M+37
00372 624F BD C000 JSR ASD
00373 * ROTATE BACK TO PARK POSITION
00374 * MUST ROTATE BACK 31080 PULSES
00375 6252 CE 77D8 LDX #30680 ;30680*M+12 PULSES
00376 6255 DF 2A STX M+42
00377 6257 CE 7968 LDX #31080
00378 625A DF 25 STX M+37
00379 625C 86 1D LDA A #$1D
00380 625E 97 00 STA A M
00381 6260 BD C000 JSR ASD
00382 6263 3F SWI
00386 6280 ORG $6280
00387 * NAM 8DETS
00388 * THIS PROGRAM WILL BE USED TO PERFORM
00389 * A MULTI-DETECTOR SCAN USING 8 DETECTORS.
00390 * USING A 1:1 PULLEY RATIO THE TRANSLATION
00391 * IS 16992 STEPS (106.2 MM). IT WILL COLLECT 1416 DATA FROM THE
00392 * PARK POSITION THE SCANNER MUST MOVE BACK
00393 * 1447 STEPS +5 FOR ACCEL.) BEFORE
00394 * STARTING THE SCAN.
00395 * MOTOR PULSES ARE SENT EVERY 7458 CYCLES

```

```

00396
00397
00398
00399
00400 6280 86 OF
00401 6282 97 2C
00402 6284 86 07
00403 6286 97 2D
00404 6288 86 0C
00405 628A 97 32
00406 628C 86 08
00407 628E 97 33
00408 6290 86 E3
00409 6292 97 34
00410 6294 86 02
00411 6296 97 35
00413
00414
00416
00417 6298 BD C278
00418 629B 86 17
00419 629D 97 00
00420 62BF CE 041C
00421 62A2 DF 2A
00422 62A4 CE 05AC
00423 62A7 DF 25
00424 62A9 BD C000
00425 62AC BD C29B ST4
00426 62AF C6 1B
00427 62B1 F7 8004
00428 62B4 BD C28C
00429 62B7 C6 1F
00430 62B9 F7 8004
00431
00432 62BC BD C1F5
00433 62BF CE 0005
00434 62C2 DF 25
00435 62C4 BD C000
00437
00438
00439
00440 6207 CE 4260
00441 62CA BD C280
00442
00443
00444 62CD BD C25D
00445 62D0 7A 002D

```

\* (APPROX. 12139 US) AND DATA PULSES ARE SENT TO  
\* THE HP EVERY 12 MOTOR PULSES. THE SCANNER IS TO  
\* ROTATE 25.71 DEG. AFTER EACH TRANSLATION & IS  
\* TO PERFORM 7 TRANSLATIONS & 6 ROTATIONS.  
LDA A #50F  
STA A M+44 ; TRANSLATIONAL DIRECTION  
LDA A #07 ; # OF TRANSLATIONS  
STA A M+45 ; # OF MOTOR STEPS / HP SIGNAL  
LDA A #12 ; DETERMINES DELAY IN TRANSLATION  
STA A M+50 ; DETERMINES DELAY IN TRANSLATION  
LDA A #08 ; DETERMINES DELAY IN TRANSLATION  
STA A M+51 ; DETERMINES DELAY IN TRANSLATION  
LDA A #227 ; DETERMINES DELAY IN TRANSLATION  
STA A M+52 ; DETERMINES DELAY IN TRANSLATION  
LDA A #02 ; DETERMINES DELAY IN TRANSLATION  
STA A M+53 ; DETERMINES DELAY IN TRANSLATION  
\* MOVE FROM PARK TO START POSITION  
\* ONE GROUP OF 1452 PULSES  
\* 1452=400 + 1052\*1  
JSR PIA ; CALLS INIT AND F AS WELL  
LDA A #517 ; TRANSLATIONAL DIRECTION  
STA A M  
LDX #1052  
STX M+42  
LDX #1452  
STX M+37  
JSR ASD  
LDA B #51B  
STA B ORA  
JSR DELAY  
LDA B #51F  
STA B ORA  
\* BEGIN ACCELERATION  
JSR ACCEL  
LDX #05  
STX M+37  
JSR ASD  
\* SCAN - UP PROVIDES A MOTOR PULSE EVERY 7458 CYCLES & A HP PULSE  
\* EVERY 12 MOTOR PULSES  
\* HP PULSE IS SENT EVERY M+46 MOTOR PULSES  
LDX #16992 ; PULSES REQUIRED FOR SCAN  
JSR TRANSL  
\* DELAY BETWEEN PULSES = 227(2\*12+8)+42+56+8\*12 = 7458 CYCLES  
\* DECELERATION  
JSR DEC5  
DEC M+45 ; IS SCAN FINISHED?

```

00446 62D3 27 OC          BEQ      JMPE4
00447 62D5 BD C28D       USR      RBD
00448 62D8 96 2C       LDA A M+44
00449 62DA 88 18       EOR A #18
00450 62DC 97 2C       STA A M+44
00451 62DE 7E 62AC     JMP      STA
00453                   *MOVE BACK TO PARK POSITION
00454                   *SHOULD MOVE BACK 15550
00455                   *HOWEVER APPEARS TO BE OUT ONE PULSE
00456 62E1 86 17       JMPE4 LDA A #17
00457 62E3 87 00       STA A M
00458 62E5 CE 382D     LDX #15149
00459 62E8 DF 2A       STX M+42
00460 62EA CE 3C8D     LDX #15549
00461 62ED DF 25       STX M+37
00462 62EF BD C000     JSR ASD
00463                   * ROTATE BACK TO PARK POSITION
00464                   * MUST ROTATE BACK 31080 PULSES
00465 62F2 CE 77D8     LDX #30680 ;30680*M+12 PULSES
00466 62F5 DF 2A       STX M+42
00467 62F7 CE 7968     LDX #31080
00468 62FA DF 25       STX M+37
00469 62FC 86 1D       LDA A #10
00470 62FE 97 00       STA A M
00471 6300 BD C000     JSR ASD
00472 6303 3F         SWI
00476 6320             ORG $6320
00477                   * NAM RAT
00478                   * THIS PROGRAM WILL BE USED TO PERFORM
00479                   * A SINGLE DETECTOR SCAN.
00480                   * USING A 1:1 PULLEY RATIO THE TRANSLATION
00481                   * IS 2560 STEPS (16.0 MM). IT WILL COLLECT 128 DATA FROM THE
00482                   * PARK POSITION THE SCANNER MUST MOVE FORWARD(+)
00483                   * 6500 STEPS -O FOR ACCEL. BEFORE
00484                   * STARTING THE SCAN.
00485                   * MOTOR PULSES ARE SENT EVERY 15.358 CYCLES
00486                   * (APPROX. 24,997 US) AND DATA PULSES ARE SENT TO
00487                   * THE HP EVERY 20 MOTOR PULSES. THE SCANNER IS TO
00488                   * ROTATE 3.214 DEG. AFTER EACH TRANSLATION & IS
00489                   * TO PERFORM 56 TRANSLATIONS & 55 ROTATIONS.
00490 6320 86 OF         LDA A #50F
00491 6322 97 2C       STA A M+44 ; TRANSLATIONAL DIRECTION
00492 6324 86 38       LDA A #56 ;# OF TRANSLATIONS
00493 6326 97 2D       STA A M+45 ;# OF MOTOR STEPS / HP SIGNAL
00494 6328 86 14       LDA A #20
00495 632A 97 32       STA A M+50

```

```

00496 632C 86 08 LDA A #08
00497 632E 97 33 STA A M+51
00498 6330 86 DF LDA A #223
00499 6332 97 34 STA A M+52
00500 6334 86 05 LDA A #05
00501 6336 97 35 STA A M+53
00503
00504
00505
00506
00507 6338 8D C278 JSR PIA
00508 6338 86 0F LDA A #50F
00509 633D 97 00 STA A M
00510 633F CE 17D4 LDX #6100
00511 6342 DF 2A STX M+42
00512 6344 CE 1964 LDX #6500
00513 6347 DF 25 STX M+37
00514 6349 8D C000 JSR ASD
00515 634C 8D C29B JSR START
00516 634F C6 18 LDA B #518
00517 6351 F7 8004 STA B ORA
00518 6354 8D C28C JSR DELAY
00519 6357 C6 1F LDA B #51F
00520 6359 F7 8004 STA B ORA
00522
00523
00524
00525 635C CE 0A00 JSR UP
00526 635F 8D C2B0 JSR TRANSL
00527
00528 6362 7A 002D DEC M+45
00529 6365 27 1A BEQ JMPE5
00530
00531 6367 86 1E LDA A #51E
00532 6369 97 00 STA A M
00533 636B CE 00F8 LDX #248
00534 636E DF 2A STX M+42
00535 6370 CE 0288 LDX #648
00536 6373 DF 25 STX M+37
00537 6375 8D C000 JSR ASD
00538 6378 96 2C LDA A M+44
00539 637A 88 18 EOR A #518
00540 637C 97 2C STA A M+44
00541 637E 7E 634C JMP ST5
00543
00544
00545

```

: DETERMINES DELAY IN TRANSLATION  
 : DETERMINES DELAY IN TRANSLATION  
 : DETERMINES DELAY IN TRANSLATION  
 \* MOVE FROM PARK TO START POSITION  
 \* ONE GROUP OF 6500 PULSES  
 \* MAKES USE OF THE R21 RAMP  
 \* 6500=400 + 6100\*1  
 : CALLS INIT AND F AS WELL  
 : TRANSLATIONAL DIRECTION (+)  
 : TELL HP RAMP IS BEGINNING  
 \* SCAN - UP PROVIDES A MOTOR PULSE EVERY 15,358 CYCLES & A HP PULSE  
 \* EVERY 20 MOTOR PULSES  
 \* HP PULSE IS SENT EVERY M+46 MOTOR PULSES  
 : PULSES REQUIRED FOR SCAN  
 \* DELAY BETWEEN PULSES =  $223(5*12+8)+42+56+8*12 = 15358$  CYCLES  
 : IS SCAN FINISHED?  
 \* ROTATE 3.214 DEG. (648 PULSES)  
 : 248 \* M+12 PULSES  
 : CHANGE TRANSLATIONAL DIRECTION  
 \* MOVE BACK TO PARK POSITION  
 \* SHOULD MOVE BACK 6500  
 \* HOWEVER APPEARS TO BE OUT ONE PULSE



```

00546 6381 86 17 JIMPE5 LDA A #S17
00547 6383 97 00 STA A M
00548 6385 CE 17D3 LDX #6089
00549 6388 DF 2A STX M+42
00550 638A CE 1963 LDX #6499
00551 638D DF 25 STX M+37
00552 638F BD C000 JSR ASD
00553
00554
00555 6392 CE 89A8 * ROTATE BACK TO PARK POSITION
00556 6395 DF 2A LDX #35240 ;35240*M+12 PULSES
00557 6397 CE 8B38 STX M+42
00558 639A DF 25 LDX #35640
00559 639C 86 1D LDA A #S1D
00560 639E 87 00 STA A M
00561 63A0 BD C000 JSR ASD
00562 63A3 3F SWI
00563 C000
00564
00565
00566 C000 ORG $C000
00567
00568 * NAM SUBROUTINES
00569 * SUBROUTINE ASD (ACCELERATION,SPEED,
00570 * DECELERATION)
00571 * MUST HAVE PARAMETERS SET INTO M THROUGH M+43 BEFORE INITIATION.
00572 * M IS THE TYPE OF MOTION AND DIRECTION ($1D & $1E ARE ROTATION WHILE
00573 * $OF & $17 ARE TRANSLATION). M+1 THROUGH M+23 ARE
00574 * THE LENGTHS OF THE RAMPS INVOLVED
00575 * M+25 THROUGH M+36 ARE THE FREQUENCY OF THE PULSES ASSOCIATED WITH
00576 * THE SETS OF RAMPS
00577 * WHILE M+24 IS A SPARE LOCATION.
00578 * M+37 M+38 IS THE TOTAL # OF PULSES NEEDED FOR THE DESIRED MOTION
00579 * M+39 IS A PROGRAM LOCATION DEVICE
00580 * M+40 IS USED TO STORE ACC A
00581 * M+41 IS MERELY A DELAY MECHANISM
00582 * M+42 M+43 = THE # OF TIMES THE RAMP AT
00583 C000 CE 0000 ASD LDX #S0000
00584 C003 7F 0027 CLR M+39
00585 C006 7F 0028 CLR M+40
00586 C009 08 ASDO
00587 C00A 96 28 LDA A M+40 ;4
00588 C00C 4C INC A ;3
00589 C00D 97 28 STA A M+40 ;2
00590
00591 * THE FOLLOWING BRANCH TO C1 THROUGH C9 SINCE BRANCHES TO
00592 * B3 THROUGH B8 WOULD BE OUT OF RANGE
00593
00594 COOF 91 01 CMP A M+1 ;5
00595 C011 2F 23 BLE C1

```

00596	C019	91	O2	CMP	A	M+2
00597	C015	2F	22	BLE	C2	
00598	C017	91	O3	CMP	A	M+3
00599	C019	2F	21	BLE	C3	
00600	C018	91	O4	CMP	A	M+4
00601	C01D	2F	20	BLE	C4	
00602	C01F	B1	O5	CMP	A	M+5
00603	C021	2F	1F	BLE	C5	
00604	C023	91	O6	CMP	A	M+6
00605	C025	2F	1E	BLE	C6	
00606	C027	91	O7	CMP	A	M+7
00607	C029	2F	1D	BLE	C7	
00608	C02B	91	O8	CMP	A	M+8
00609	C02D	2F	1C	BLE	C8	
00610	C02F	91	O8	CMP	A	M+9
00611	C031	2F	1B	BLE	C9	
00612	C033	7E	C051	JMP	J5	
00613	C036	7E	C0E7	C1		
00614	C039	7E	C0EC	C2		
00615	C03C	7E	C0F1	C3		
00616	C03F	7E	C0F6	C4		
00617	C042	7E	C0FB	C5		
00618	C045	7E	C100	C6		
00619	C048	7E	C105	C7		
00620	C04B	7E	C10A	C8		
00621	C04E	7E	C10F	C9		
00623				JMP	B9	
00624				JMP	B1	
00626				JMP	B2	
00628				JMP	B3	
00630				JMP	B4	
00631				JMP	B5	
00632				JMP	B6	
00633				JMP	B7	
00634				JMP	B8	
00635				JMP	B9	
00636				JMP	B9	
00637				JMP	B9	
00638				JMP	B9	
00639				JMP	B9	
00640				JMP	B9	
00641				JMP	B9	
00642				JMP	B9	
00643				JMP	B9	
00644				JMP	B9	
00645				JMP	B9	

\* THE FOLLOWING (PRE BLE B10) IS NECESSARY SINCE THE BLE INSTRUCTION  
 \* USES TWO S COMPLEMENT ARITHMETIC WHICH RESTRICTS THE  
 \* SIZE OF AN 8 BIT NUMBER TO +127 & THE SIZE OF A RAMP SPEC TO +126

:B10 IS OUT OF RANGE FOR BRANCH  
 :B11 IS OUT OF RANGE FOR BRANCH

```

00646 C077 7F 0028 P1 CLR M+40
00647 C07A 09 DEX
00648 C07B D6 28 LDA B M+43
00649 C07D 27 06 BEQ P4
00650 C07F 7A 002B DEC M+43
00651 C082 7E C08F JMP ASD2 M+42
00652 C085 D6 2A P4 LDA B M+42
00653 C087 27 16 BEQ P6
00654 C089 7A 002A DEC M+42
00655 C08C 7A 002B DEC M+43
00656 C08F 96 28 LDA A M+40
00657 C091 4C ASD2 INC A M+40
00658 C092 97 28 STA A M+40
00659 C094 08 INX M+12
00660 C095 91 0C CMP A M+12
00661 C097 2F 03 BLE C12
00662 C099 7E C077 JMP P1
00663 C09C 7E C11E C12 JMP B12
00664 C09F 86 03 LDA A #03
00665 C0A1 97 27 STA A M+39
00666 C0A3 7F 0028 CLR M+40
00667 C0A6 09 DEX
00668 C0A7 96 28 LDA A M+40
00669 C0A9 4C INC A M+40
00670 C0AA 97 28 STA A M+40
00671 C0AC 08 INX
00672 C0AD 91 0D CMP A M+13
00673 C0AF 2F 68 BLE B11
00674 C0B1 91 0E CMP A M+14
00675 C0B3 2F 5F BLE B10
00676 C0B5 91 0F CMP A M+15
00677 C0B7 2F 56 BLE B9
00678 C0B9 86 04 LDA A #04
00679 C0BB 97 27 STA A M+39
00680 C0BD 7F 0028 CLR M+40
00681 C0C0 09 DEX
00682 C0C1 96 28 LDA A M+40
00683 C0C3 4C INC A M+40
00684 C0C4 97 28 STA A M+40
00685 C0C6 08 INX
00686 C0C7 91 10 CMP A M+16
00687 C0C9 2F 3F BLE B6
00688 C0CB 91 11 CMP A M+17
00689 C0CD 2F 36 BLE B7
00690 C0CF 91 12 CMP A M+18
00691 C0D1 2F 2D BLE B6
00692 C0D3 91 13 CMP A M+19
00693 C0D5 2F 24 BLE B5

```

∴ B12 IS OUT OF RANGE FOR A BRANCH

```

00684 C007 91 14      CMP A M+20
00695 C009 2F 1B      BLE B4
00696 C00B 91 15      CMP A M+21
00697 C00D 2F 12      BLE B3
00698 C00F 91 16      CMP A M+22
00699 C0E1 2F 09      BLE B2
00700 C0E3 91 17      CMP A M+23
00701 C0E5 2F 00      BLE B1
00702 C0E7 96 19      LDA A M+25
00703 C0E9 7E C120    JMP J
00704 C0EC 96 1A      LDA A M+26
00705 C0EE 7E C120    JMP J
00706 C0F1 96 1B      LDA A M+27
00707 C0F3 7E C120    JMP J
00708 C0F6 96 1C      LDA A M+28
00709 C0F8 7E C120    JMP J
00710 C0FB 96 1D      LDA A M+29
00711 C0FD 7E C120    JMP J
00712 C100 96 1E      LDA A M+30
00713 C102 7E C120    JMP J
00714 C105 96 1F      LDA A M+31
00715 C107 7E C120    JMP J
00716 C10A 96 20      LDA A M+32
00717 C10C 7E C120    JMP J
00718 C10F 96 21      LDA A M+33
00719 C111 7E C120    JMP J
00720 C114 96 22      LDA A M+34
00721 C116 7E C120    JMP J
00722 C119 96 23      LDA A M+35
00723 C11B 7E C120    JMP J
00724 C11E 96 24      LDA A M+36
00725 C120 C6 1F      LDA B #1F
00726 C122 F7 8004    STA B ORA
00727 C125 C6 09      LDA B #09
00728 C127 78 0029 D1 ASL M+41
00729 C12A 5A          DEC B
00730 C12B 26 FA          BNE D1
00731 C12D 8C 0000      CPX #0000
00732 C130 4A          DEC A
00733 C131 26 F2          BNE DEL
00734 C133 D6 00          LDA B M
00735 C135 F7 8004      STA B ORA
00736 C138 9C 25          CPX M+37
00737 C13A 27 21          BEQ Z2
00738 C13C 96 27          LDA A M+39
00739 C13E 81 01          CMP A #01

```

```

)B*12=9*12=108
)

```

```

:2
:5
:2
:6
:4
:3
:2
:4
:3
:2
:4
:3
:5
: IS MOTION COMPLETE ? 4
:2

```

00740 C140 27 OF  
 00741 C142 81 O2  
 00742 C144 27 OE  
 00743 C146 81 O3  
 00744 C148 27 O0  
 00745 C14A 81 O4  
 00746 C14C 27 OC  
 00747 C14E 7E CO09  
 00748 C151 7E CO59 Z3  
 00749 C154 7E CO8F Z4  
 00750 C157 7E COA7 Z5  
 00751 C15A 7E COC1 Z6  
 00752 C15D C6 1F Z2  
 00753 C15F F7 8004  
 00754 C162 39  
 00757  
 00758  
 00759  
 00760 C163 86 FF  
 00761 C165 97 19  
 00762 C167 86 81  
 00763 C169 97 1A  
 00764 C16B 86 4A  
 00765 C16D 97 1B  
 00766 C16F 86 2F  
 00767 C171 97 1C  
 00768 C173 86 22  
 00769 C175 97 1D  
 00770 G177 86 13  
 00771 C179 97 1E  
 00772 C17B 86 OC  
 00773 C17D 97 1F  
 00774 C17F 86 09  
 00775 C181 97 20  
 00776 C183 86 07  
 00777 C185 97 21  
 00778 C187 86 05  
 00779 C189 97 22  
 00780 C18B 86 04  
 00781 C18D 97 23  
 00782 C18F 86 03  
 00783 C191 97 24  
 00784 C193 39  
 00787  
 00788  
 00789

BEQ Z3  
 CMP A #02  
 BEQ Z4  
 CMP A #03  
 BEQ Z5  
 CMP A #04  
 BEQ Z6  
 JMP ASDO  
 JMP ASD1  
 JMP ASD2  
 JMP ASD3  
 JMP ASD4  
 LDA B #51F  
 STA B ORA  
 RTS

:4  
 :2  
 :4  
 :2  
 :4  
 :2  
 :4  
 :2  
 :4  
 :3

\* THE FOLLOWING FREQUENCIES ARE APPROXIMATE ONLY  
 \* & ARE SLIGHTLY DIFFERENT FOR ACCELERATION & DECELERATION  
 \* F IS THE REQUIRED FREQUENCIES FOR ACCELERATION/DECELERATION

F  
 LDA A #255 :20.2HZ  
 STA A M+25 :39.9HZ  
 LDA A #129 :69.3 HZ  
 STA A M+26 :108.6 HZ  
 LDA A #74 :148.9 HZ  
 STA A M+27 :261.4 HZ  
 LDA A #47 :402.3 HZ  
 STA A M+28 :548 HZ  
 LDA A #34 :677 HZ  
 STA A M+29 :917 HZ  
 LDA A #19 :1115 HZ  
 STA A M+30 :1422 HZ  
 LDA A #12 :548 HZ  
 STA A M+31 :677 HZ  
 LDA A #9 :917 HZ  
 STA A M+32 :1115 HZ  
 LDA A #7 :1422 HZ  
 STA A M+33 :548 HZ  
 LDA A #5 :677 HZ  
 STA A M+34 :917 HZ  
 LDA A #4 :1115 HZ  
 STA A M+35 :1422 HZ  
 LDA A #3 :548 HZ  
 STA A M+36 :677 HZ  
 RTS

\* INIT. GIVES THE LENGTHS OF RAMPS  
 \* 360 DEGREES = 360/ 9\*464/128\*50.044=72564 STEPS  
 \* 25.7 DEGREES=5180.25 STEPS



```

00835 C1EC 86 52          LDA A #82
00836 C1EE 97 16          STA A M+22
00837 C1FO 86 53          LDA A #83
00838 C1F2 97 17          STA A M+23
00839 C1F4 39            RTS
00842
00843 C1F5 BD C194        * ACCELERATION
00844 C1F8 96 2C        ACCEL JSR INIT
00845 C1FA 97 00        LDA A M+44
                                STA A M
00846 C1FC 7F 002A        CLR M+42
00847 C1FF 7F 002B        CLR M+43
00848 C202 CE 00C8        LDX #200
00849 C205 DF 25          STX M+37
00850 C207 39            RTS
00853
00854 C208 96 2C        * DECELERATION
00855 C20A 97 00        DECEL LDA A M+44
00856 C20C 7F 0001        STA A M
00857 C20F 7F 0002        CLR M+1
00858 C212 7F 0003        CLR M+2
00859 C215 7F 0004        CLR M+3
00860 C218 7F 0005        CLR M+4
00861 C21B 7F 0006        CLR M+5
00862 C21E 7F 0007        CLR M+6
00863 C221 7F 0008        CLR M+7
00864 C224 7F 0009        CLR M+8
00865 C227 7F 000A        CLR M+9
00866 C22A 7F 000B        CLR M+10
00867 C22D 7F 000C        CLR M+11
00868 C230 7F 000D        CLR M+12
00869 C233 7F 000E        CLR M+42
00870 C236 CE 00C8        CLR M+43
00871 C239 DF 25          LDX #200
00872 C23B BD C000        STX M+37
00873 C23E BD C194        JSR ASD
00874 C241 39            JSR INIT
00877 C242 CE 0053        RTS
00878 C245 DF 25          LDX #83
00879 C247 86 33          STX M+37
00880 C249 97 28          LDA A #51
00881 C24B CE 0033        STA A M+40
00882 C24E 86 04          LDX #51
00883 C250 97 27          LDA A #04
00884 C252 96 2C          STA A M+39
00885 C254 97 00          LDA A M+44
00886 C256 BD C0C1        STA A M
                                JSR ASD4
                                :32+51

```

```

00887 C259 BD C194 JSR INIT
00888 C25C 39 RTS
00889 * USED FOR DECELERATION FROM 100 HZ. < F. MAX. <400 HZ.
00892 C25D CE 0053 DEC5 ;78+5
00893 C260 DF 25 LDX #83
00894 C262 86 4E LDA A #78
00895 C264 97 28 STA A M+40
00896 C266 CE 004E LDX #78
00897 C269 86 04 LDA A #04
00898 C26B 97 27 STA A M+39
00899 C26D 96 2C LDA A M+44
00900 C26F 97 00 STA A M
00901 C271 BD C0C1 JSR #3D4
00902 C274 BD C194 JSR INIT
00903 C277 39 RTS
00904 * USED FOR DECELERATION FROM F. MAX. < 100 HZ.
00907 C278 7F 8005 PIA CLR CRA ;SET CRA FOR DDRA
00908 C27B C6 1F LDA B #31F ;BITS 0-4 O/P.5-7 I/P
00909 C27D F7 8004 STA B DDRA ;SET CRA FOR ORA
00910 C280 C6 04 LDA B #04
00911 C282 F7 8005 STA B CRA
00912 C285 BD C194 JSR INIT
00913 C288 BD C163 JSR F
00914 C28B 39 RTS
00915 * U P HAS BEEN INITIALIZED
00916 * BITS 0+1 = ROTATION, 2= O/P TO HP, 3+4 = TRANSLATION, 5= I/P FROM HP.
00917 * 6+7 ARE NOT PRESENTLY USED.
00918 * BITS 0-4 ARE ACTIVE ON THE POSITIVE TRANSITION, BIT 2
00921 C28C 39 DELAY RTS ;5
00924 * R8D (ROTATE FOR 8 DETECTORS)
00925 * PRODUCES 25.7 DEGREES ROTATION
00926 * ACCEL. + DECEL. = 400 STEPS
00927 * A BIT PATTERN IS NOT REQUIRED FOR 25.7 DEG.
00928 C28D CE 143C R8D LDX #5180 ; 5180 STEPS = 25.7 DEGREES
00929 C290 DF 25 STX M+37 ; 4780*M+12
00930 C282 CE 12AC LDX #4780
00931 C295 DF 2A STX M+42
00932 C297 BD C000 JSR ASD
00933 C29A 39 RTS
00936 * START SENDS A SIGNAL TO THE HP
00937 * AND WAITS FOR A SIGNAL IN RETURN
00938 C29B C6 1B START LDA B #31B ROT. & TRANSL. BITS HIGH
00939 *
00940 C29D F7 8004 STA B ORA
00941 C2A0 BD C28C JSR DELAY
00942 C2A3 C6 1F LDA B #31F

```



```

00943 C2A5 F7 8004 STA B ORA
00944 C2AB F6 8004 LDA B ORA
00945 C2AB C4 20 AND B #20
00946 C2AD 27 F9 BEQ J3
00947 C2AF 39 RTS
00950
00951
00952
00953
00954
00955 C280 C6 01
00956 C282 D7 2E STA B M+46
00957 C284 08 INX
00958 C285 96 34 LOOP6
00959 C287 7A 002E LDA A M+52
00960 C28A 26 17 BNE N2
00962 C28C C6 18 LDA B #51B
00963 C28E F7 8004 STA B ORA
00964 C2C1 BD C28C JSR DELAY
00965 C2C4 C6 1F LDA B #51F
00966 C2C6 F7 8004 STA B ORA
00967 C2C9 F7 8004 STA B ORA
00968 C2CC D6 32 LDA B M+50
00969 C2CE D7 2E STA B M+46
00970 C2D0 7E C2E8 JMP J1
00971
00972 C2D3 78 0029 N2
00973 C2D6 78 0029 ASL M+41
00974 C2D9 78 0029 ASL M+41
00975 C2DC 78 0029 ASL M+41
00976 C2DF 78 0029 ASL M+41
00977 C2E2 78 0029 ASL M+41
00978 C2E5 78 0029 ASL M+41
00979 C2E8 09 J1
00980 C2E9 27 23 DEX
00981 C2EB D6 33 BEQ J2
00982 C2ED 78 0029 J4 LDA B M+51
00983 C2FO 5A DEC B M+41
00984 C2F1 26 FA BNE J4
00985 C2F3 D6 2C LDA B M+44
00986 C2F5 F7 8004 STA B ORA
00987 C2F8 BD C28C JSR DELAY
00988 C2FB C6 1F LDA B #51F
00989 C2FD F7 8004 STA B ORA
00990 C300 D6 35 LOOP5
00991 C302 78 0029 J6 LDA B M+53
ASL M+41
ASL M+41
ASL M+41
ASL M+41
ASL M+41
ASL M+41
DEX
BEQ J2
LDA B M+51
ASL M+41
DEC B
BNE J4
LDA B M+44
STA B ORA
JSR DELAY
LDA B #51F
STA B ORA
LDA B M+53
ASL

```

: WAIT FOR HP SIGNAL  
 \* TRANSLATION - A SIGNAL IS SENT TO THE HP  
 \* EVERY M+50 MOTOR STEPS. M+51, M+52 AND M+53  
 \* DETERMINE THE DELAY BETWEEN MOTOR STEPS  
 \* DELAY BETWEEN STEPS  
 \* M+52((M+53\*12)+8) + 42 +M+51\*12 +56  
 TRANSL LDA B #01  
 STA B M+46  
 INX  
 LDA A M+52  
 DEC M+46  
 BNE N2  
 LDA B #51B  
 STA B ORA  
 JSR DELAY  
 LDA B #51F  
 STA B ORA  
 STA B ORA  
 LDA B M+50  
 STA B M+46  
 JMP J1  
 ASL M+41  
 ASL M+41  
 ASL M+41  
 ASL M+41  
 ASL M+41  
 ASL M+41  
 DEX  
 BEQ J2  
 LDA B M+51  
 ASL M+41  
 DEC B  
 BNE J4  
 LDA B M+44  
 STA B ORA  
 JSR DELAY  
 LDA B #51F  
 STA B ORA  
 LDA B M+53  
 ASL

: PULSES IN INX = # OF PULSES FOR TRANSLATION  
 : PRODUCES DESIRED DELAY BETWEEN PULSES 3 CYCLES  
 : 6  
 : 4  
 : 2) SEND SIGNAL TO HP  
 : 5)  
 : 9+5)  
 : 2) 42  
 : 5)  
 : 3) HP SIGNAL EVERY M+50 STEPS  
 : 4)  
 : 3)  
 : 6) TIME TO J1 IS THE SAME EITHER WAY  
 : 6)  
 : 6)  
 : 6) 42  
 : 6)  
 : 6)  
 : 6)  
 : 4  
 : 4  
 : 3  
 : 6 )  
 : 2 )B\*12=M+51+12  
 : 4 )  
 : 3  
 : 5  
 : 9+5  
 : 2  
 : 5  
 : 2  
 : 2 )  
 : 6 )

```

00992 C305 5A
00993 C306 26 FA
00994 C308 4A
00995 C309 26 F5
00996 C308 7E C2B5
00997 C30E 39 J2
01000
DEC B
BNE J6
DEC A
BNE L00P5
JMP L00P6
RTS
END
:2 ) M+53*12
:4 )
:2
:4
:3

```

Symbol Table

ORA	8004	DDRA	8004	CRA	8005	M	0000	ST	602C	JMPE	605C	ST1	608C	K5	60EA
MC1	61A6	JMPE2	61B5	ST3	620C	JMPE3	6241	ST4	62AC	JMPE4	62E1	ST5	634C	JMPE5	6381
C1	C039	C2	C039	C3	C03C	C4	C03F	C5	C042	C6	C045	C7	C048	CB	C04B
ASD1	C059	C10	C066	K1	C069	C11	C070	K2	C073	P1	C077	P4	C085	ASD2	C08F
ASD3	COA7	ASD4	COA1	B1	COE7	B2	COEC	B3	GOF1	B4	COF6	B5	COFB	B6	C100
B8	C10F	B10	C114	B11	C119	B12	C11E	J	C120	DEL	C125	D1	C127	Z3	C151
Z6	C15A	Z2	C15D	F	C163	INIT	C194	ACCEL	C1F5	DECEL	C208	DEC32	C242	DEC5	C25D
R8D	C28D	START	G29B	U3	C2AB	TRANSL	C2B0	L00P6	C2B5	N2	C2D3	J1	C2E8	J4	C2ED
J2	C30E	JMPE1	6107	ST2	6179	ASD	C000	ASDO	CO09	C9	CO4E	J5	CO51	C12	C09C
P6	C09F	B7	C105	B8	C10A	Z4	C154	Z5	C157	PIA	C278	DELAY	C28C		

\*\*\* SOME PROGRAM LINE NUMBERS MAY BE MISSING DUE TO DELETION OF SOME COMMENTS. THIS WAS DONE FOR FORMATTING PURPOSES.

\*\*\* APPENDIX D - CONTAINS READ SUBROUTINE \*\*\*

Motorola M68SAM Cross-Assembler

```

00001      8004      EQU      $8004
00002      8004      EQU      $8004
00003      8005      EQU      $8005
00004      8006      EQU      $8006
00005      8006      EQU      $8006
00006      8007      EQU      $8007
00007      0000      EQU      $0000
00008      M        EQU      READ
00009      C300     ORG      $C300
00010
00011      * 4 TYPES OF INFORMATION WILL BE
00012      * SENT FROM THE CAMAC.
00013      * (1) 8 BIT DATA SENT THROUGH A SIDE
00014      * BITS B7-B0 (HIGH-LOW)
00015      * (2) 9 BIT ADDRESS FOR DATA (512 BYTES RAM)
00016      * B SIDE B0 (HIGH), A SIDE B7-B0 (LOW)
00017      * (3) 9 BIT ADDRESS FOR STARTING PROGRAMS
00018      * IN RAM (AS IN (2)) AND
00019      * (4) 16 BIT ADDRESS FOR STARTING PROGRAMS IN ROM
00020      * PIA A SIDE B7-B0 IS SENT TWICE.
00021      * THE FIRST BYTE SENT IS THE HIGH
00022      * BYTE OF THE ADDRESS.
00023      * THE TYPE OF INFORMATION
00024      * BEING SENT IS ENCODED IN B SIDE
00025      * BITS 162.
00026      * TYPE 1 =B1=B2=0
00027      * TYPE 2 =B1=0, B2=1
00028      * TYPE 3 =B1=B2=1
00029      * TYPE 4 =B1=1, B2=0
00029      C300 7F 8005      CLR      CRA
00030      C303 7F 8007      CLR      CRB
00031      C306 7F 8004      CLR      DDRA
00032      C309 C6 F8        LDA B  #$F8
00033      C308 F7 8006      STA B  DDRB
00034      C30E C6 E6        LDA B  #$E6
00035
00036      * CRA = 1110 0110
00037      * B5=1 CA2 = 0/P;
00038      * B4=B3=0 HANDSHAKE MODE, CA2 GOES
00039      * LOW ON READ ORA & RETURNS HIGH
00040      * WHEN IRQA1 IS SET BY CA1;
00041      * B2=1 ORA; B1=1 +VE TRANSITIONS OF
00042      * CA1 SET IRQA1; B0=0 DISABLES IRQA1
00043      * INTERRUPT BY CA1.
00043      C310 F7 8005      STA B  CRA
00044      C313 C6 FD        LDA B  #$FD
00044
                                ; SET CRB
                                ; SET CRA FOR DDRA
                                ; SET CRB FOR DDRB
                                ; A SIDE I/P'S
                                ; B SIDE BITS 0-2 I/P,
                                ; BITS 3-7 O/P
                                ; SET CRA

```

```

00045
00046
00047
00048
00049
00050
00051
00052 C315 F7 8007
00053 C318 FE C31E
00054 C318 FF A000
00055 C31E B6 8005 READ
00056 C321 84 80
00057 C323 27 F9
00058 C325 B6 8006
00059 C328 B7 01F6
00060 C328 84 04
00061 C32D 26 10
00062 C32F B6 8006
00063 C332 84 02
00064 C334 26 26
00065 C336 B6 8004
00066 C339 A7 00
00067 C33B 08
00068 C33C 7E C31E
00069 C33F B6 8006 B2
00070 C342 84 01
00071 C344 B7 01F4
00072 C347 B6 8004
00073 C34A B7 01F5
00074 C34D FE 01F4
00075 C350 F6 01F6
00076 C353 C4 02
00077 C355 26 03
00078 C357 7E C31E
00079 C35A 6E 00 B91
00080 C35C B6 8004 B1
00081 C35F B7 01F4
00082 C362 B6 8005 REA
00083 C365 84 80
00084 C367 27 F9
00085 C369 B6 8004
00086 C36C B7 01F5
00087 C36F FE 01F4
00088 C372 6E 00
00089
          STA B
          CRB
          LDX READ
          STX $A000
          LDA A CRA
          AND A #80
          BEQ READ
          LDA A ORB
          STA A M+502
          AND A #04
          BNE B2
          LDA A ORB
          AND A #02
          BNE B1
          LDA A ORA
          STA A X
          INX
          JMP READ
          LDA A ORB
          AND A #01
          STA A M+500
          LDA A ORA
          STA A M+501
          LDX M+500
          LDA B M+502
          AND B #02
          BNE B91
          JMP READ
          X
          LDA A ORA
          STA A M+500
          LDA A CRA
          AND A #80
          BEQ REA
          LDA A ORA
          STA A M+501
          LDX M+500
          JMP X
          END
          ; VECTORIZE JBUG SO THAT IRQ WILL
          ; CAUSE A JUMP TO READ SR
          ; CHECK IF MESSAGE
          ; HAS BEEN SENT
          ; $01F6= SCRATCH LOCATION
          ; IS B2=0 ??
          ; B2=0
          ; IS B1=0 ??
          ; B2=0, B1=0
          ; B2=1
          ; MASK BITS SIDE B 1-7
          ; $01F4= SCRATCH LOCATION
          ; $01F5= SCRATCH LOCATION
          ; IS B1=0 ??
          ; B2=1, B1=0
          ; B2=1, B1=1
          ; B2=0, B1=1
          * CRB = 1111 1101
          * B5=1 CB2= 0/P; B4=1 CB2 FOLLOWS B3
          * AS CHANGED BY WRITE CRB INSTRUCTION;
          * B3=1 NORMALLY HIGH, ACTIVE HIGH TO LOW;
          * B2=1 ORB; B1=0 -VE TRANSITION OF CB1 SET
          * IRQB1; B0=1 ENABLES IRQB MPU INTERRUPT
          * BY CB1.
    
```

Symbol Table

ORA	8004	DDRA	8004	CRA	8005	ORB	8006	DDRB	8006	CRB	8007	M	0000
READ	C31E	B2	C33F	B91	C35A	B1	C35C	REA	C362				

\*\*\* SOME PROGRAM LINE NUMBERS MAY BE MISSING DUE TO DELETION OF SOME COMMENTS. THIS WAS DONE FOR FORMATTING PURPOSES.